

**A MODEL DEVELOPMENT OF ORGANOSOLV PRETREATMENT  
FOR VARIOUS TYPES OF BIOMASS**

**LIM SIEW CHE**

**A project report submitted in partial fulfilment of the  
requirements for the award of Bachelor of Engineering  
(Honours) Chemical Engineering**

**Lee Kong Chian Faculty of Engineering and Science  
Universiti Tunku Abdul Rahman**

**April 2020**

**DECLARATION**

I hereby declare that this project report is based on my original work except for citations and quotations which have been duly acknowledged. I also declare that it has not been previously and concurrently submitted for any other degree or award at UTAR or other institutions.

Signature : 

Name : LIM SIEW CHE

ID No. : 1501602

Date : 18<sup>th</sup> MAY 2020

**APPROVAL FOR SUBMISSION**

I certify that this project report entitled “**A MODEL DEVELOPMENT OF ORGANOSOLV PRETREATMENT FOR VARIOUS TYPES OF BIOMASS**” was prepared by **LIM SIEW CHE** has met the required standard for submission in partial fulfilment of the requirements for the award of Bachelor of Engineering (Honours) Chemical Engineering at Universiti Tunku Abdul Rahman.

Approved by,

Signature :



DR. STEVEN LIM  
ASSISTANT PROFESSOR  
LEE KONG CHAN FACULTY OF ENGINEERING AND SCIENCE  
UNIVERSITI TUNKU ABDUL RAHMAN

Supervisor :

Dr. Steven Lim

Date :

18<sup>th</sup> MAY 2020

Signature :



Co-Supervisor :

Dr. Lim Chun Hsion

Date :

18<sup>th</sup> MAY 2020

The copyright of this report belongs to the author under the terms of the copyright Act 1987 as qualified by Intellectual Property Policy of Universiti Tunku Abdul Rahman. Due acknowledgement shall always be made of the use of any material contained in, or derived from, this report.

© 2020, Lim Siew Che. All right reserved.

## ACKNOWLEDGEMENTS

I would like to thank everyone who had contributed to the successful completion of this project. I would like to express my deep and sincere gratitude to my research supervisor, Dr. Steven Lim and co-supervisor, Dr. Lim Chun Hsion for providing me their invaluable advice, guidance and enormous patience throughout the development of the research.

In addition, a special thanks to my helpful and responsible senior, Mr. Danny Chin. He has taught me the methodology to carry out the research works as clearly as possible. It was a great privilege and honour to study under his guidance. I am extremely grateful to Mr. Pavi, Ms. Wong Wan Ying, Ms. Heng Zheng Wei and Ms. Tan Yin Yin as well. They had offered me important suggestions and assistance unconditionally throughout this research project.

Lastly, I am very much thankful to my loving parents for their love, prayers, caring and sacrifices for educating and preparing me for my future. Also, I express my gratitude to my friends who had helped and given me encouragement all the time.

## ABSTRACT

Organosolv pretreatment is declared as a reliable approach to transform lignocellulosic biomass into sustainable energy, such as biofuel and value-added chemicals. A comprehensive study of organosolv pretreatment for coconut husk, spent coffee ground and sugarcane bagasse had performed by using aqueous ethylene glycol (30 v/v%) under 80 °C for 40 minutes, with solid to liquid of 1:20. It was found that the raw coconut husk comprised of  $30.73 \pm 1.7$  % alpha-cellulose,  $20.60 \pm 4.1$  % beta-cellulose,  $12.62 \pm 6.4$  % gamma-cellulose and  $36.89 \pm 1.3$  % lignin. Whereas, spent coffee ground composed of  $22.68 \pm 1.0$  % alpha-cellulose,  $19.56 \pm 6.2$  % beta-cellulose,  $35.28 \pm 7.5$  % gamma-cellulose and  $22.43 \pm 0.2$  % lignin. While raw sugarcane bagasse contained  $41.01 \pm 4.3$  % alpha-cellulose,  $9.506 \pm 7.2$  % beta-cellulose,  $24.73 \pm 2.7$  % gamma-cellulose and  $24.62 \pm 0.3$  % lignin. The highest delignification yield, hemicellulose removal rate, cellulose recovery and solid yield was observed for spent coffee ground with  $14.60 \pm 2.5$  %,  $22.29 \pm 1.7$  %,  $26.50 \pm 2.8$  % and  $87.07 \pm 0.6$  %, respectively. Furthermore, SEM-EDX, XRD and FTIR analysis had been carried out for the raw and treated biomass to study the impacts brought by pretreatment process in terms of structural morphology composition, crystallinity and functional groups. Various combination of biomass mixture had underwent the organosolv pretreatment to verify the result obtained. It was found the sample (E5) comprised of 50 wt.% SCG and 50 wt.% SB showed the best performance of organosolv pretreatment with the highest delignification yield of  $15.98 \pm 1.4$  %, highest hemicellulose removal rate of  $24.77 \pm 3.9$  % and highest total cellulose recovery of  $24.34 \pm 2.5$  %. Several models had been developed to examine the possible factors that will impact the delignification yield and hemicellulose degradation rate. It was concluded that the higher the delignification yield and hemicellulose removal rate, the higher the cellulose recovery.

## TABLE OF CONTENTS

|   |             |
|---|-------------|
| <b>DECLARATION</b>  | <b>i</b>    |
| <b>APPROVAL FOR SUBMISSION</b>                            | <b>ii</b>   |
| <b>ACKNOWLEDGEMENTS</b>                                   | <b>iv</b>   |
| <b>ABSTRACT</b>   | <b>v</b>    |
| <b>TABLE OF CONTENTS</b>                                  | <b>vi</b>   |
| <b>LIST OF TABLES</b>                                     | <b>ix</b>   |
| <b>LIST OF FIGURES</b>                                    | <b>x</b>    |
| <b>LIST OF SYMBOLS / ABBREVIATIONS</b>                    | <b>xiii</b> |
| <br>  |             |
| <b>CHAPTER</b>  |             |
| <b>1 INTRODUCTION</b>                                     | <b>1</b>    |
| 1.1 Overview of Energy Consumption                        | 1           |
| 1.2 Introduction to Biorefinery                           | 4           |
| 1.3 Biomass for Bioenergy                                 | 5           |
| 1.3.1 Lignocellulosic Biomass as Biorefinery<br>Feedstock | 6           |
| 1.4 Pretreatment of Lignocellulosic Biomass               | 8           |
| 1.4.1 Introduction to Organosolv Pretreatment             | 9           |
| 1.5 Importance of the Study                               | 10          |
| 1.6 Problem Statement                                     | 11          |
| 1.7 Aim and Objectives                                    | 12          |
| 1.8 Scope and Limitation of the Study                     | 13          |
| 1.9 Contribution of the Study                             | 14          |
| 1.10 Outline of the Report                                | 14          |
| <br>  |             |
| <b>2 LITERATURE REVIEW</b>                                | <b>16</b>   |
| 2.1 Lignocellulosic Biomass in Focus                      | 16          |
| 2.1.1 Coconut Husk  | 16          |
| 2.1.2 Spent Coffee Ground                                 | 18          |

|          |  |           |
|----------|--|-----------|
| 2.1.3    | Sugarcane Bagasse                                | 19        |
| 2.2      | Component Structure of Lignocellulosic Biomass   | 20        |
| 2.3      | Chemical Composition of Biomass in Focus         | 23        |
| 2.4      | Overview of Organosolv Pretreatment              | 24        |
| 2.4.1    | Organosolv Pretreatment Factors                  | 26        |
| 2.4.2    | Ethylene Glycol-based Organosolv Pretreatment    | 27        |
| 2.5      | Pretreatment of Lignocellulosic Biomass in Focus | 28        |
| 2.5.1    | Coconut Husk                                     | 28        |
| 2.5.2    | Spent Coffee Ground                              | 29        |
| 2.5.3    | Sugarcane Bagasse                                | 30        |
| 2.6      | Characterisation Analysis of Treated Biomass     | 31        |
| 2.6.1    | Structural and Morphology Change                 | 31        |
| 2.6.2    | Crystallinity Change                             | 33        |
| 2.6.3    | Functional Groups Change                         | 35        |
| 2.6.4    | Thermal Stability Change                         | 36        |
| <b>3</b> | <b>METHODOLOGY AND WORK PLAN</b>                 | <b>38</b> |
| 3.1      | Overview of Methodology                          | 38        |
| 3.2      | Materials and Apparatus                          | 38        |
| 3.2.1    | Materials and Chemicals                          | 39        |
| 3.2.2    | Apparatus and Equipment                          | 39        |
| 3.3      | Biomass Sample Preparation                       | 39        |
| 3.3.1    | Coconut Husk                                     | 39        |
| 3.3.2    | Sugarcane Bagasse                                | 39        |
| 3.3.3    | Spent Coffee Ground                              | 42        |
| 3.4      | Organosolv Pretreatment of Biomass Samples       | 42        |
| 3.5      | Compositional Analysis                           | 43        |
| 3.5.1    | Determination of Solid Recovery                  | 44        |
| 3.5.2    | Cellulose Content Analysis (TAPPI T203 cm-99)    | 44        |
| 3.5.3    | Lignin Content Analysis (TAPPI T222 om-02)       | 48        |
| 3.5.4    | Chemical Component Removal and Recovery Rate     | 50        |

|          |   |           |
|----------|---|-----------|
| 3.6      | Spectroscopic Analysis  | 51        |
| 3.6.1    | Structural Morphology Analysis  | 51        |
| 3.6.2    | X-ray Diffraction (XRD)   | 52        |
| 3.6.3    | Fourier Transformation-infrared (FTIR)                                      | 52        |
| <b>4</b> | <b>RESULTS AND DISCUSSION</b>   | <b>53</b> |
| 4.1      | Organosolv Pretreatment of Pure Biomass Samples                             | 53        |
| 4.1.1    | Compositional Analysis  | 53        |
| 4.1.2    | Scanning Electron Microscopy(SEM) Analysis                                  | 57        |
| 4.1.3    | Energy Dispersive X-ray (EDX) Analysis                                      | 61        |
| 4.1.4    | Fourier Transform-Infrared (FTIR) Analysis                                  | 63        |
| 4.1.5    | X-ray Diffraction (XRD) Analysis  | 69        |
| 4.2      | Organosolv Pretreatment of Biomass Mixture                                  | 72        |
| 4.2.1    | Chemical Compositional Analysis   | 72        |
| 4.2.2    | Structural and Morphology Analysis  | 75        |
| 4.2.3    | FTIR Analysis   | 77        |
| 4.2.4    | XRD Analysis  | 79        |
| 4.3      | Model Development of Organosolv Pretreatment                                | 81        |
| 4.3.1    | Lignin Composition and Delignification Yield                                | 81        |
| 4.3.2    | Hemicellulose Composition and<br>Hemicellulose Removal Rate                 | 82        |
| 4.3.3    | Delignification Yield and Hemicellulose<br>Removal Rate                     | 83        |
| 4.3.4    | Delignification Yield, Hemicellulose Removal<br>Rate and Cellulose Recovery | 84        |
| <b>5</b> | <b>CONCLUSIONS AND RECOMMENDATIONS</b>                                      | <b>86</b> |
| 5.1      | Conclusions   | 86        |
| 5.2      | Recommendations for Future Work   | 87        |
|          | <b>REFERENCES</b>   | <b>89</b> |

**LIST OF TABLES**

|             |  |    |
|-------------|--|----|
| Table 1.1:  | Merits and Demerits of different Generations of Biofuels (Sudhakar et al., 2018)   | 5  |
| Table 2.1:  | The Chemical Composition of Major Components in Lignocellulosic Biomass in Focus   | 24 |
| Table 3.1:  | Materials and Chemicals used in the Experiment                                     | 40 |
| Table 3.2:  | Apparatus and Equipment used in the Experiment                                     | 41 |
| Table 3.3:  | Analytical Instruments used for Characterisation Procedure                         | 41 |
| Table 3.4:  | Run of Experiments   | 43 |
| Table 3.5:  | Preparation Step of Reagents Required for Cellulose Analysis                       | 44 |
| Table 4.1:  | Chemical Composition of Raw and Treated Biomass Samples                            | 56 |
| Table 4.2:  | Chemical Components Recovery and Removal Rate for Various Types of Biomass Samples | 56 |
| Table 4.3:  | Element Quantification in Dried Weight Percent of Biomass Samples by EDX Analysis  | 62 |
| Table 4.4:  | Polymers and Functional Groups of their respective Vibrational Frequencies         | 67 |
| Table 4.5:  | Functional Groups of their respective Vibrational Frequencies                      | 68 |
| Table 4.6:  | Crystallinity Index of Raw and Treated Biomass Samples                             | 69 |
| Table 4.7:  | Chemical Composition of Treated Biomass Mixture                                    | 72 |
| Table 4.8:  | Chemical Components Recovery and Removal Rate of Treated Biomass Mixtures          | 74 |
| Table 4.9:  | Element Quantification of Treated Biomass Mixtures from EDX Analysis               | 74 |
| Table 4.10: | Crystallinity Index of Raw and Treated Biomass Mixtures                            | 79 |

## LIST OF FIGURES

|             |   |    |
|-------------|---|----|
| Figure 1.1: | Global Energy Consumption Statistic by Regions from year 1990 to 2018 (Top) and Global Energy Consumption breakdown by Energy in 2018 (Bottom) (Enerdata, 2019)   | 1  |
| Figure 1.2: | Primary Energy Consumption by Source in Malaysia from year 1965 to 2018, measured in terawatt-hours (TWh) (Ritchie and Roser, 2018)                               | 2  |
| Figure 1.3: | Carbon Dioxide (CO <sub>2</sub> ) Concentration in the Atmosphere (ppm) and Annual Emission (billion tons) from year 1750 to 2020 (Lindsey, 2020)                 | 3  |
| Figure 1.4: | Classification of Lignocellulosic Biomass by Sources (Zabed et al., 2016)   | 7  |
| Figure 1.5: | Schematic Pretreatment Process of Lignocellulosic Material (Huzir et al., 2018)   | 8  |
| Figure 1.6: | The Classification of Pretreatment Method (Baruah et al., 2018)   | 9  |
| Figure 2.1: | Global Coconut Production (in Tons) in 2018 (Burton, 2018)  | 16 |
| Figure 2.2: | Cross Section of a Coconut Fruit (Rajah, 2018)  | 17 |
| Figure 2.3: | Schematic of the Anatomy of a Coffee Cherry (Zarrinbakhsh et al., 2016)   | 18 |
| Figure 2.4: | Raw Sugarcane Bagasse (Romanov, 2020)   | 20 |
| Figure 2.5: | The Structural Organisation of Plant Cell Wall and the Distribution of Components (Anwar, Gulfraz and Irshad, 2014)   | 21 |
| Figure 2.6: | The Chemical Structure of Cellulose Component in Plant Cell Wall (Baruah et al., 2018)  | 21 |
| Figure 2.7: | The Chemical Structure of Hemicellulose Component in Plant Cell Wall (Baruah et al., 2018)  | 22 |
| Figure 2.8: | The Chemical Structure of Lignin Component in Plant Cell Wall (Baruah et al., 2018)   | 23 |
| Figure 2.9: | Mechanism of Cleavage of $\alpha$ - (Top), $\beta$ - and $\gamma$ -ether Linkages (Bottom) in Acid-catalysed Ethanol Pretreatment of Biomass (Zhang et al., 2016) | 26 |

|              |  |    |
|--------------|--|----|
| Figure 2.10: | SEM images of (a) Raw CH and (b) AAG, S/L 1:30, 60 min Treated CH under 500× magnification (Ebrahimi et al., 2017)   | 32 |
| Figure 2.11: | SEM images of (a) Raw SCG and (b) NaOH, 110 °C, 15 min treated SCG under 1000× magnification (Wongsiridetchai et al., 2018)  | 32 |
| Figure 2.12: | SEM images of (a) Raw SB and (b) 25 vol.% Aqueous Ethanol Treated SB under 3000× magnification (Nantnarphirom et al., 2017)  | 33 |
| Figure 2.13: | X-ray Diffraction Spectra of a Cellulose Crystallinity by using Peak Height Method (Chandrasaha, Rajamane and Jeyalakshmi, 2014)   | 34 |
| Figure 2.14: | X-ray Crystallography of Raw CH and NaOH treated CH (Chandrasaha, Rajamane and Jeyalakshmi, 2014)  | 34 |
| Figure 2.15: | FTIR spectrum of raw CH and AAG treated CH (Ebrahimi et al., 2017)   | 35 |
| Figure 2.16: | (A) TG and (B) DTG distribution of Raw and Treated SB (Zhang et al., 2018c)  | 36 |
| Figure 3.1:  | Flowchart of the Research Methodology  | 38 |
| Figure 3.2:  | Colour Changes of Mixture during Back Titration  | 46 |
| Figure 3.3:  | Settling of Beta-Cellulose Precipitate after 24 hours  | 47 |
| Figure 3.4:  | Reflux Condensation of Lignin Solution   | 49 |
| Figure 4.1:  | Chemical Components Recovery and Removal Rate for Various Types of Biomass Samples   | 55 |
| Figure 4.2:  | SEM images of CH (A1) Raw Fibre-500× (B1) Raw Fibre-1000× (C1) Raw Powder-1000× (D1) Raw Powder-2000× (A2) Treated Fibre-500× (B2) Treated Fibre-1000× (C2) Treated Fibre-1000× (D2) Treated Fibre-2000× | 58 |
| Figure 4.3:  | Surface Morphology of SCG (A1) Raw SCG-500× (B1) Raw SCB-1000× (C1) Raw SCG-2000× (A2) Treated SCG-500× (B2) Treated SCG-1000× (C2) Treated SCG-2000×  | 60 |
| Figure 4.4:  | SEM images of SB (A1) Raw Fibre-500× (B1) Raw Fibre-1000× (C1) Raw Fibre-2000× (A2) Treated Fibre-   |    |

|              |   |    |
|--------------|---|----|
|              | 500× (B2) Treated Fibre-1000× (C2) Treated Fibre-2000×                                | 61 |
| Figure 4.5:  | FTIR Spectrum of Raw and Treated Biomass Samples                                      | 63 |
| Figure 4.6:  | FTIR Spectrum of Raw and Treated Coconut Husk   | 64 |
| Figure 4.7:  | FTIR Spectrum of Raw and Treated Spent Coffee Ground                                  | 65 |
| Figure 4.8:  | FTIR Spectrum of Raw and Treated Sugarcane Bagasse                                    | 66 |
| Figure 4.9:  | Diffractiongram of Raw and Treated Coconut Husk                                       | 71 |
| Figure 4.10: | Diffractiongram of Raw and Treated Spent Coffee Ground                                | 71 |
| Figure 4.11: | Diffractiongram of Raw and Treated Sugarcane Bagasse                                  | 71 |
| Figure 4.12: | SEM images of Treated Biomass Mixtures under Magnification ranging from 400× to 1000× | 77 |
| Figure 4.13: | FTIR Spectrum of Treated Biomass Mixtures   | 78 |
| Figure 4.14: | Diffractiongrams of Treated Biomass Mixtures  | 80 |
| Figure 4.15: | Relationship between Lignin Composition (%) and Delignification Yield (%)             | 82 |
| Figure 4.16: | Relationship between Hemicellulose Composition (%) and Hemicellulose Removal Rate (%) | 83 |
| Figure 4.17: | Relationship between Delignification Yield (%) and Hemicellulose Removal Rate (%)     | 84 |
| Figure 4.18: | Relationship between Delignification Yield (%) and Cellulose Recovery (%)             | 85 |
| Figure 4.19: | Relationship between Hemicellulose Removal Rate (%) and Cellulose Recovery (%)        | 85 |

## LIST OF SYMBOLS / ABBREVIATIONS

|           |  |
|-----------|--|
| $A$       | Volume of pulp filtrate used in the oxidation, mL          |
| $A_{215}$ | Absorbance at 215 nm                                       |
| $A_{280}$ | Absorbance at 280 nm                                       |
| $C$       | Total Cellulose Content, g                                 |
| $C_f$     | Total Cellulose Content after treatment, g                 |
| $C_i$     | Total Cellulose Content before treatment, g                |
| $D$       | Dilution ratio   |
| $G$       | guaiacyl lignin unit                                       |
| $H$       | Total Hemicellulose Content, g                             |
| $H_f$     | Total Hemicellulose Content after treatment, g             |
| $H_i$     | Total Hemicellulose Content before treatment, g            |
| $I_{002}$ | Maximum peak intensity of the 002 lattice reflection       |
| $I_A$     | Valley intensity between the peak of the 002 and 001 plane |
| $K$       | Weight of dried Klason Lignin, g                           |
| $L$       | Total Lignin content, g                                    |
| $L_i$     | Total Lignin Content before treatment, g                   |
| $L_f$     | Total Lignin Content after treatment, g                    |
| $N$       | Normality of the ferrous ammonium sulphate solution, N     |
| $S$       | syringyl lignin unit                                       |
| $V_1$     | Titration Volume of the pulp filtrate, mL                  |
| $V_2$     | Blank Titration Volume of alpha-cellulose analysis, mL     |
| $V_3$     | Titration Volume of gamma-cellulose solution, mL           |
| $V_4$     | Blank Titration Volume of gamma-cellulose analysis, mL     |
| $V_F$     | Filtrate Volume, L   |
| $W$       | Weight of dried sample, g                                  |
| $\alpha$  | alpha linkage  |
| $\beta$   | beta linkage   |
| $\gamma$  | gamma linkage  |

|   |   |
|---|---|
| AAG   | acidified aqueous glycerol              |
| ATR   | Attenuated Total Reflectance            |
| Au  | aurum/gold                              |
| C   | carbon                                  |
| CaO   | calcium oxide                           |
| CH  | coconut husk                            |
| (CH <sub>2</sub> OH) <sub>2</sub>             | ethylene glycol                         |
| C <sub>2</sub> H <sub>4</sub> Cl <sub>2</sub> | 1,2-dichloroethane                      |
| C <sub>2</sub> H <sub>5</sub> OH              | ethanol                                 |
| Cl  | chlorine                                |
| CO <sub>2</sub>                               | carbon dioxide gas                      |
| CrI   | crystallinity index, %                  |
| DTG   | Derivative Thermogravimetric Graph      |
| E   | experiment number                       |
| EDX   | Energy Dispersive X-ray Spectroscopy    |
| EG  | ethylene glycol                         |
| EIA   | Energy Information Administration       |
| etc.  | et cetera                               |
| FeCl <sub>3</sub>                             | iron (III) chloride                     |
| FTIR  | Fourier Transform-infrared Spectroscopy |
| G   | generation of biofuel                   |
| GHG(s)  | greenhouse gas(es)                      |
| H   | <i>p</i> -hydroxyphenyl lignin unit     |
| HCl   | hydrogen chloride                       |
| H <sub>3</sub> PO <sub>4</sub>                | phosphoric acid                         |
| H <sub>2</sub> SO <sub>4</sub>                | sulphuric acid                          |
| K <sub>2</sub> Cr <sub>2</sub> O <sub>7</sub> | potassium dichromate                    |
| LCB(s)  | lignocellulosic biomass(es)             |
| NaOH  | sodium hydroxide                        |
| NH <sub>3</sub>                               | ammonia                                 |
| M   | model                                   |
| Mg  | magnesium                               |
| O   | oxygen                                  |
| ppm   | parts per million                       |

|                  |                              |
|------------------|------------------------------|
| R <sup>2</sup>   | coefficient of determination |
| S                | sulphur                      |
| SB               | sugarcane bagasse            |
| SCG              | spent coffee ground          |
| SEM              | Scanning Electron Microscopy |
| Si               | silicon element              |
| SiO <sub>2</sub> | silica                       |
| S/L              | solid to liquid ratio        |
| TG               | thermogravimetric            |
| TGA              | Thermogravimetric Analysis   |
| TWh              | terawatt-hours               |
| UV-Vis           | Ultraviolet Spectrometer     |
| XRD              | X-ray Diffractometer         |

## CHAPTER 1

### INTRODUCTION

#### 1.1 Overview of Energy Consumption

Energy is indispensable in almost all aspects of life across the globe. It plays a vital role in ecological maintenance, human civilisation, and well-being of life (Ozturk et al., 2017). The major energy resources in the world are mostly retrieved from fossil fuels, particularly the non-renewable hydrocarbon sources. Crude oil is the dominant energy source for the transportation and production of materials in the world, followed by coal and natural gas as illustrated in Figure 1.1.

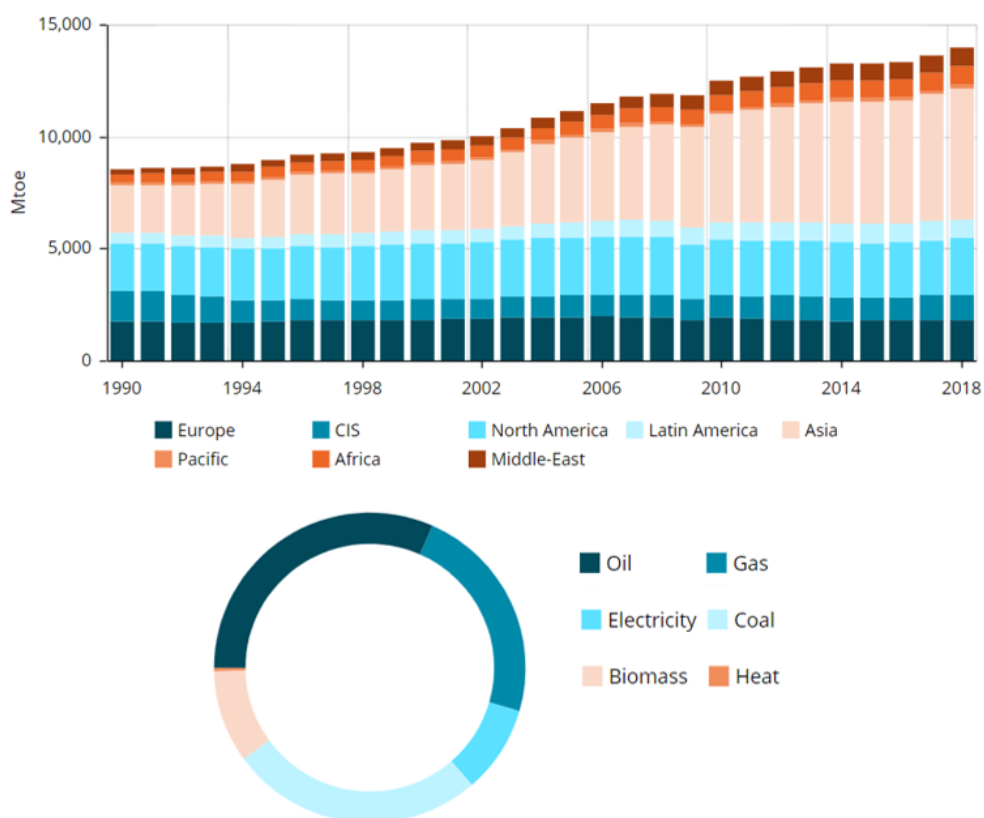


Figure 1.1: Global Energy Consumption Statistic by Regions from year 1990 to 2018 (Top) and Global Energy Consumption breakdown by Energy in 2018 (Bottom) (Enerdata, 2019)

About 13 million m<sup>3</sup> of oil is used daily and this is expected to rise by 2030 to approximately 18.4 million m<sup>3</sup> per day (Ahorsu, Medina and Constantí, 2018). China, the world's largest energy consumer since 2009, is also ranked for the first in coal consumption, accounting for about 379 % of the world's total consumption. More than 1 billion tons of coal is exploited for power generation and fulfilling strong industrial demand in China (Worldometer, 2017). While the worldwide natural gas consumption is driven by the United States, especially for new gas-fired plants (+15 gigawatts) and buildings, with an overall consumption of 848 billion m<sup>3</sup> in 2018 (Enerdata, 2019). Same goes to Malaysia, the utilisation of renewable energy is still lacking as shown in Figure 1.2, due to the underdeveloped technology and low participation of local companies (Bernama, 2019).

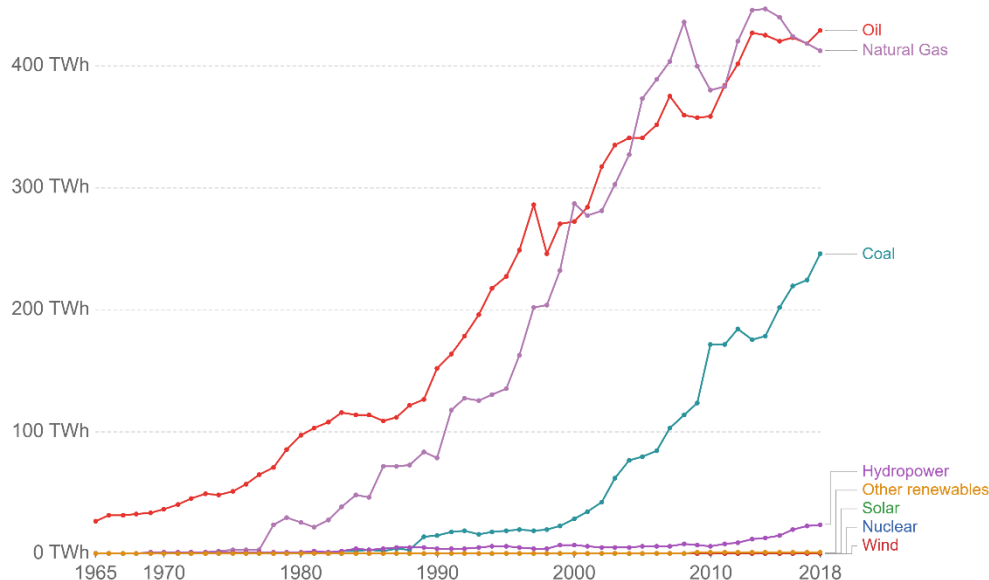


Figure 1.2: Primary Energy Consumption by Source in Malaysia from year 1965 to 2018, measured in terawatt-hours (TWh) (Ritchie and Roser, 2018)

The increase of global energy demand on these finite natural resources is giving rise to the energy crisis. Besides, the excessive utilisation of fossil-fuel-driven energy has led to the serious environmental issues including but not limited to air pollution, water source contamination, greenhouse effect and global warming (Terán Hilaes et al., 2017). The increase concentration of greenhouse gas (GHG), especially carbon dioxide (CO<sub>2</sub>) in the atmosphere

causes the rise in the global average temperature and leads to the climate change. The CO<sub>2</sub> concentration is escalating drastically in past ten years and recorded the highest at 414.7 ppm in 2019 May (Lindsey, 2020). Based on Figure 1.3, the total emission of CO<sub>2</sub> is estimated to be more than 36 billion tons in 2020 (Lindsey, 2020). The increase of environmental pollution together with the dwelling of fossil-fuel-driven energy have given rise to the concern of sustainable energy around the world (Zhao, Cheng and Liu, 2009).

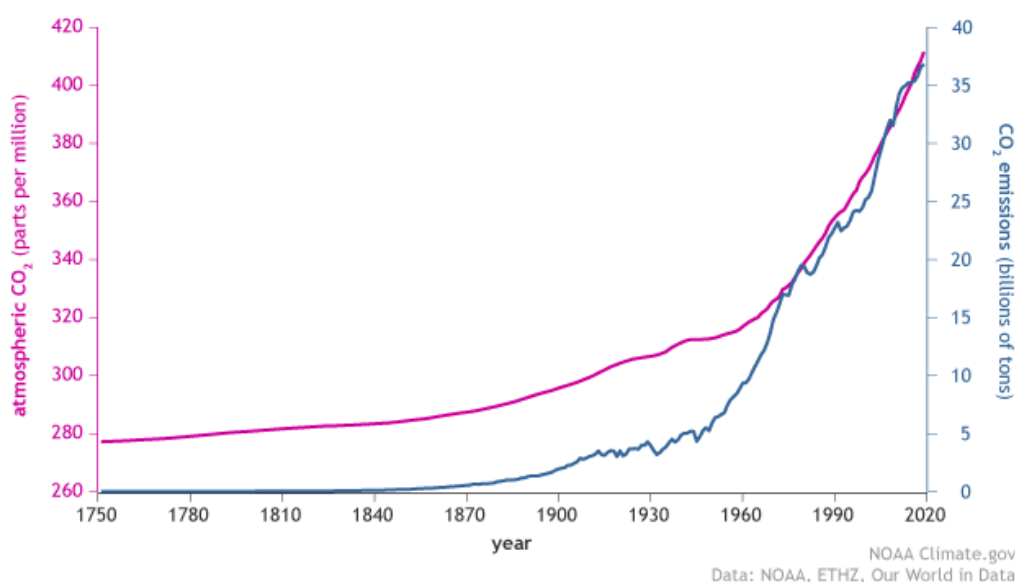


Figure 1.3: Carbon Dioxide (CO<sub>2</sub>) Concentration in the Atmosphere (ppm) and Annual Emission (billion tons) from year 1750 to 2020 (Lindsey, 2020)

Therefore, it is essential to discover sustainable energy which is readily available and environmental friendly. It must be a renewable energy with little or no GHGs emission, such as solar energy, wind energy, hydropower, bioenergy, etc. Among the renewable resources, biomass is identified as a reliable source of green energy to replace fossil fuels due to its renewable basis and potential to diminish the social and environmental impacts brought by finite stocks. Recently, the “waste to wealth” notion that converts low value biomass into bioenergy which can be used either directly or in the form of biofuel has drawn the world’s attention due to its strong financial potential (Ozturk et al., 2017).

## 1.2 Introduction to Biorefinery

The concept of biorefinery has successfully aroused the interest of many countries to process the biomass into a spectrum of marketable green products such as biofuels, value-added fine chemicals, and economical energy sources from enzymatic hydrolysis and biological decomposition (Sidiras, 2015). For instance, bioethanol is regarded as a clean fuel that is commonly produced by cellulosic biomass to run the automobiles without modification of car engine (Kim and Dale, 2004). Bioenergy production especially bioethanol is expected to increase due to the increase of energy demand resulted from the population growth.

The development of bioenergy could be an efficient approach to decrease carbon footprint and reduce the impacts brought by burning of fossil fuels (Lalman, Shewa and Gallagher, 2016). In addition, the production of biofuel from renewable energy will promote the circular economy with better use of land and improve the agricultural growth. Recently, attempts have been made to utilise biomass in biorefinery sector to produce biofuels which could bring positive effects to the economy, technology, society and environment of the planet. These biofuels are categorised into four generations based on the biorefinery feedstock and processing technology.

The first generation (1G) biofuel is conventional biofuel that generated by commercially available technique and readily fermentable biomass feedstock such as wheat, sugarcane, corn, soybeans, rapeseed, palm oil, etc. Second generation (2G) biofuels are generated primarily from lignocellulosic biomass (LCB) which including wheat straws, corn stovers, sawdust and bagasse that require pretreatment prior to fermentation process (Lalman, Shewa and Gallagher, 2016). The 2G biofuel has eliminated the “food versus fuel” drawback of 1G biofuels by employing non-food crops biomass. Third generation (3G) biofuel is essentially bio-oil produced from marine based biomass such as microalgae and macroalgae (seaweed) which do not compete for land use. Fourth generation (4G) biofuel aims to produce super-clean carbon negative biofuels by implying carbon sequestration concept in raw material and process technology (Sudhakar et al., 2018). Table 1.1 compares the benefits and limitations of different generation of biofuels.

Table 1.1: Merits and Demerits of different Generations of Biofuels (Sudhakar et al., 2018)

| <b>Type of Biofuel</b> | <b>Advantages</b>  | <b>Disadvantages</b>   |
|------------------------|--|--|
| <b>1G</b>              | <ul style="list-style-type: none"> <li>▪ Direct and well-developed technology</li> <li>▪ Easy to scale up</li> <li>▪ Cost-competitive process</li> </ul>               | <ul style="list-style-type: none"> <li>▪ Compete with food supply</li> <li>▪ Occupied large land area for crops cultivation</li> <li>▪ Moderate yield</li> </ul> |
| <b>2G</b>              | <ul style="list-style-type: none"> <li>▪ Non-food crops</li> <li>▪ Abundant sources</li> <li>▪ Environmental sustainable</li> <li>▪ Reduce carbon footprint</li> </ul> | <ul style="list-style-type: none"> <li>▪ Difficulty in industry scale up</li> <li>▪ High capital cost</li> <li>▪ Not widely established</li> </ul>               |
| <b>3G</b>              | <ul style="list-style-type: none"> <li>▪ High biomass yield</li> <li>▪ Less energy input</li> <li>▪ Widespread availability</li> <li>▪ Carbon neutral</li> </ul>       | <ul style="list-style-type: none"> <li>▪ Low energy output</li> <li>▪ Pilot-scale in developing</li> </ul>   |
| <b>4G</b>              | <ul style="list-style-type: none"> <li>▪ Targeted carbon negative</li> <li>▪ High production rate</li> </ul>   | <ul style="list-style-type: none"> <li>▪ Laboratory scale/primary stage of research</li> </ul>   |

Currently, 2G biofuel production is considered as the most favourable approach to produce biofuel. It has solved the food and energy security problem by utilising LCB to replace edible food as biorefinery feedstock. Cellulosic ethanol, Fischer-Tropsch diesel and biomethanol are examples of 2G biofuel which can yield greater energy output with lower environmental impacts than fossil fuels. The top three cellulosic ethanol installed capacity is the United States, China and Canada. It is also important to mention that, Malaysia had implemented the mandatory application of B5 biodiesel since 2014. The B5 biodiesel is a mixture of 5 % palm methyl ester with diesel (Ahorsu, Medina and Constantí, 2018).

### **1.3 Biomass for Bioenergy**

Biomass refers to any organic matter that originates from living or non-living sources and is available on a renewable basis (Ahorsu, Medina and Constantí, 2018). The common types of biomass are agricultural crops and wastes, forestry

wood products, industrial residues, municipal solid wastes, human and animal manure. According to the latest report of Energy Information Administration (EIA), biomass contributes 46 % of the total renewable energy consumption. The consumption of bioenergy is believed to give rise in economic growth, especially for developing countries. It is able to reduce the foreign dependency on oil and beneficial to the rural employment, thus decreasing the poverty rate (Bildirici and Özaksoy, 2018).

Malaysia is rich with agriculture biomass owing to its favourable weather for agriculture sector and the presence of thick tropical rainforest for timber industry, producing nearly 168 million tons of biomass including oil palm waste, coconut fibres, timber residues and sugarcane bagasse. It has been estimated that the country can generate more than 2.4 gigawatts of biomass and 0.41 gigawatts of biogas. By assuming the utilisation of an extra 22 million tons oil palm biomass in 2020 with a higher value creation, this could significantly contribute to improve Malaysia's economy, proposed by The National Biomass Strategy 2020 (Ozturk et al., 2017).

### **1.3.1 Lignocellulosic Biomass as Biorefinery Feedstock**

Although there are various types of biomass can be used in biofuel production, the available amount of biomass must be sufficient to ensure sustainable bioenergy conversion and the source of biomass must not compete with food crops. Thus, production of biofuels from non-grain feedstock, especially lignocellulosic biomass (LCB) has become a focal point in many nations (Zhao, Cheng and Liu, 2009). This is represented by 2G biofuel production as per mentioned.

LCB is the most chosen biorefinery feedstock as it can be obtained abundantly in nature with low production cost (Zhao, Cheng and Liu, 2009). Another advantage is due to its high carbohydrate content which can generate the fermentable sugars necessary for enzymatic hydrolysis in bioethanol production. Agricultural residues and forestry waste are the most abundantly found LCB. The dried stem of food crops such as soya, rice, wheat, corn, barley and sorghum are inappropriate for human consumption and are mostly categorised as agro-waste. Besides, LCB could be obtained from dedicated whole plant, industrial wastes and municipal solid wastes. LCB is further

classified into hardwoods, softwoods and grasses material (De Bhowmick, Sarmah and Sen, 2018), as shown in Figure 1.4.

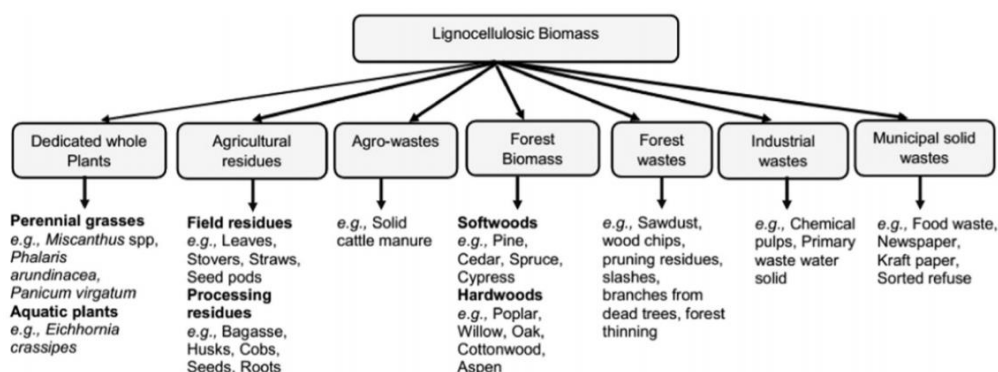


Figure 1.4: Classification of Lignocellulosic Biomass by Sources (Zabed et al., 2016)

Typically, most of the LCB contains about 40 – 50 % cellulose, 20 – 30 % of hemicellulose, and 10 – 25 % lignin content (Nantnarphirom et al., 2017). High lignin content LCB such as coconut shell, palm kernel and drupe fruit endocarps of olive are potential feedstock to provide energy as comparable to coal (Welker et al., 2015). Whereas, the agro and forestry LCB that composed of mainly carbohydrate component are suitable for bioethanol production via advanced enzymatic hydrolysis and fermentation (Ahorsu, Medina and Constantí, 2018).

Hydrolysis of LCB will produce various sugar monomers that are extremely valuable for biofuel production such as, biodiesel, bioethanol and biogas, organic acids, aldehydes and phenols. However, LCB is classified as a recalcitrance feedstock because it is resistant to chemical breakdown and biodegradation. The natural properties of LCB with high crystalline structure of cellulose, strong degree of lignification and complexity of cell wall constituents have resulted in the inhibition of carbohydrates hydrolysis process (Amore, Ciesielski and Lin, 2016). The formation of plant cell wall with holocellulose attached together by lignin leads to the low accessibility of microcrystalline cellulose fibres and thus reducing the efficiency of the cellulase chemical activities (Baruah et al., 2018). Therefore, several pretreatment methods have to be incorporated to overcome the biomass recalcitrance property.

#### 1.4 Pretreatment of Lignocellulosic Biomass

The main role of biomass pretreatment is to modify or suppress the structural and compositional impediments to enzymatic saccharification and enhance fermentable sugars yield from cellulose and hemicellulose components. The reaction mechanism of organosolv pretreatment is illustrated in Figure 1.5.

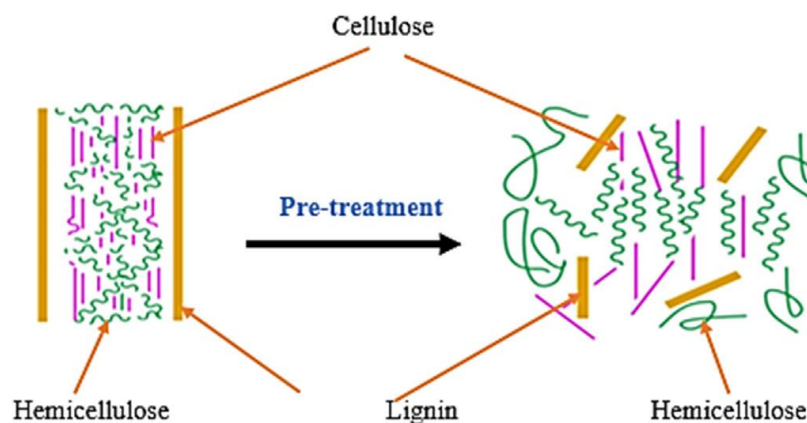


Figure 1.5: Schematic Pretreatment Process of Lignocellulosic Material (Huzir et al., 2018)

An effective pretreatment must be able to decrease the particle size of biomass, and reduce the formation of degradation by-product that will hinder the growth of fermentative microorganisms. Furthermore, pretreatment is important to minimise feedstock consumption rate, energy input and catalyst usage throughout the biofuel production. Hence, it will help to lower down the downstream processing cost, operating cost and capital cost indirectly (De Bhowmick, Sarmah and Sen, 2018).

Biomass pretreatment can be performed in a variety of methods as shown in Figure 1.6. Physical pretreatment is aimed to increase the specific surface area by reducing the particle size of biomass. It is also helpful in decreasing degree of polymerisation and decrystallisation. Chemical pretreatment is the most common method used for delignification of lignocellulosic materials and to recover as much as possible carbohydrate monosaccharides from cellulose and hemicellulose polymers by optimising the chemical reagents. Physicochemical pretreatment is making benefits of both physical and chemical pretreatments. Biological or microbial pretreatment involves no chemicals but utilises microbial degradation of fungi and bacteria

to alter the fundamental properties of biomass. Among the pretreatment processes, organosolv pretreatment of LCB by using organic solvent is identified as one of the most reliable delignification methods that is widely applied.

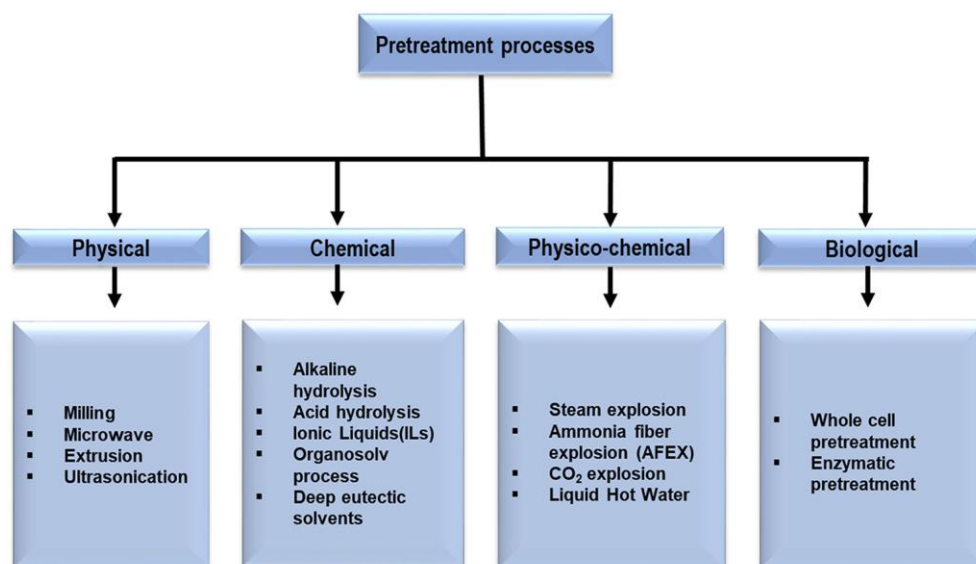


Figure 1.6: The Classification of Pretreatment Method (Baruah et al., 2018)

#### 1.4.1 Introduction to Organosolv Pretreatment

Organosolv pretreatment was originally developed as a greener pulping technique in the pulp and paper industries. The development of organosolv pretreatment was driven by the need to tackle the environmental problems due to sulphur containing wastes from traditional kraft and sulphite pulping techniques. It also aims to increase production yield and create more economically viable options (Nitsos and Rova, 2018). Organosolv pulping begins from 1893 and has been used as a pretreatment method for delignification and production of other valuable coproducts like acetone, butanol, ethanol and biogas production (Salapa et al., 2017).

Organosolv pretreatment can be conducted by using different kinds of organic or aqueous-organic solvents with or without a catalyst (Salapa et al., 2017). The process can be improved by adding catalyst to either decrease the pretreatment temperature or enhance the delignification yield. Normally acids (HCl, H<sub>2</sub>SO<sub>4</sub>, and H<sub>3</sub>PO<sub>4</sub>), bases (CaO, NaOH and NH<sub>3</sub>) and some salts are used as catalyst. A broad variety of organic solvents such as ethylene glycol, ethanol,

methanol, acetone, peracetic acid, organic acid, and tetrahydrofurfuryl are blended with water to treat various types of LCB.

The cooking of LCB in an organic solvent leads to the deconstruction and solvation of both lignin and hemicellulose content during pretreatment process. Organosolv pretreatment will produce high purity cellulose with minor degradation, high-quality lignin solid precipitate and a hemicellulose solution (Nitsos and Rova, 2018). High-quality lignin can be isolated from this process as a valuable by-product for different industrial applications. Additionally, organic solvent can be easily recovered by distillation and recycled back for pretreatment process (Baruah et al., 2018). Moreover, organosolv pretreatment usually has less modification on the cellulose structure, but it depolymerises the cellulose and removes amorphous lignin and hemicellulose, resulting in the changes of crystallinity (Park, Kim and Kim, 2018)

From the environmental aspect, the organosolv pretreatment has successfully met some sustainable process requirements. It decreases the concentration and quantity of dangerous chemicals used in the traditional paper pulping processes, and excludes the neutralisation of process streams. It reduces the quantity of wastes produced from the reaction because lignin is obtained as a value-added product instead of a waste generated from the biofuel industries. Furthermore, several organic solvents such as methanol and ethanol, can be acquired from renewable sources which improves their application to sustainable production of biofuels (Zhang et al., 2016). It also enables the manufacturing of bio-based molecules that could be the raw material for natural or biodegradable resins, polymer and many others, compared to their fossil-based counterparts (Nitsos and Rova, 2018).

However, the recovery of organic solvents is an energy intensive process. Besides, most of the organic solvents are extremely flammable and volatile that leads to the pretreatment to be carried out under specially controlled conditions (Baruah et al., 2018).

## **1.5 Importance of the Study**

The research studies based on the organosolv pretreatment of LCB have been proven to have a significant contribution to biorefinery field. Since it means to produce bioenergy that will probably replace the use of non-renewable energy.

Organosolv pretreatment is preferable over the other pretreatment methods because it causes lesser negative impacts on the cellulose component of LCB and enables high-quality lignin isolation for other profitable end use (Zhao, Cheng and Liu, 2009).

In addition, a mathematical model is established based on the results obtained from the experiment, which including the chemical compositions, delignification yield, hemicellulose removal rate, cellulose recovery rate, etc. A mathematical model is important in providing a framework for the research conduction and giving direction for the establishment of systems and the completion of work. The well-developed model will be able to answer a wide range of research questions. Thus, it is deemed as an effective technique to assist researchers to relate more precisely to the fact (Mahmood and Shafique, 2010).

Moreover, it is advantageous in allowing the researchers to forecast things that have never been discovered. Hence, providing a direction for them to make future planning on the particular investigation. For instance, the pretreatment result of an undiscovered LCB can be identified based on its chemical compositions and the organosolv pretreatment efficiency could be determined, as long as the data insert is within the boundary set. Hence, the suitability of the LCB as a 2G biofuel feedstock could be identified based on the efficiency of organosolv pretreatment.

Besides, considering that the organosolv pretreatment is one of the most expensive processing step in biorefinery production, the use of model to obtain the result for other undiscovered LCBs would definitely help to decrease the costs and risks of the process. Furthermore, this method requires very little of time and resources, and can be used to test as much as scenario if it is built within a broad range of hypothesis, without undergoing dozens of experiments and steps to collect sufficient data to answer a question with certainty (Duzevik, 2017).

## **1.6 Problem Statement**

A desired mathematical model of organosolv pretreatment is required to determine the delignification yield, hemicellulose removal rate and cellulose recovery of coconut husk, spent coffee ground and sugarcane bagasse. In the previous research, the model is lacking of sensitivity for its result. The

sensitivity of the model depends on one or more input variables within the specific boundary (Abbott, 2015). In this study, the lignin and hemicellulose composition of LCBs represent the independent variables, while the dependent variables are the chemical components removal and recovery rates.

The experiment is carried out under the same organosolv pretreatment operating conditions. The existing model consists of narrow range of input value, causing the result is limited within the boundaries set because the types of biomass chosen in the previous study consists of a small discrepancy in term of their cellulose, hemicellulose and lignin content. Therefore, the LCBs which have a great difference in chemical component percentage are proposed for current study to broaden the range of input data. Thus, the shortlisted LCBs are coconut husk, spent coffee ground and sugarcane bagasse, which is rich of lignin, hemicellulose and cellulose content, respectively. Hence, the mathematical model is able to be applied for a wider variety of biomass in future.

The research on the utilisation of organic solvents to LCB pretreatment has progressed significantly in recent years, but extensive reviews describing organosolv pretreatment are still limited (Zhang et al., 2016). Most of the investigations were done based on a specific organic solvent on a single type of biomass. The pretreatment efficiency is dependent on several parameters set while conducting the experiment, such as temperature, contact time, concentration of pretreatment solvent and ratio of organic solvent to water. Since organosolv pretreatment will have a considerable effect on the economics of biofuels production, it will become feasible if the methodology for pretreatment process is standardised for all kind of biomass. Hence, this study is mainly focusing on the same experimental procedure to treat coconut husk, spent coffee ground and sugarcane bagasse, and the efficiency of organosolv pretreatment is determined.

## **1.7 Aim and Objectives**

This research study is aimed to develop a model of organosolv pretreatment for various types of biomass with the following objectives:

- (i) To analyse the cellulose, hemicellulose and lignin content of coconut husk, spent coffee ground, sugarcane bagasse before and after the organosolv pretreatment.

- (ii) To characterise the chemical and physical properties of coconut husk, spent coffee ground, sugarcane bagasse before and after the organosolv pretreatment.
- (iii) To design mathematical model of organosolv pretreatment to determine the relationship between chemical compositions, delignification yield, hemicellulose removal rate and cellulose recovery based on the experimental results obtained.
- (iv) To determine the other possible factors that will affect the efficiency of organosolv pretreatment.

### **1.8 Scope and Limitation of the Study**

A model is an abstraction of an actual situation or object, but it may appear much less complicated than reality itself. To develop a complete model, all the aspects of reality that is being investigated must be taken into account. However, despite how complex of the model is, it is impossible to include all the variables that may influence the outcomes (Rogers, 2012). Thus, the models are always constrained by basic assumptions, uncertainties and structures which can compromise to its reliability, and lead to incorrect conclusions (National Research Council, 2007).

In this research, similar methodology from the study of Chin et al. (2019) is applied to coconut husk, spent coffee ground and sugarcane bagasse to investigate the cellulose recovery, lignin and hemicellulose removal rates after organosolv pretreatment process. The model is beneficial in forecasting the efficacy of organosolv pretreatment, but it is constrained by the pretreatment conditions and the biomass types. The constraints of mathematical model are emphasised by the truth that models typically are not full depictions. Indeed, the result generated by the model cannot be the perfect representation of experiment results. In fact, in attempting to understand an object or system completely, several models, each on behalf of a section of the object or system are required. Collectively, the models are potential to provide a more complete representation, or at least a more comprehensive understanding of the real object or system (Rogers, 2012).

The present study focuses on the organosolv pretreatment of coconut husk, spent coffee ground, and sugarcane bagasse by using water-ethylene

glycol solvent (30 v/v%) at 80 °C for 40 minutes, with solid to liquid ratio of 1:20. The solid yield and compositional analysis of biomass samples will be done before and after the pretreatment process. The alpha-, beta- and gamma-cellulose and lignin content were determined according to TAPPI T203 cm-99 and TAPPI T222 om-02 analysis, respectively. Furthermore, characterisation instruments including Scanning Electron Microscopy (SEM), Energy Dispersive X-ray Spectroscopy (EDX), Fourier Transform Infrared Spectroscopy (FTIR) and X-ray Diffractometer (XRD) will be employed to give fundamental insight into the impacts that contributed by organosolv pretreatment process on biomass samples. Mathematical models are established to determine the relationship between chemical compositions, delignification yield, hemicellulose removal rate and cellulose recovery based on the experimental results obtained. Similar procedures of experiment were repeated on the different combination of biomass mixtures to verify the accuracy of the model developed.

### **1.9 Contribution of the Study**

This study provides a fundamental insight in the effects of ethylene glycol pretreatment on coconut husk, spent coffee ground and sugarcane bagasse under 80 °C for 40 minutes, with solid to liquid ratio of 1:20. Mathematical models are developed to investigate the relationships between chemical compositions, delignification yield, hemicellulose removal rate and cellulose recovery. It also means to predict the efficiency of organosolv pretreatment for undiscovered LCB in future. This study will also offer a chance to explore the other possible factors that will affect the efficacy of ethylene glycol-based organosolv pretreatment. Besides, the interaction of various types of biomass could be determined by having different proportion of biomass mixture in organosolv pretreatment. The research study related to biorefinery process based on renewable feedstock (LCB) is important to minimise GHGs emissions and dependency of fossil fuel.

### **1.10 Outline of the Report**

The general introduction of energy consumption, biorefinery, lignocellulosic biomass and organosolv pretreatment were outlined in Chapter 1. In the Chapter

2 of this report, a comprehensive literature review on the coconut husk, spent coffee ground and sugarcane bagasse, reaction mechanism of organosolv pretreatment and preliminary results of treated biomass samples were discussed extensively. The methodology of the experiment conducted for ethylene glycol pretreatment, chemical composition analysis and spectroscopic characterisation were explained accordingly in Chapter 3. Subsequently, the pretreatment results for pure biomass samples and biomass mixtures were examined and discussed in Chapter 4. The investigation of models developed was presented in the last part of Chapter 4. Lastly, the achievements and fulfilments were concluded based on the results obtained, and recommendations were suggested to improve the research framework in the future study.

## CHAPTER 2

### LITERATURE REVIEW

#### 2.1 Lignocellulosic Biomass in Focus

Malaysia produces various types of lignocellulosic biomass with most of them could be a potential candidate for biorefinery feedstock. In this study, the selection of LCB prior to organosolv pretreatment is based on their availability in Malaysia and distinction in the major chemical components. Thus, the shortlisted biomass samples are coconut husk, spent coffee ground and sugarcane bagasse. Coconut husk and sugarcane bagasse are common agricultural wastes that can be found easily in the local market. Whereas, spent coffee ground can be obtained from the café and western restaurant. Furthermore, coconut husk, spent coffee ground and sugarcane bagasse are rich in lignin, hemicellulose and cellulose components, respectively.

##### 2.1.1 Coconut Husk

Coconut (*Cocos nuciferas L.*) is one of the most widely planted crops in tropic and subtropical zone countries with a worldwide coconut production of around 67 million tons (Shahbandeh, 2020). Indonesia represents the largest coconut producer with an annual productivity rate of 18.3 million tons, followed by the Philippines, India, Brazil and Sri Lanka as shown in Figure 2.1 (Burton, 2018). Malaysia is ranked the top 10 coconut producer in the world, with a recent production of 646,932 tons, occupying an area of 85,000 hectares (Tan, 2019).

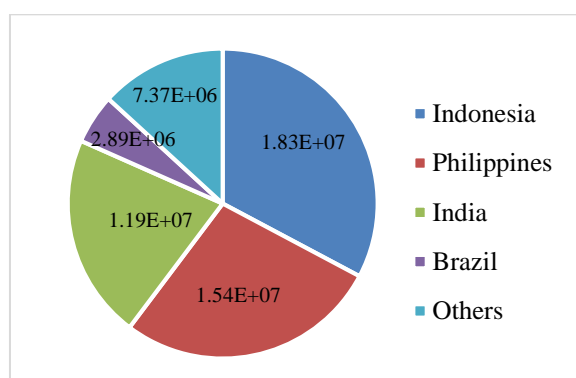


Figure 2.1: Global Coconut Production (in Tons) in 2018 (Burton, 2018)

Coconuts are Malaysia's fourth largest industrial crop with majority crop yield comes from Sabah and Sarawak (Tan, 2019). The main products such as coconut meat, oil, milk and juice are the primary interest in most of the local coconut processing industries. However, the coconut residues or wastes which including the coconut shell and coconut husk are not given much attention and normally discarded. A coconut fruit produces 40 % of coconut husks with 30 % of fibre. Around 36.2 % of coconut husk is not well utilised, which is equivalent to 24 million tons of coconut husk is produced as agricultural waste yearly (Rawangkul et al., 2010). The disposal of these wastes in rubbish dumps, landfills, slopes and some public areas had contributed to the disease spreading, landscapes degradation, unpleasant smell, and the formation of methane gas due to anaerobic digestion (Eduardo et al., 2016).

In fact, there is a great potential of these by-products in the field of biorefinery, especially the coconut husk (CH). Coconut husk or coir is a coarse fibre found in the mesocarp (fibrous outer shell) of a coconut, as illustrated in Figure 2.2. It takes up 80 – 85 % of the overall weight of a nut and is recognised by its length, ranging from 1 to 20 cm. A layer of wax of non-polar aliphatic origin was coated on the CH fibre, presenting a globular shape (Esmeraldo et al., 2010). It is composed of cellulose, lignin, pyroligneous acid, charcoal, tar, tannin, and potassium (Zafar, 2019). CH is extremely robust and tough natural fibre due to its high lignin content, approximately 40 %. Thus, it is difficult to decompose naturally and required more than 8 years to fully degrade into the environment (Eduardo et al., 2016).

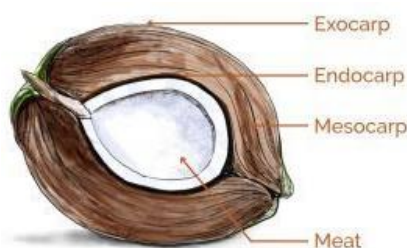


Figure 2.2: Cross Section of a Coconut Fruit (Rajah, 2018)

However, CH is a potential raw material to produce 2G bioethanol and biohydrogen via fermentation owing to its higher holocellulose (cellulose and hemicellulose) content of about 38 % (Ebrahimi et al., 2017). Many approaches

have been suggested to increase value to the CH, and minimise the environmental issues brought by of this LCB (Eduardo et al., 2016). Its' surface porosity, particle size and fibre-resin adhesion can be altered easily by chemical pretreatments. For instance, organosolv pretreatment could be an effective alternative to degrade lignin, release cellulose and improve enzymatic hydrolysis yield of CH (Ebrahimi et al., 2017). As a result, there is a growing interest to produce new bio-based composite materials from CH (Esmeraldo et al., 2010).

### 2.1.2 Spent Coffee Ground

Coffee is one of the world's most popular beverages and the second biggest traded product after crude oil (Alghooneh et al., 2017). According to International Coffee Organisation (ICO), it was estimated that about 11 million tons of coffee was processed in 2017 and majority consumed by EU, the USA, Brazil and Japan (Lee et al., 2019). Due to extensive consumption of fresh coffee, large amount of by-products such as spent coffee ground (SCG) and coffee silverskin (CS) are generated from foodservices (café and restaurants) and instant coffee industries. An average value of 7.9 million tons of SCG is generated annually with 93 % of it was ended up in landfills. Direct discharge of unutilised SCG leading to serious contamination and environmental issues, as it consists of toxic substances such as caffeine, tannins and polyphenols (Nguyen et al., 2017). Figure 2.3 illustrates the anatomy of a coffee cherry.

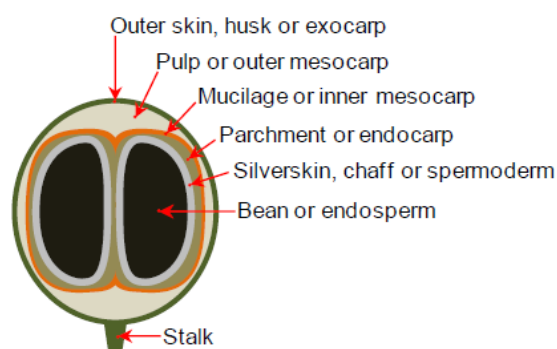


Figure 2.3: Schematic of the Anatomy of a Coffee Cherry (Zarrinbakhsh et al., 2016)

The coffee bean is obtained from the deepest central of a coffee cherry by separating out the husk, pulp, parchment, and mucilage. SCGs are the remaining insoluble residue after dehydration, milling and brewing of coffee beans (Zarrinbakhsh et al., 2016). The generated SCG occupies more than 90 % of initial dry mass of a coffee bean (Lee et al., 2019).

However, SCG is a rich lignocellulose residue which consists of cellulose, hemicellulose, lignin, lipids and antioxidant compounds, representing a potential energy source (Lee et al., 2019). The presence of organic compounds is an important feature as an appropriate biorefinery feedstock in the production of biofuels and highly value chemicals (Pereira et al., 2019).

Recently, several studies on the conversion of SCG to value-added chemicals by overcoming the covalent linkages between the lignin and hemicellulose through organosolv pretreatment to improve hydrolysis of holocellulose contents into industrially significant monosaccharides have been investigated (Lee et al., 2019). Therefore, the valorisation of SCG as an useful by-products is beneficial to the environment and economy (Zarrinbakhsh et al., 2016).

### **2.1.3 Sugarcane Bagasse**

Sugarcane is an essential crop that use to produce white sugar from the juice extracted. Around 80 % of the world's sugar production is originated from tropical and subtropical regions. The sugar production in 2019 was found to be 197 million tons and is projected to increase to approximately 200 million tons in 2020. Recently, India becomes the world leader of sugarcane production with a production rate of 36 million tons of sugar, accounting 19 % of the world's total sugar production (Walton, 2020). The other top sugarcane producers are Brazil, Thailand and China, which contribute 70 % of the world's sugarcane production including India (Vallejos et al., 2015).

Additionally, sugarcane is an important agro-industrial crops to be used as the feedstock for 1G biofuel production. It is normally burned in sugar and ethanol mills to generate energy (Vallejos et al., 2015). Brazil is the world's second cellulosic ethanol producer that highly makes use of the cane ethanol in their auto fleets due to the considerable domestic demand for the alternative fuel (Walton, 2020).

However, the juice extraction of sugarcane will produce 260 to 290 kg of bagasse in every single tonne of sugarcane at 50 % moisture (Vallejos et al., 2015). Sugarcane bagasse (SB) is a solid residue produced from sugarcane after juice extraction as shown in Figure 2.4. SB was initially treated as agro-waste that usually discarded away or combusted, which was unsustainable and not environmental friendly.



Figure 2.4: Raw Sugarcane Bagasse (Romanov, 2020)

In recent advancement, this cheap and abundant agricultural residue has become a potential feedstock for 2G bioethanol production due to its significant amount of carbohydrates and energy-rich structure (Mesa et al., 2016). Besides, SB-generated bioethanol emits less CO<sub>2</sub> to the atmosphere because it is less carbon intensive than fossil fuel, thus reducing air pollution. It is a valuable biomass which could be used in power generation, paper and pulp sectors and as solar energy reservoir (Niju and Swathika, 2019).

## 2.2 Component Structure of Lignocellulosic Biomass

All lignocellulosic materials are mainly comprised of three biopolymers, which are cellulose,  $(C_6H_{10}O_5)_x$ , hemicellulose  $(C_5H_8O_4)_y$  and lignin  $[C_9H_{10}O_3(OCH_3)_{0.9-1.7}]_z$  components, together with minor amounts of other components such as proteins, ash and lipid (Baruah et al., 2018). These major components are formed as a result of plant photosynthesis by carbohydrates (Chan et al., 2019). The composition of LCB are strongly dependent on the types of biomass and the source it is derived from. Figure 2.5 shows the structural organisation of plant cell wall (Anwar, Gulfranz and Irshad, 2014).

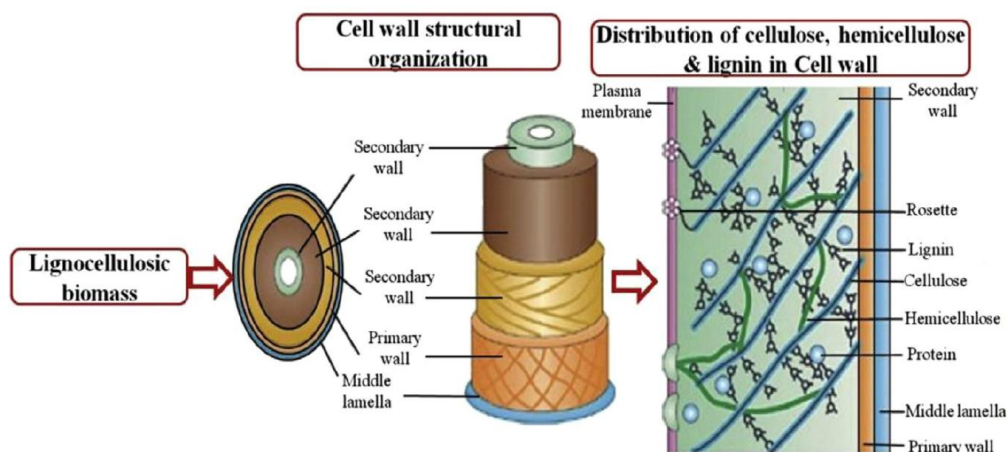


Figure 2.5: The Structural Organisation of Plant Cell Wall and the Distribution of Components (Anwar, Gulfranz and Irshad, 2014)

Cellulose is the most abundant biopolymer presence in plants, which acts as a basic construction of microfibrils in the cell wall. It is a highly stable polymer comprised of unbranched, parallel, and straight chain of many D-glucopyranose units linked by  $\beta$ -(1,4)-glycosidic bonds (Amore, Ciesielski and Lin, 2016), as illustrated in Figure 2.6. Cellulose molecules appears as bundles which gathered together to form microfibrils containing both crystalline and amorphous structures. They are highly crystalline owing to the strong hydrogen bonds and Van der Waals interactions which decrease the flexibility of cellulose. Hence, leading to water insoluble characteristic and resistant to most organic solvents except under extreme pH concentration of solution (Anwar, Gulfranz and Irshad, 2014). Cellulose possesses the highest degree of polymerisation among lignocellulosic polymers, which is around 1000 or higher, thus responsible for its high rigidity (De Bhowmick, Sarmah and Sen, 2018), compatibility with living tissue, and stereochemical regularity (Baruah et al., 2018).

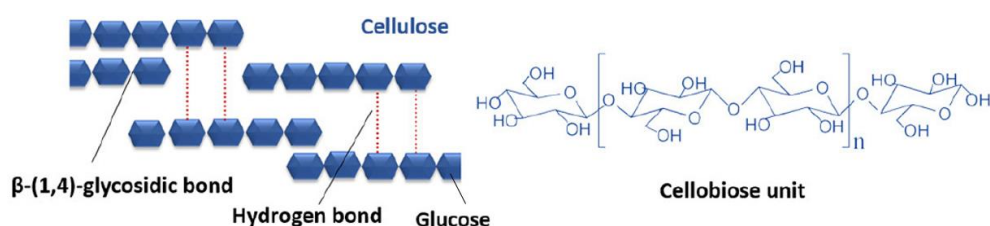


Figure 2.6: The Chemical Structure of Cellulose Component in Plant Cell Wall (Baruah et al., 2018)

Hemicellulose is the second most abundant heterogeneous polymers, which joins tightly to the surface of cellulose fibrils by non-covalent bonds and resulting an amorphous matrix region (Anwar, Gulfranz and Irshad, 2014). It composed of small chains of various polysaccharides such as galactomannan, glucuronoxylan, xylan, xyloglucan, arabinoxylan and glucomannan that are joins together by  $\beta$ -(1,4)- or  $\beta$ -(1,3)-glycosidic bonds (Baruah et al., 2018), as show in Figure 2.7. However, they are readily hydrolysed by alkali and acid treatments to produce bioethanol and other energy products (Amore, Ciesielski and Lin, 2016). Grass biomass normally comprises arabinan, galactan and xylan. Whereas, hardwood and softwood contains primarily mannan (Anwar, Gulfranz and Irshad, 2014). Hemicellulose has lower degree of polymerisation than cellulose, about 100 to 200 (De Bhowmick, Sarmah and Sen, 2018). Therefore, it is non-crystalline in native state and is readily degraded into monosaccharides (Baruah et al., 2018).

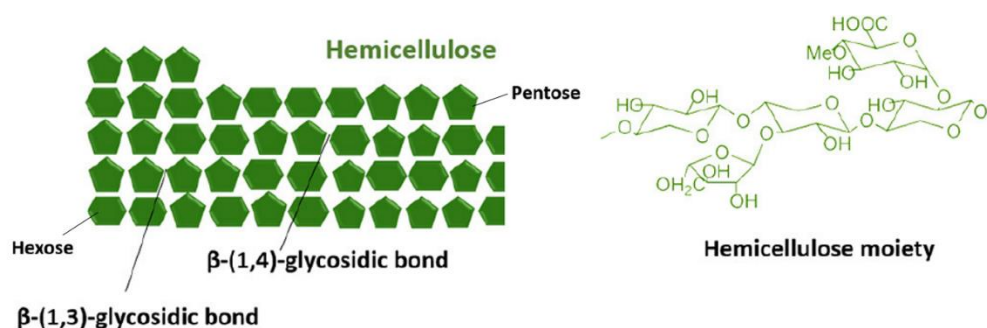


Figure 2.7: The Chemical Structure of Hemicellulose Component in Plant Cell Wall (Baruah et al., 2018)

Lignin is a heterogeneous cross-linked aromatic biopolymer that normally exists in the lowest composition in LCB. It binds covalently with cellulose and hemicellulos, providing a protective layer and mechanical strength to the plant cell wall. Lignin is a tridimensional phenolic polymer that comprises phenyl propane structural units which varied according to the substitute of the methoxyl groups present in the aromatic rings (Baruah et al., 2018). The three basic phenylpropanoid subunits are *p*-hydroxyphenyl (H), guaiacyl (G) and syringyl (S). The HGS subunits are polymerised from *p*-coumaryl, coniferyl, and sinapyl alcohols respectively, as presented in Figure 2.8. Lignin is held by

aryl ether linkages (C-O-O,  $\beta$ -O-4,  $\alpha$ -O-4) and carbon-carbon bonds (5-5,  $\beta$ - $\beta$ ) with no-ordered repeating units. The composition of lignin varies among softwood, hardwood and grass species (Amore, Ciesielski and Lin, 2016). The variation in composition has important effect on degree of delignification and deconstruction of biomass (De Bhowmick, Sarmah and Sen, 2018).

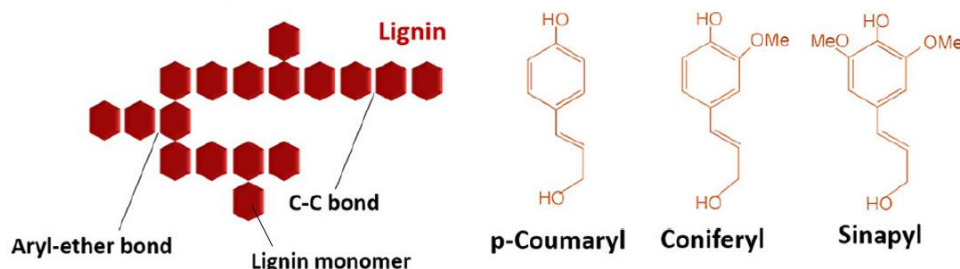


Figure 2.8: The Chemical Structure of Lignin Component in Plant Cell Wall (Baruah et al., 2018)

Lignin gives considerably recalcitrance towards enzymatic saccharification and prohibit interaction between molecules and inner structure (Chin et al., 2019). Hence, lignin is regarded as a hindrance in cellulose biodegradability because it does not involve in hydrolysis process to produce alcohol but could be beneficial for extraction aromatic chemical compounds (De Bhowmick, Sarmah and Sen, 2018).

### 2.3 Chemical Composition of Biomass in Focus

Coconut husk is one of the hardest natural fibre due to its high lignin content, ranging from 35.80 % – 40.10 %. This makes it a durable and high strength fibre but resulting in a strong recalcitrant network toward enzymatic hydrolysis. The mature CH consists of a considerable amount of cellulose, from 24.70 % to 34.80 %, which could be a potential source of fermentable sugars such as glucose and can be utilised to produce 2G bioethanol. CH presented a low hemicellulose content of 12.26 % – 18.30 % (Eduardo et al., 2016) (Ebrahimi et al., 2017).

Unlike other LCB, spent coffee ground contains many hemicellulose content. SCG was found to contain 33.50 % – 39.10 % hemicellulose, 23.15 % – 23.90 % lignin and 8.60 % – 12.40 % cellulose (Ballesteros, Teixeira and

Mussatto, 2014). Hemicellulose extracted from SCGs contained 21.10 % mannans, 13.80 % galactans and 1.70 % arabinans, while xylose was not found in SCG (Wongsiridetchai et al., 2018). With a significant amount of hemicellulose, it can be assumed that SCG is rich in galactomannan and glucomannan. SCG also composes of a small fraction of lipid which takes up 13.40 % of its overall weight (Ravindran et al., 2018). Since SCG consists of mainly mannans, it can be digested by mannanase and used as a substrate for manno-oligosaccharide production (Wongsiridetchai et al., 2018).

The sugarcane bagasse is primarily comprised of three-dimensional cellulose networks intertwined by hemicelluloses and lignin (Espirito Santo et al., 2018). It is rich with cellulose content of 41.00 % – 55.00 %. The strong hydrogen bonds and the orientation of the linkages cause the rigidity of cellulose which is difficult to be broken down. Hemicellulose and lignin content was found in the range of 20.00 % – 25.00 % and 25.00 % – 28.00 %, respectively (Niju and Swathika, 2019) (Zhang et al., 2018c).

Table 2.1 summaries the chemical composition of cellulose, hemicellulose and lignin contents in each of the LCB in focus. It is clearly evidenced that the three types of LCBs have a very different chemical composition in nature. According to Kérzia et al. (2017), the variation of LCB species, harvest time, soil type, age, locality, etc. will affect the lignocellulosic material composition.

Table 2.1: The Chemical Composition of Major Components in Lignocellulosic Biomass in Focus

| <b>Type of Lignocellulosic Biomass</b> | <b>Chemical Composition (%)</b> |                      |               |
|--|---------------------------------|----------------------|---------------|
|  | <b>Cellulose</b>                | <b>Hemicellulose</b> | <b>Lignin</b> |
| <b>Coconut Husk</b>                    | 24.70 – 34.80                   | 12.26 – 18.30        | 35.80 – 40.10 |
| <b>Spent Coffee Ground</b>             | 8.600 – 12.40                   | 33.50 – 39.10        | 23.15 – 23.90 |
| <b>Sugarcane Bagasse</b>               | 41.00 – 55.00                   | 20.00 – 25.00        | 25.00 – 28.00 |

## 2.4 Overview of Organosolv Pretreatment

The primarily purpose of organosolv pretreatment is to solubilise lignin and degrade hemicellulose content of LCB prior to enzymatic saccharification. Lignin is identified as a major hindrance that blocks the accessibility of enzymes

to polysaccharides in LCB. Hemicellulose acts as a barrier that prevents the interaction between cellulase and cellulose through adsorption of enzyme and avoids enzyme from accessing the cellulose surface (Zhao, Cheng and Liu, 2009).

Therefore, most of the organosolv pretreatments are principally lignin removal and hemicellulose solvation, in order to increase the accessible surface area and pore volume of LCB for enhancing the enzymatic digestibility. The following steps are the reaction mechanisms associated with alcohol organosolv pretreatment:

1. Cleavage of lignin's internal bonds and lignin–hemicellulose bonds (ether and 4-O-methylglucuronic acid ester bonds to the  $\alpha$ -carbons of the lignin units).
2. Cleavage of the  $\beta$ -glycosidic bonds in hemicelluloses and cellulose at severe process conditions.
3. Acid-catalysed degradation of the monosaccharides into furfural and 5-hydroxymethyl furfural.
4. Condensation reactions between lignin and reactive aldehydes.

In highly acidic condition, readily broken  $\alpha$ -aryl ether linkages are most easily hydrolysed, but  $\beta$ -aryl ether bonds are likely to be broken, depending on the process conditions (Zhao, Cheng and Liu, 2009) The cleavage of these two ether linkages plays a major role for lignin breakdown prior to dissolution of the fragments. The broken of  $\gamma$ -ether linkages has minor effect in lignin fragmentation during organosolv pretreatment as shown in Figure 2.9 (Zhang et al., 2016).

In the absence of acid catalyst, organosolv pretreatment starts with the auto-ionisation of water. The resulted hydronium ions and acetic acid released from hemicellulose acts as catalysts that promote the breakdown of  $\alpha$ - and  $\beta$ -aryl ether linkages in lignin, even though  $\alpha$ -aryl ether linkage cleavage is dominant (Zhang et al., 2016).

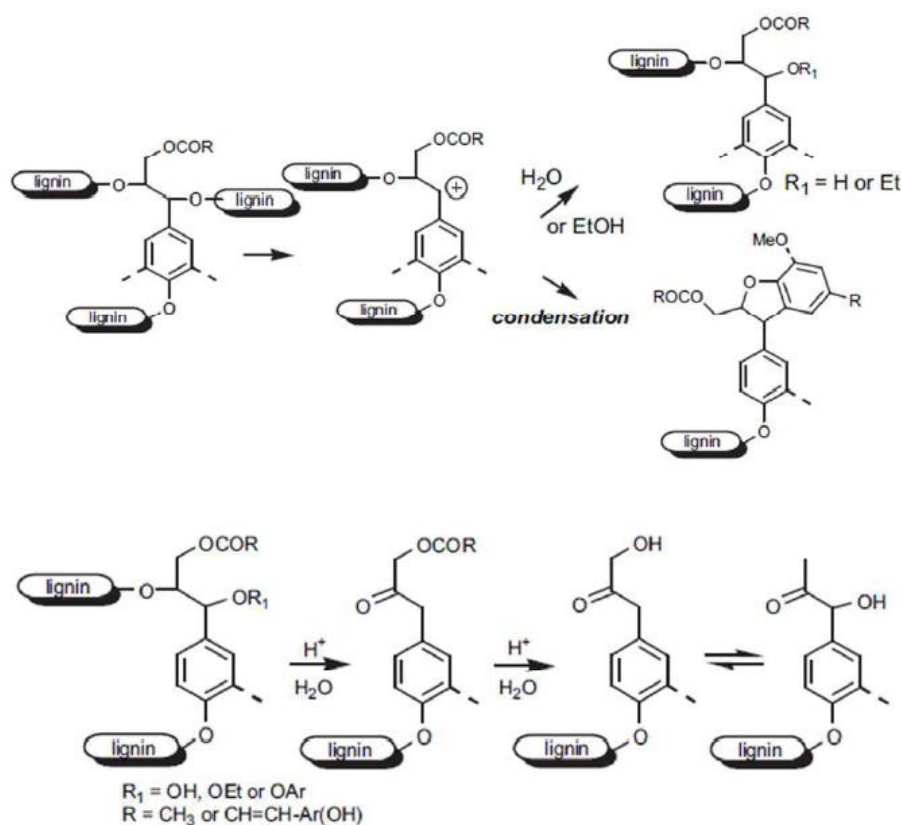


Figure 2.9: Mechanism of Cleavage of  $\alpha$ - (Top),  $\beta$ - and  $\gamma$ -ether Linkages (Bottom) in Acid-catalysed Ethanol Pretreatment of Biomass (Zhang et al., 2016)

#### 2.4.1 Organosolv Pretreatment Factors

The efficiency of organosolv pretreatment on LCB is affected by many chemical and physical factors, such as lignin and hemicellulose concentration, lignin structure, particle size, organic solvent, the presence of catalyst, temperature, etc. The degree of lignin dissolution, fragmentation, and condensation are determined by the properties and proportion of organic solvent together with the reaction pH of an organosolv pretreatment (Zhang et al., 2016).

According to Ebrahimi et al. (2017), high boiling point organic solvent such as glycerol and ethylene glycol do not have the capability to break down the lignocellulosic matrix under pretreatment temperature lower than 110 °C. Besides, the addition of a small quantity of acids like HCl or H<sub>2</sub>SO<sub>4</sub> or alkaline or ionic liquids in the solvents will improve the hydrolytic cleavage of LCB ether linkages, and thus enhancing the rate of delignification. Recent researches also reported that blending the solvent with 20 wt.% of water or less during the pretreatment process can decrease the solution viscosity, and offers higher

biomass loading, as well as elimination of more hemicellulose and lignin contents.

LCB contains lignin that is varied between species due to their native proportion of syringyl (*S*) and guaiacyl (*G*) lignin units. Hence, variation of species would give different *S/G* ratios, allowing for the opportunity to enhance pretreatment efficiency. A more appropriate native lignin may tolerate with milder pretreatment conditions with lower temperature, lesser retention time and lower solvent concentration (Santos et al., 2013).

Several investigation have been conducted to study the relationship between *S/G* ratio and kraft pulping of hardwoods. An analysis with model showed that the  $\beta$ -aryl ether linkage of syringyl lignin is cleaved much more easily than that of guaiacyl lignin. Since  $\beta$ -ether linkage represents the major structure in lignin and is highly associated with the *S/G* ratio. However, the correlation between the pulping efficiency and the *S/G* ratio was too weak in other researches, suggesting that besides *S/G* ratio, other lignin structural features might play a role in delignification process (Santos et al., 2013).

#### **2.4.2 Ethylene Glycol-based Organosolv Pretreatment**

Nakanun and Takanti reported the earliest use of ethylene glycol (EG) to obtain cellulose pulp in 1941 (Rodríguez et al., 2018). EG is used frequently as a high boiling point alcohol in organosolv pretreatment of biomass. It offers an advantage to carry out the pretreatment process under atmospheric pressure with a high degree of delignification (Zhang, Pei and Wang, 2016).

Zhang et al. (2016) studied the pretreatment of waste newspaper with pure EG solution in the present of 2 %  $\text{H}_2\text{SO}_4$  at 150 °C for 15 min and resulted in 94 % hemicellulose digestibility. Chin et al. (2019) investigated the EG pretreatment of natural microbial degraded empty fruit bunch for sugar based substrate recovery. It was found that the pretreatment with 50 v/v% EG in the present of 3 v/v% NaOH performed the best result with 67.2 % delignification and 90.6 % alpha-cellulose recovery. Additionally, under the same concentration of EG by using 5 v/v%  $\text{H}_2\text{SO}_4$  and 5 v/v%  $\text{FeCl}_3$  were able to degrade alpha cellulose considerably.

EG was proven as a more effective delignification agent than ethanol by Nitsos and Rova (2018). Japanese Cypress was pretreated with aqueous ethanol

and aqueous EG at different concentrations. The pretreatment was undertaken at a variety of temperatures, ranging from 140 to 230 °C in the presence of acetic acid as a catalyst. The ethanol-pretreated biomass showed a lower degree of enzymatic digestibility of about 10 % even at the maximum severity used in the experiment. The use of EG displayed a marginal increase in digestibility with a 30 % glucose yield. This implies that EG has better solvent properties than ethanol in Japanese Cypress pretreatment (Nitsos and Rova, 2018).

EG pretreatment is advantageous for its mild pretreatment conditions but less attractive to be applied because it requires higher energy for solvent recovery and relatively high material costs (Zhao, Cheng and Liu, 2009). The low equipment requirements and cheap organic solvents are more favourable in organosolv pretreatment for economical considerations (Zhang, Pei and Wang, 2016).

## **2.5 Pretreatment of Lignocellulosic Biomass in Focus**

Pretreatment processes are important to modify the structure of biomass by eliminating the lignin content, depolymerising the hemicellulose and increasing cellulose crystallinity, depending on the process conditions of pretreatment. This reduces the biomass recalcitrance and leads to better yields of glucose during enzymatic hydrolysis (Espirito Santo et al., 2018). There is limited literature review of organosolv pretreatment on coconut husk, spent coffee grounds and sugarcane bagasse. Since there are various types of LCB, the solvents that can be used for pretreatment are also diverse.

### **2.5.1 Coconut Husk**

From the study of Ebrahimi et al. (2017), hydrochloric acidified 90 % aqueous glycerol pretreatment of CH at 130 °C for 30 min with a solid to liquid (S/L) ratio of 1:20, able to remove 38.8 % of lignin content and yield 76.2 % of glucan digestibility. When S/L ratio increased to 1:30, lignin removal rate increased to 40.9 % and glucan digestibility decreased to 75.3 %. However, for 90 % aqueous glycerol pretreatment under the same conditions without acid catalyst, the lignin removal and glucan digestibility percentages were recorded low, as 10.1 % and 13.5 % respectively. Ebrahimi et al. (2017) justified that glycerol alone has low capability to break down the lignocellulosic matrix under lower temperatures.

than 110 °C. Therefore, a pretreatment temperatures of 130 °C was applied and 1.2 wt.% of hydrochloric acid was added to the solvent to enhance the delignification yield, and thus the efficiency to cleave the biomass structure.

There is limited research study of organosolv pretreatment on CH due to its insignificant effect and unsatisfactory results. However, more literature of alkaline pretreatment on CH was found. Based on the study of Eduardo et al., (2016), the lignin content of fibre decreased to 29.91 % from 40.10 % after pretreatment with 5 % NaOH solution at 121 °C for 40 minutes. Accordingly, the cellulose content increase from 24.7 % to 55.17 % and the hemicellulose content decreased from 12.26 % to 7.80 %.

According to Fatmawati, Agustriyanto and Liasari, (2013), the cellulose recovery of 8.13 % and delignification yield of 14.5 % were obtained by using 3 % NaOH solution at 60 °C. It was reported that the cellulose content improved by increasing the concentration of NaOH (from 3 % to 11 %) and pretreatment temperature (from 60 °C to 80 °C). The lignin removal rate began to decrease at 100 °C for all tested NaOH concentrations.

### **2.5.2 Spent Coffee Ground**

In the study of Nguyen et al. (2017), 20 wt.% of dry SCG was treated with 60 % aqueous ethanol at 150 °C for 2 hours. A significant reduction in the concentration of lignin was observed from  $37.1 \pm 1.2$  % to  $18.5 \pm 0.5$  %. The mannose content increased slightly from 19.3 % to 22.7 % after pretreatment but decreased for other sugar monomers (glucose, galactose and arabinose). This presumably means that the ethanol pretreatment of SCG is more efficient in breaking down the polysaccharides, which are particularly recalcitrant due to the complicated nature of their galactomannans, arabinogalactans, and cellulose components.

Organosolv pretreatment was conducted by Lee et al., (2019) to undergo lignocellulosic deconstruction of SCG by using methanol with the aid of H<sub>2</sub>SO<sub>4</sub> as catalyst. It was noticed that higher lignin removal rate was achieved for lower pretreatment temperature, 110 °C when compare to 180 °C, and higher H<sub>2</sub>SO<sub>4</sub> concentration. The highest delignification yield of 62.3 % was recorded at 110 °C with 5 vol.% of H<sub>2</sub>SO<sub>4</sub> concentration and methanol to SCG ratio of 4.

However, in the study of Ravindran et al. (2017), organosolv pretreatment has been shown to be harmful to the carbohydrate content in SCG. Organosolv pretreatment was carried out by using 25 mL of aqueous ethanol mixture (50 – 70 v/v%) with 1 wt.% SCG and 1 wt.% of H<sub>2</sub>SO<sub>4</sub> served as a catalyst. The pretreatment was carried at 120 °C for 30 min. The acid catalyst used in organosolv pretreatment is corrosive in nature and can result in inhibitory compounds when reacting with cellulose and hemicellulose fractions in SCG. A large quantity of acid soluble lignin was successfully removed, but there was a reduction in cellulose content as well. A maximum reducing sugar of 283.12 mg/g of substrate was obtained from pretreated SCG when subjected to enzymatic hydrolysis. It was observed that the hemicellulose content was found to be fairly conserved and the galactan fraction was maximised in organosolv treated SCG.

### **2.5.3 Sugarcane Bagasse**

In the Zhang et al. (2018b) research study, iron (III) chloride-catalysed aqueous ethanol pretreatment was performed at 160 °C to remove lignin and hemicellulose in SB leaving the cellulose-rich residue. After 10 min of pretreatment, the hemicellulose content is reduced from 20.2 % to 3.3 % with 55.2 % of Klason lignin removal rate. The hemicellulose content reduced from 3.3 % to 0.9 % when the pretreatment time increased from 10 min to 90 min. Accordingly, the delignification yield rose gradually when prolong the pretreatment time.

According to Espirito Santo et al. (2018), increased of pretreatment time would improve the efficiency of lignocellulose composition fractionation. These effects may explain an observed increase in solvation of lignin under ethanol/water solutions (50 v/v%) pretreatment at 190 °C at different treatment durations. Specifically, the SB treated for 150 min consist the highest cellulose content and the least remaining lignin content. Mesa et al. (2016) had carried out a sequential organosolv pretreatment process of SB. The used of H<sub>2</sub>SO<sub>4</sub> as catalyst in the first step of aqueous ethanol (45 v/v%) pretreatment enhanced the selectively of xylose (hemicellulose fraction) removal, while the use of NaOH in the following pretreatment procedure improved the efficiency of delignification.

Vallejos et al. (2015) studied the combination of the hot water auto-hydrolysis and aqueous ethanol (50 v/v%) organosolv delignification of SB at 190 °C for 150 min with liquor to solid ratio of 9, allowed extraction of 86.7 % of lignin and produced a solid with 90.0 % of cellulose content. Under the same conditions with liquor to solid ratio of 3, delignification yield decreased and cellulose content dropped to 82.9 %. At low liquor to solid ratio fractionation, the direct separation of the hemicelluloses, lignin and cellulose content was achieved more easily, but the lignin removal rate was decreased.

## **2.6 Characterisation Analysis of Treated Biomass**

After subjecting to chemical attack, the treated LCBs would suffer from physical and chemical changes. Some instrumental analysis such as Scanning Electron Microscopy (SEM), X-ray Diffractometer (XRD), Fourier Transform Infrared Spectroscopy (FTIR) and Thermogravimetric analysis (TGA) were employed to characterise and monitor the fundamental properties change of CH, SCG and SB contributed by organic solvent and chemical pretreatments. Each technique has specific functions and is used to determine different properties of biomass.

### **2.6.1 Structural and Morphology Change**

The structural morphology of biomass is determined by using SEM analysis. The untreated CH surface is rather smooth and had none or very few pores as shown in Figure 2.10 (a). The tiny white stains was observed on the fibre surface, suggested that it was attached with some impurities or other elements. Referring to SEM image in Figure 2.10 (b), the acidified aqueous glycerol treated (AAG) CH presented a rougher surface and unstructured fibre matrix, denoted that the solubilisation and elimination of lignin content after organosolv pretreatment. The increased of surface roughness indicated the increased of accessible surface area of cellulose for enzymatic saccharification (Ebrahimi et al., 2017).

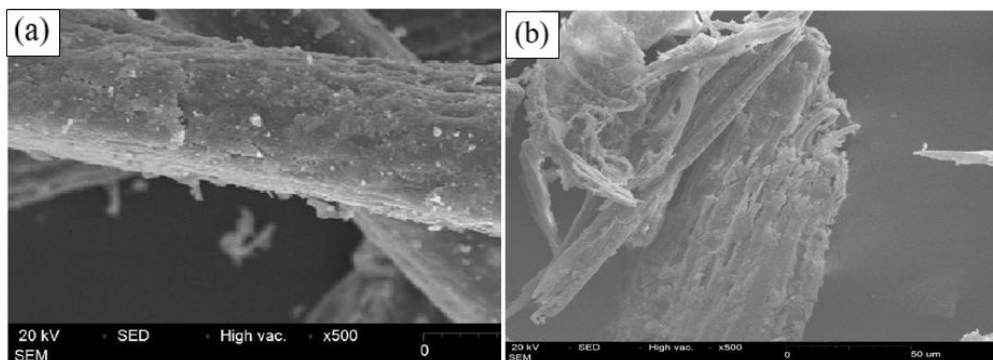


Figure 2.10: SEM images of (a) Raw CH and (b) AAG, S/L 1:30, 60 min Treated CH under 500× magnification (Ebrahimi et al., 2017)

Native SCG is very different from other lignocellulosic substrates in terms of particle shape, size and appearance. It was found to be highly porous, non-fibrous and exhibit a sheet like structure in nature (Ballesteros et al., 2014), as shown in Figure 2.11 (a). The porous nature of the SCG may be due to the solvation of some components of coffee grounds during hot-water brewing. Structural disintegration and obvious holes formation was clearly displayed on treated SCG in Figure 2.11 (b). This can be attributed to the efficiency of the pretreatment in the removal of hemicellulose and lignin fractions after NaOH pretreatment at 110 °C for 15 min (Wongsiridetchai et al., 2018).

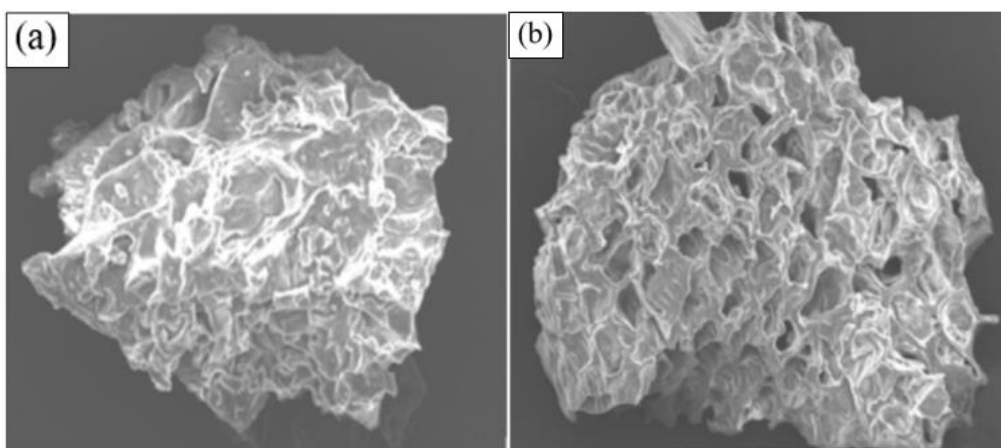


Figure 2.11: SEM images of (a) Raw SCG and (b) NaOH, 110 °C, 15 min treated SCG under 1000× magnification (Wongsiridetchai et al., 2018)

Figure 2.12 (a) illustrates an intact surface of SB fibre. This surface layer was being gradually removed during 25 vol.% aqueous ethanol pretreatment.

The loosely packing of fibre and separation of bundles can be clearly observed in Figure 2.12 (b). The effect of organosolv pretreatment on SB surface was presumably caused by the removal of lignin composition and elimination of hemicellulose (Espirito Santo et al., 2018). Besides, the treated SB exhibited a highly porous surface which increased the specific surface area of bagasse (Nantnarphirom et al., 2017).

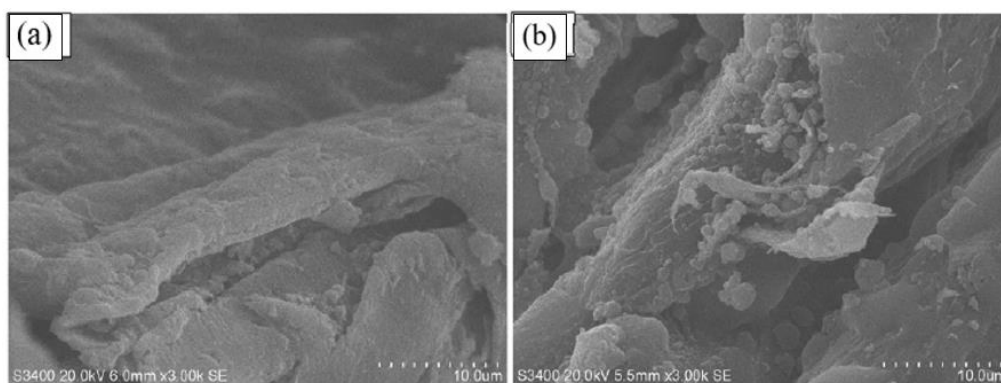


Figure 2.12: SEM images of (a) Raw SB and (b) 25 vol.% Aqueous Ethanol Treated SB under 3000 $\times$  magnification (Nantnarphirom et al., 2017)

### 2.6.2 Crystallinity Change

The crystallinity analysis by XRD of raw and treated biomass is important in identifying the compositional change due to the organosolv pretreatment (Espirito Santo et al., 2018). The presence of crystalline cellulose determine the crystallinity of LCB. Whereas, the amorphous nature of LCB is contributed by amorphous cellulose, hemicellulose and lignin components (Ravindran et al., 2018). In a typical XRD spectrum as shown in Figure 2.13, the peaks associated with amorphous and crystalline fractions of LCB are  $18^\circ$  ( $I_A$ ) and  $22^\circ$  ( $I_{002}$ ) respectively (Espirito Santo et al., 2018), but these vary depending on the type of biomass.

The treated biomass always showed an increment of crystallinity index (CrI) owing to the elimination of hemicellulose and lignin, and the removal some amorphous cellulose, depending on the process conditions. For a LCB being treated under mild conditions, CrI will improve linearly according to the cellulose concentration in the LCB. When a harsher pretreatment is applied, the resulted CrI will stabilise and stop rising with the increase amount of cellulose

in the sample. This could be explained by the unstructured of cellulose bundles due to the more vigorous pretreatment leading to the decreased in cellulose crystallinity (Espirito Santo et al., 2018).

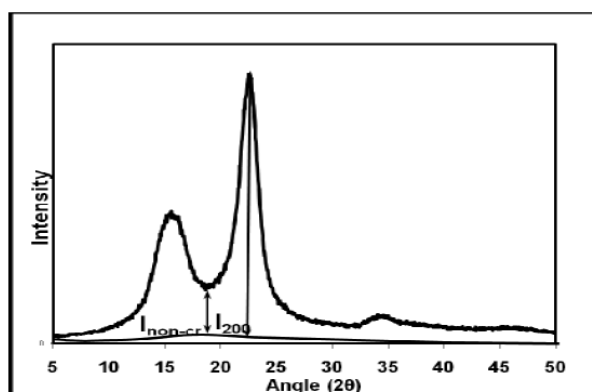


Figure 2.13: X-ray Diffraction Spectra of a Cellulose Crystallinity by using Peak Height Method (Chandrasaha, Rajamane and Jeyalakshmi, 2014)

Figure 2.14 shows the crystallinity peaks for raw CH, and NaOH treated CH. It can be observed that raw CH is amorphous in nature with no sharp peak was observed. The crystallinity was achieved with strong intensity of peaks after pretreatment. This reflects the fact that the amorphous regions such as lignin and hemicellulose were removed after pretreatment and leading to the exposure of crystalline cellulose (Chandrasaha, Rajamane and Jeyalakshmi, 2014).

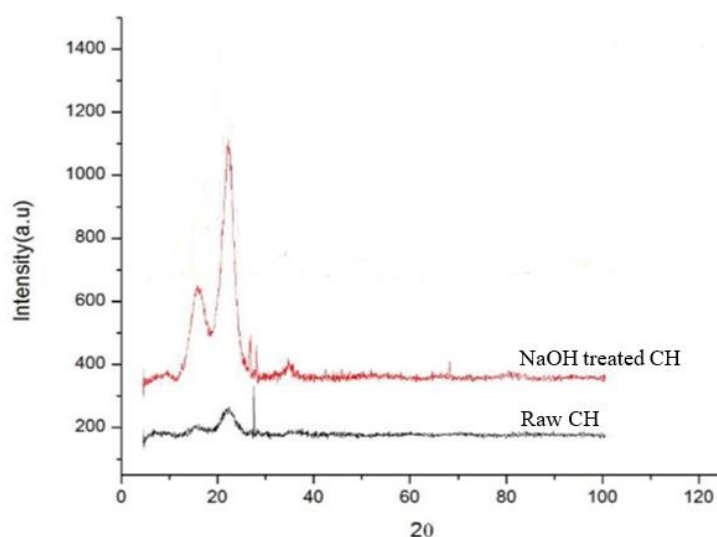


Figure 2.14: X-ray Crystallography of Raw CH and NaOH treated CH (Chandrasaha, Rajamane and Jeyalakshmi, 2014)

### 2.6.3 Functional Groups Change

FTIR spectroscopy is used to determine the efficacy of pretreatment by analysing the change in functional groups of LCB samples. Ebrahimi et al. (2017) suggested that, the untreated biomass has lower absorption strength than treated biomass along the entire spectrum because of the intact and recalcitrant structure of raw materials are having a very weak absorption of the functional groups. This can be observed in Figure 2.15 where the band strength of FTIR spectra for raw CH is lower than that of AAG treated CH.

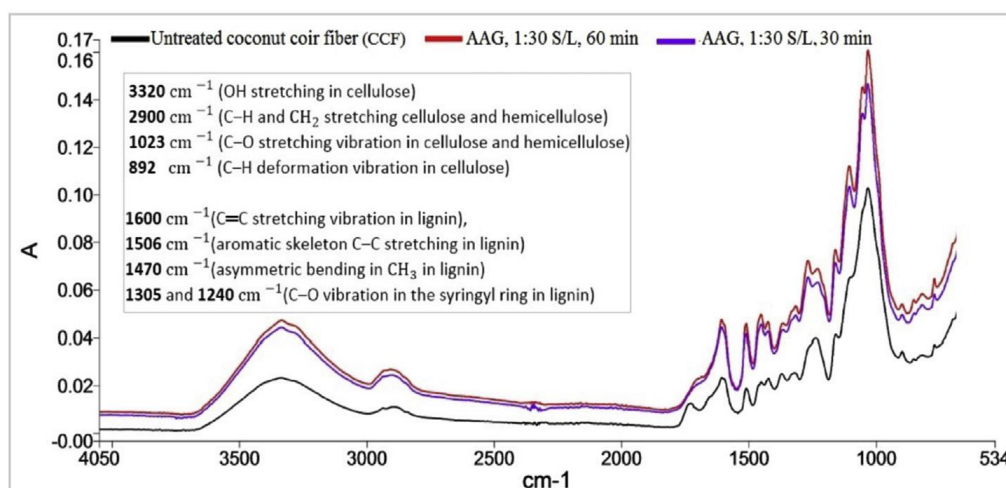


Figure 2.15: FTIR spectrum of raw CH and AAG treated CH (Ebrahimi et al., 2017)

Typically, characteristic peaks of  $2900\text{ cm}^{-1}$  (C-H and  $\text{CH}_2$  stretching),  $1362\text{ cm}^{-1}$  (C-H bending vibration) and  $1126\text{ cm}^{-1}$  (C-O-C asymmetric bridge stretching vibration) are related to cellulose and hemicellulose content. The increase band intensities at these peaks implying that the highly ordered hydrogen bonds in the crystalline cellulose were disrupted after pretreatment. The treated LCB will exhibit an increase intensities in the region of  $1200 - 1000\text{ cm}^{-1}$ , which is associated with C-O stretch and deformation bands in cellulose and lignin. This may be related to the increase in porosity and the proportion of the cellulose content in pretreated CH samples (Ebrahimi et al., 2017).

Peak at  $1740\text{ cm}^{-1}$  is corresponding to the aromatic skeletal vibration and carbonyl group where lignin and hemicellulose probably exist (Bakri et al.,

2018). The absorption band appears from  $900 - 800 \text{ cm}^{-1}$  is associated with the glycosidic bond in cellulose (Ebrahimi et al., 2017).

Characteristic peaks at  $1600 \text{ cm}^{-1}$  (C=C stretching vibration),  $1506 \text{ cm}^{-1}$  (aromatic skeleton C-C stretching),  $1470 \text{ cm}^{-1}$  (asymmetric bending in  $\text{CH}_3$ ), and both  $1305$  and  $1240 \text{ cm}^{-1}$  (C-O vibration in the syringyl ring in lignin) are associated with lignin content. The reduction in band strength or absence of these peaks indicated the cleavage of lignin linkages (Ebrahimi et al., 2017).

#### 2.6.4 Thermal Stability Change

Thermogravimetric analysis was employed to explore the thermal stability of biomass. The thermogravimetric (TG) curve measures the weight loss of the biomass when the temperature rises, while the rate at which the mass loss occurs was showed by the derivative thermogravimetric (DTG) graph (Zarrinbakhsh et al., 2016).

Figure 2.16 shows TGA and DTG graphs of SB. Two primary weight loss peaks were observed in between  $200$  and  $400 \text{ }^\circ\text{C}$ , which are  $302 \text{ }^\circ\text{C}$  and  $350 \text{ }^\circ\text{C}$  with DTG of  $-0.51$  and  $-0.95\% \cdot ^\circ\text{C}^{-1}$ , respectively. The first peak was contributed by the degradation of hemicellulose. The second peak was ascribed to the depolymerisation of cellulose and lignin. This indicated that the degradation temperature of hemicellulose is lower than the depolymerisation temperature of cellulose and lignin (Zhang et al., 2018c).

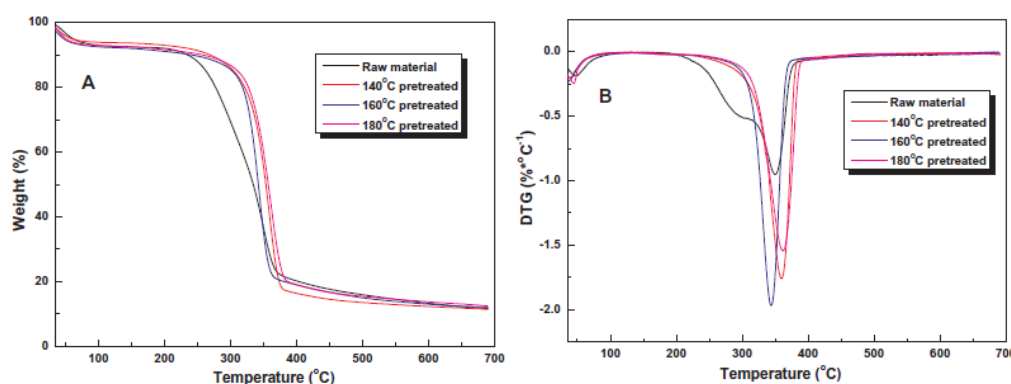


Figure 2.16: (A) TG and (B) DTG distribution of Raw and Treated SB (Zhang et al., 2018c)

For ethanol treated SB with FeCl<sub>3</sub> at 140 °C, only one peak of weight loss was presented in TGA graph at 361 °C with DTG of  $-1.76\% \cdot ^\circ\text{C}^{-1}$ , which was associated with the depolymerisation of cellulose and lignin. This phenomenon reflected that most of hemicellulose was eliminated after FeCl<sub>3</sub>-catalysed ethanol pretreatment (Zhang et al., 2018c).

## CHAPTER 3

### METHODOLOGY AND WORK PLAN

#### 3.1 Overview of Methodology

The overall view of the research experiment procedure is presented in the form of process flow chart as shown in Figure 3.1.

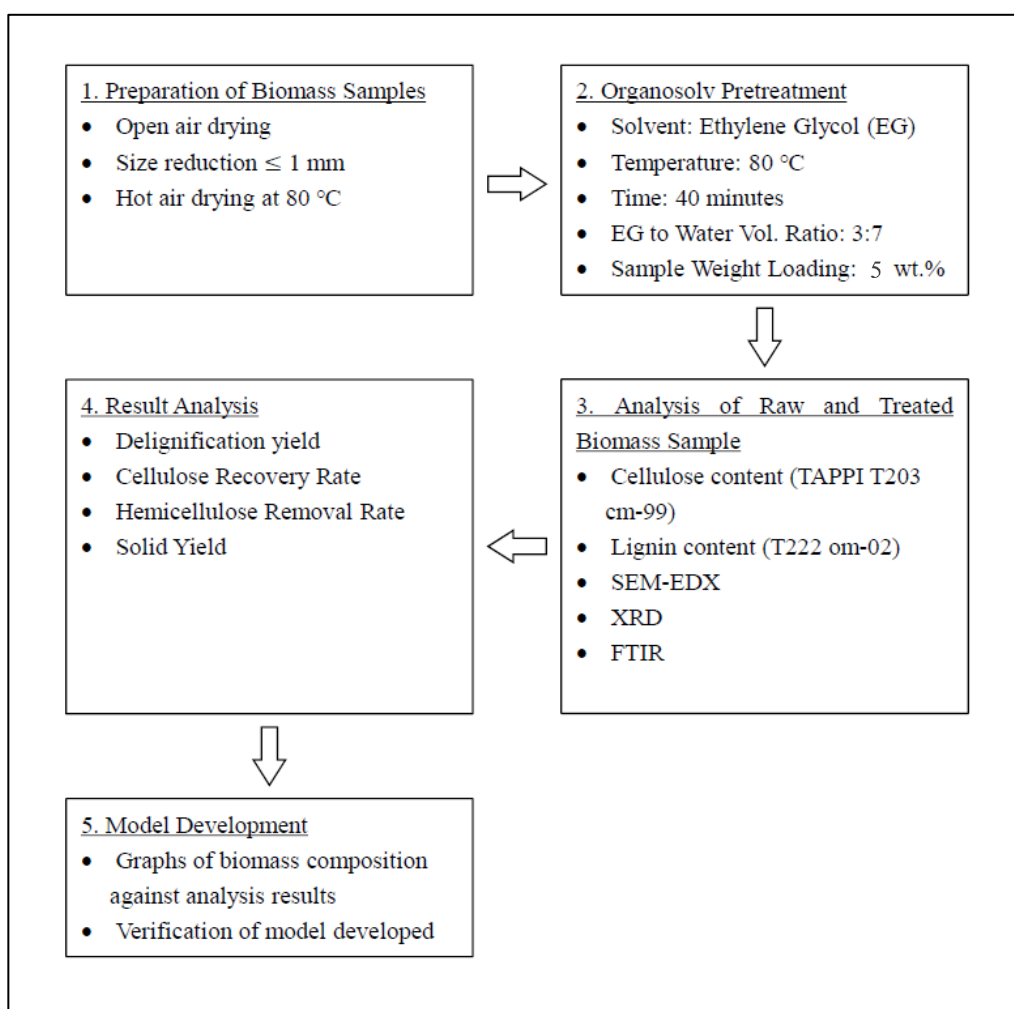


Figure 3.1: Flowchart of the Research Methodology

#### 3.2 Materials and Apparatus

The materials, chemicals, apparatus and equipment necessary for this research study are listed accordingly.

### **3.2.1 Materials and Chemicals**

The coconut husk (CH), sugarcane bagasse (SB) and spent coffee ground (SCG) were selected as the lignocellulosic materials for this research study due to their variation in chemical composition. The matured coconuts were obtained from a grocery in Bahau, Negeri Sembilan. SB was supplied by a vendor of sugarcane drink from Sg. Long night market. SCG was collected from the Amitie Café. The chemicals required were purchased from Merck Sdn Bhd. Table 3.1 provides a complete list of raw materials and chemicals required for the experiment.

### **3.2.2 Apparatus and Equipment**

The apparatus and equipment used during conducting the experiment are listed in Table 3.2. Table 3.3 shows all the analytical instruments involved for the characterisation procedure.

## **3.3 Biomass Sample Preparation**

Three types of lignocellulosic materials were prepared separately with slightly different in preparation procedure.

### **3.3.1 Coconut Husk**

CH were ripped off from the outer shell of a matured coconut. The air-dried CH were cut into  $5 \pm 1$  cm of length, and then grounded into 1 mm mesh size powder in a grinder. The desired particle size of CH is achieved by using a 1 mm mesh size sieve. The fine coconut husk powder were dried completely in a forced-air oven under 80 °C for overnight. CH sample was stored in an airtight container prior to subsequent usage.

### **3.3.2 Sugarcane Bagasse**

SB were dried in an oven under 80 °C for 24 hours. The partially dried bagasse was cut into  $5 \pm 1$  cm of length, and then grinded into finer powder to pass through 1 mm mesh size screen. The bagasse powder were dried again in a forced-air oven at 80 °C until all the moisture content is removed. SB sample was stored in tightly-capped bottles for subsequent usage.

Table 3.1: Materials and Chemicals used in the Experiment

| <b>Materials / Chemicals</b>   | <b>Source</b>         | <b>Brand (Purity)</b> | <b>Usage Purpose</b>                                 |
|--|-----------------------|-----------------------|--|
| <b>Coconut Husks</b>   | Grocery               | -                     | Lignocellulosic material for organosolv pretreatment |
| <b>Sugarcane Bagasse</b>   | Sugarcane Drink Stall | -                     | Lignocellulosic material for organosolv pretreatment |
| <b>Spent Coffee Grounds</b>  | Amitie Café           | Roaster Hill          | Lignocellulosic material for organosolv pretreatment |
| <b>1,2-Dichloroethane, C<sub>2</sub>H<sub>4</sub>Cl<sub>2</sub></b>  | UTAR                  | Merck (99.99%)        | Lipid extraction of spent coffee ground              |
| <b>Ethanol, C<sub>2</sub>H<sub>5</sub>OH</b>   | UTAR                  | Merck (99.99%)        | Lipid extraction of spent coffee ground              |
| <b>Ethylene Glycol, (CH<sub>2</sub>OH)<sub>2</sub></b>   | Merck Sdn Bhd         | Merck (99.99%)        | Organic solvent for pretreatment                     |
| <b>Sodium Hydroxide, NaOH</b>  | UTAR                  | Merck (99.99%)        | TAPPI cellulose analysis                             |
| <b>Potassium Dichromate,<br/>K<sub>2</sub>Cr<sub>2</sub>O<sub>7</sub></b>  | UTAR                  | Merck (99.99%)        | TAPPI cellulose analysis                             |
| <b>Sulphuric Acid, H<sub>2</sub>SO<sub>4</sub></b>   | Merck Sdn Bhd         | Merck (96 – 98%)      | TAPPI cellulose and lignin analysis                  |
| <b>Ferrous Ammonium Sulphate,<br/>(NH<sub>4</sub>)<sub>2</sub>Fe(SO<sub>4</sub>)<sub>2</sub>·6H<sub>2</sub>O</b> | UTAR                  | Merck (99.99%)        | TAPPI cellulose analysis                             |
| <b>Ferriin indicator</b>   | Merck Sdn Bhd         | Merck (99.99%)        | TAPPI cellulose analysis                             |

Table 3.2: Apparatus and Equipment used in the Experiment

| <b>Apparatus / Equipment</b> | <b>Brand (Model)</b>       | <b>Usage Purpose</b>   |
|------------------------------|----------------------------|--|
| <b>Oven</b>                  | Memmert                    | To dry the lignocellulosic materials.                                |
| <b>Grinder</b>               | Dickson (DFY-500)          | To finely grind the lignocellulosic materials.                       |
| <b>Sieve</b>                 | Prada Test Sieve<br>(1 mm) | To obtain desired size of lignocellulosic materials.                 |
| <b>Hot Plate</b>             | IKA RH Basic-2             | To heat up organic solvent and water.                                |
| <b>Heating Mantle</b>        | MTops<br>(MS-DMS633)       | To heat up the mixture of solution.                                  |
| <b>Reflux Condenser</b>      | Favorit                    | To reflux the evaporated acid soluble lignin during lignin analysis. |

Table 3.3: Analytical Instruments used for Characterisation Procedure

| <b>Equipment</b>                                      | <b>Brand (Model)</b>   | <b>Function</b>   |
|---|------------------------|---|
| <b>Scanning Electron Microscopy (SEM)</b>             | Hitachi<br>(S-3400N)   | To determine the morphology of the biomass samples.                         |
| <b>Energy Dispersive X-ray Spectroscopy (EDX)</b>     | Ametek                 | To determine the elemental composition of biomass samples.                  |
| <b>X-ray Diffractometer (XRD)</b>                     | Shidmazu<br>(XRD-6000) | To investigate crystallinity of cellulose content.                          |
| <b>Fourier Transform-infrared Spectroscopy (FTIR)</b> | Nicolet (IS10)         | To analyse chemical structure and functional groups of the biomass samples. |
| <b>Ultraviolet Spectrometer (UV-Vis)</b>              | Shidmazu               | To determine the acid soluble lignin content in the biomass sample          |

### 3.3.3 Spent Coffee Ground

SCG is rich in triglycerides with a lipid amount ranging from 7.0 to 30.4 % w/w on a dry weight basis, and the values may vary between 11 and 20 w/w%, reported by Efthymiopoulos et al. (2018). Thus, oil extraction of dried SCG by using solvent extraction method was performed before organosolv pretreatment to ensure the accuracy of analysis results as the oil content would affect the compositional tests. A solvent mixture of 1,2-dichloroethane and ethanol (1:1, v/v) was used to remove the lipid composition in SCG according to the protocol described by Cequier-Sánchez et al. (2008) with minor modification, with a solid to solvent ratio of 1:10 w/v. Dried SCG was put into a cellulose thimble and immersed in a beaker with the solvent mixture. The beaker was covered with aluminium foil to prevent the evaporation of solvent, and then left for 24 hours in the fume hood. Then, the mixture was filtered and the solid residuals were dried in an oven at 80 °C until completely dried. SCG sample was kept well prior to organosolv pretreatment.

### 3.4 Organosolv Pretreatment of Biomass Samples

Organosolv pretreatment was carried out by using 30 v/v% aqueous ethylene glycol to treat dried biomass samples at 80 °C for 40 min with solid to liquid ratio of 1:20. There are total of nine sets of biomass samples to be treated, which included raw CH, raw SB, SCG, and different combinations of biomass mixture. The organosolv pretreatment conditions were controlled to ensure that the pretreatment efficiency is depending on the chemical composition variation of biomass samples only. Table 3.4 summarises the number of experiment to be carried out with different weight percent of lignocellulosic biomass. To ensure the accuracy of the results, the experiments were performed in triplicate and the results were averaged.

An organic solvent of 70 mL distilled water and 30 mL ethylene glycol were added into a 250 mL beaker. The medium was heated to 80 °C and stirred constantly with a magnetic stirrer at 250 rpm by using a hotplate. The beaker was covered with aluminium foil throughout the heating process to prevent the evaporation of medium to the atmosphere. The temperature of the medium was monitored and measured by using a thermometer. 5 g of dried biomass sample

was added into the beaker and left for 40 minutes once the medium temperature reached 80 °C.

After 40 minutes, excess volume of distilled water was added into the beaker to stop the desired pretreatment process. The pretreated sample was filtered by using a filter bag to separate the solid residue from organosolv liquor. Then, the resulted pretreated solid was rinsed with distilled water for five times to remove the residue organic solvent, lignin and hemicellulose components. At the intervals of washing process, the solid-water mixture was stirred for 1 ~ 2 minutes at 250 rpm to achieve sufficient washing. The pretreated solid residue was dried in an oven at 80 °C until a constant weight was obtained after several times of weighing. The pretreated samples were kept in a sealed plastic bag and then subjected to compositional and spectroscopic analysis.

Table 3.4: Run of Experiments

| Experiment No. | Biomass Weight Percent in Dry Weight Basis (wt.%) |     |     |
|----------------|---|-----|-----|
|                | CH  | SCG | SB  |
| 1              | 100   | 0   | 0   |
| 2              | 0   | 100 | 0   |
| 3              | 0   | 0   | 100 |
| 4              | 50  | 50  | 0   |
| 5              | 0   | 50  | 50  |
| 6              | 50  | 0   | 50  |
| 7              | 25  | 75  | 0   |
| 8              | 0   | 25  | 75  |
| 9              | 25  | 0   | 75  |

### 3.5 Compositional Analysis

Compositional analysis was conducted to assess and quantify the lignin, alpha-cellulose, beta-cellulose and gamma-cellulose content in untreated and treated lignocellulosic biomass samples. The analysis was carried out according to the Technical Association of the Pulp and Paper Industry (TAPPI). Besides, solid recovery of treated samples was determined to measure the weight loss percentage after organosolv pretreatment.

### 3.5.1 Determination of Solid Recovery

The solid recovery represents the remaining weight of lignocellulosic biomass samples after organosolv pretreatment. The biomass sample was dried completely before weighted gravimetrically on weighing machine. The percentage of solid recovery was computed by Equation 3.1.

$$\text{Solid Recovery (\%)} = \frac{\text{Pretreated dry solid weight (g)}}{\text{Untreated dry solid weight (5 g)}} \times 100\% \quad (3.1)$$

### 3.5.2 Cellulose Content Analysis (TAPPI T203 cm-99)

T203 cm-99 method (TAPPI, 1999) was used to determine alpha-, beta- and gamma-cellulose composition in lignocellulosic biomass before and after organosolv pretreatment. Alpha-cellulose is a higher-molecular-weight cellulose in pulp, which is insoluble under the test condition of 17.5 % sodium hydroxide solution. Whereas, beta-cellulose represents the soluble fraction that forms precipitate after acidification. Alpha- and beta-cellulose are described as non-degraded and degraded cellulose in pulp, respectively. Gamma-cellulose is the remaining fraction in the solution which consists of mainly hemicellulose component. Table 3.5 shows the preparation of essential reagents for cellulose analysis based on 1 L volume basis.

Table 3.5: Preparation Step of Reagents Required for Cellulose Analysis

| <b>Reagent</b>   | <b>Preparation Procedure</b>  |
|--|---|
| <b>17.5 % NaOH Solution</b>                                    | <ol style="list-style-type: none"> <li>1. 175 g of sodium hydroxide pellets was weighted and dissolved with 500 mL of distilled water.</li> <li>2. The solution was poured into a 1 L volumetric flask and filled with distilled water until the line marked.</li> <li>3. The flask was covered and inverted upside down.</li> </ol>      |
| <b>0.5 N K<sub>2</sub>Cr<sub>2</sub>O<sub>7</sub> Solution</b> | <ol style="list-style-type: none"> <li>1. 24.52 g of potassium dichromate powder was weighted and dissolved with 500 mL of distilled water.</li> <li>2. The solution was poured into a 1 L volumetric flask and filled with distilled water until the line marked.</li> <li>3. The flask was covered and inverted upside down.</li> </ol> |

Table 3.5 (Continued)

|   |   |
|---|---|
| <b>0.1 N Ferrous Ammonium Sulfate Solution</b>    | 1. 40.5 g of ferrous ammonium sulfate powder was weighted and dissolved with 500 mL of distilled water.     |
|   | 2. Add 10 mL of 98 % sulphuric acid into the solution.  |
|   | 3. The mixture was poured into 1 L volumetric flask and filled with distilled water until the line marked.  |
|   | 4. The flask was covered and inverted upside down.  |
| <b>3.0 N H<sub>2</sub>SO<sub>4</sub> Solution</b> | 1. 83.5 mL of 98 % sulphuric acid was measured and diluted with 500 mL of distilled water.                  |
|   | 2. The solution was poured into 1 L volumetric flask and filled with distilled water until the line marked. |
|   | 3. The flask was covered and inverted upside down.  |

The following procedure was performed to obtain the cellulose pulp solution:

1. 1.5 g of dried sample and 75 mL of 17.5 % sodium hydroxide solution was added into a 250 mL beaker.
2. The suspension was stirred with a glass rod until it was evenly distributed.
3. The glass rod was rinsed with additional 25 mL of 17.5% NaOH solution in the beaker to remove the adhered sample.
4. The suspension was left for 30 minutes in the sealed beaker.
5. 100 mL of distilled water was added into the suspension and stirred thoroughly.
6. The suspension was left for another 30 minutes time in the sealed beaker.
7. The suspension was stirred again and filtered by using filter bag. The first 20 mL of filtrate was disposed of and the remaining filtrate was collected to undergo subsequent procedure.

### 3.5.2.1 Alpha-Cellulose Analysis

The following procedure was carried out to determine alpha-cellulose content after obtaining pulp filtrate:

- 1.1 25 mL of filtrate and 10 mL of 0.5 N potassium dichromate solution were pipetted into a 250 mL conical flask.

- 1.2 50 mL of 98 % sulphuric acid was added into the conical flask slowly while the flask was swirled and then remained hot for 15 minutes.
- 1.3 50 mL of distilled water was added into the mixture and left to cool to room temperature in the covered conical flask.
- 1.4 Four to six drops of Ferroin indicator were added to the mixture after cooled and titrated with 0.1 N ferrous ammonium sulphate solution until it turned into dark purple solution from green colour as shown in Figure 3.2.
- 1.5 The procedure was repeated for blank analysis by replacing the pulp filtrate with 12.5 mL of 17.5 % NaOH solution and 12.5 mL of distilled water.

In Step 1.2, the solubility of pulp was observed. If the pulp shows a high solubility with the back-titration of dichromate takes less than 10 mL, procedure is repeated by using 10 mL of pulp filtrate in Step 1.1 and 30 mL of 98 % sulphuric acid in Step 1.2. The composition of alpha-cellulose was calculated by using Equation 3.2.

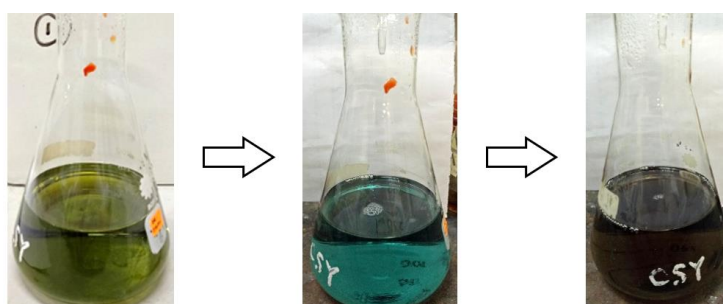


Figure 3.2: Colour Changes of Mixture during Back Titration

$$\text{Alpha Cellulose Composition [\%]} = 100 - \frac{6.85(V_2 - V_1) \times N \times 20}{A \times W} \quad (3.2)$$

where

$V_1$  = Titration volume of the pulp filtrate, mL

$V_2$  = Blank titration volume of alpha-cellulose analysis, mL

$N$  = Normality of the ferrous ammonium sulphate solution, N

$A$  = Volume of pulp filtrate used in the oxidation, mL

$W$  = Weight of dried sample, 1.5 g

### 3.5.2.2 Beta- and Gamma-Cellulose Analysis

The following procedure was carried out to determine beta-cellulose after obtaining pulp filtrate:

- 2.1 50 mL of pulp filtrate and 50 mL of 3 N sulphuric acid were pipetted into a 250 mL conical flask with stopper, and shaken upside down.
- 2.2 The stoppered conical flask was submerged in a hot water bath at 70 to 90 °C for 5 minutes to allow the formation of beta-cellulose precipitate.
- 2.3 The hot mixture was poured into a clean and dry 25 mL centrifuge tube and left for 24 hours to allow the settling of precipitate as shown in Figure 3.3.
- 2.4 50 mL of clean solution (from centrifuge tube) and 10 mL of 0.5 N potassium dichromate solution were pipetted into a 250 mL conical flask.
- 2.5 90 mL of 98 % sulphuric acid was added into the conical flask slowly while the flask was swirled and then remained hot for 15 minutes.
- 2.6 Step 1.3 to 1.5 were repeated for gamma-cellulose solution titration and blank analysis.

In Step 2.5, the solubility of pulp was observed. If the pulp shows a high solubility with the back-titration of dichromate takes less than 10 mL, procedure is repeated by using 25 mL of pulp filtrate in Step 2.4 and 50 mL of 98 % sulphuric acid in Step 2.5. The composition of gamma and beta-cellulose were calculated by using Equation 3.3 and 3.4 respectively.

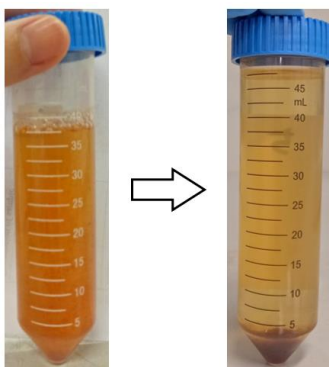


Figure 3.3: Settling of Beta-Cellulose Precipitate after 24 hours

$$\text{Gamma Cellulose Composition [\%]} = \frac{6.85(V_4 - V_3) \times N \times 20}{25 \times W} \quad (3.3)$$

where

$V_3$  = Titration volume of gamma-cellulose solution, mL

$V_4$  = Blank titration of gamma-cellulose analysis, mL

$$\begin{aligned} \text{Beta Cellulose Composition [\%]} \\ = 100 - \text{alpha cellulose \%} - \text{gamma cellulose \%} \end{aligned} \quad (3.4)$$

### 3.5.3 Lignin Content Analysis (TAPPI T222 om-02)

Lignin is an aromatic and amorphous substance that provides major support to plant cell wall. It consists of phenolic monomers including p-coumaryl, coniferyl and sinapyl alcohol. Lignin content of biomass samples was determined and categorised into acid-soluble and acid-insoluble fractions. Acid-insoluble lignin is defined as the fraction of lignin that is resistant to 72 % sulphuric acid. It is also known as Klason lignin, which was quantified by T222 om-02 method (Tappi, 2011). The acid soluble lignin was evaluated via UV-Spectrometer according to Moreira-Vilar et al., (2014) methodology. The reagent required for Klason lignin analysis is 72 % sulphuric acid solution. The acid was prepared by diluted the 665 mL of 98 % sulphuric acid in 1 L volumetric flask.

The following procedure was performed to determine Klason lignin composition:

- 3.1 0.5 g of dried sample and 15 mL of 72 % sulphuric acid solution were added into a 250 mL beaker.
- 3.2 The mixture was stirred and macerated evenly with a glass rod.
- 3.3 The beaker was sealed with parafilm and then left in the fume cupboard for 24 hours.
- 3.4 The mixture was transferred to a 500 mL round bottom flask and 325 mL of distilled water was added subsequently to dilute the 72 % of sulphuric acid solution to 3 %.

- 3.5 The solution was boiled for 4 hours by introducing reflux condenser (seen in Figure 3.4) in order to maintain a constant volume of the solution. The solution was left cooled after boiling process.
- 3.6 The Klason lignin, represented by solid residue was separated from the solution by using vacuum filtration and rinsed with distilled water for several times.
- 3.7 Klason lignin was dried at 80 °C and measured gravimetrically.
- 3.8 The acid-soluble lignin, represented by filtrate was collected after the vacuum filtration without mixing any impurity.
- 3.9 The filtrate was diluted for 4 times in a clean 15 mL centrifuge tube and analysed with UV-Vis spectrophotometer at wavelength 215 nm and 280 nm. An average absorbance was obtained by repeating this step for 3 times.

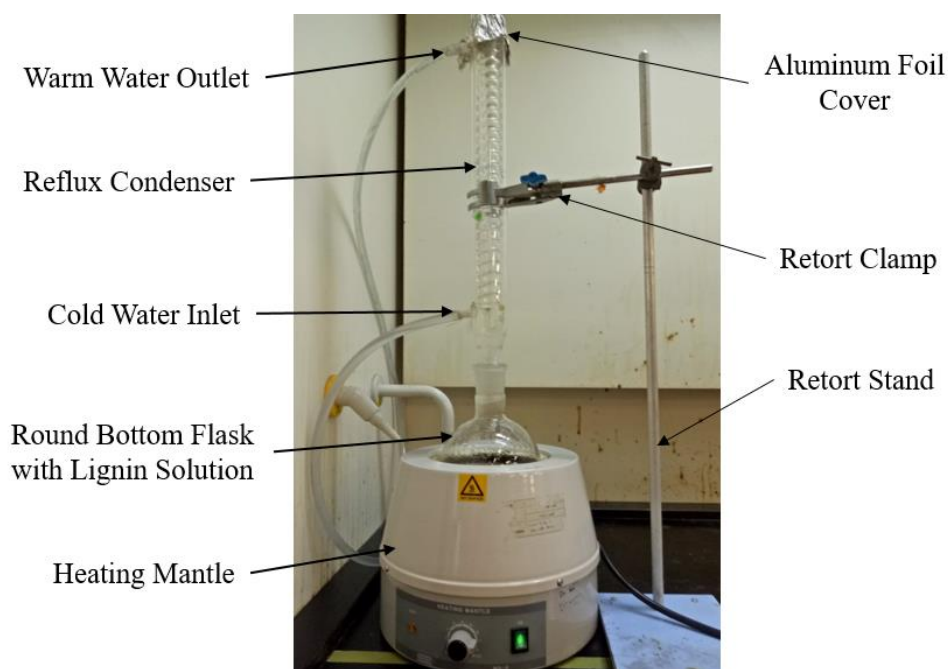


Figure 3.4: Reflux Condensation of Lignin Solution

The composition of Klason lignin and acid-soluble lignin were calculated by using Equation 3.5 and 3.6.

$$\text{Klason Lignin Composition [\%]} = K/W \times 100\% \quad (3.5)$$

where

$K$  = Weight of dried Klason Lignin, g

$W$  = Weight of dried sample, 0.5 g

$$\begin{aligned} & \text{Acid Soluble Lignin Composition [\%]} \\ &= \frac{\left[ \frac{(4.53 \times A_{215}) - A_{280}}{300} \right] DV_F}{W} \times 100\% \end{aligned} \quad (3.6)$$

where

$D$  = Dilution ratio

$V_F$  = Filtrate Volume, 0.335 L

$A_{215}$  = Absorbance at 215 nm

$A_{280}$  = Absorbance at 280 nm

### 3.5.4 Chemical Component Removal and Recovery Rate

The weight of total lignin content,  $L$  is the summation of the weight for Klason lignin and acid-soluble lignin as presented by Equation 3.7. The percentage of total lignin content in the tested sample was calculated by Equation 3.8. Equation 3.9 was used to determine the lignin removal rate.

$$\text{Total Lignin Content, } L \text{ [g]} = K + \left[ \frac{(4.53 \times A_{215}) - A_{280}}{300} \right] DV_F \quad (3.7)$$

$$\text{Total Lignin Content [\%]} = \frac{L}{0.5} \times 100\% \quad (3.8)$$

$$\text{Delignification Yield [\%]} = \frac{L_i - L_f}{L_i} \times 100\% \quad (3.9)$$

where

$L$  = Total lignin content, g

$L_i$  = Total lignin content before treatment, g

$L_f$  = Total lignin content after treatment, g

The weight of alpha-, gamma-, and beta-cellulose were computed by using Equation 3.10, 3.11 and 3.12 respectively. Gamma cellulose content also known as hemicellulose content,  $H$ .

$$\begin{aligned} \text{Alpha Cellulose Content [g]} \\ = 1.5 \text{ g} - \left( \frac{L}{0.5 \text{ g}} \times 1.5 \text{ g} \right) \left( \frac{\text{Alpha Cellulose \%}}{100 \%} \right) \end{aligned} \quad (3.10)$$

$$\begin{aligned} \text{Gamma Cellulose Content, } H \text{ [g]} \\ = 1.5 \text{ g} - \left( \frac{L}{0.5 \text{ g}} \times 1.5 \text{ g} \right) \left( \frac{\text{Gamma Cellulose \%}}{100 \%} \right) \end{aligned} \quad (3.11)$$

$$\begin{aligned} \text{Beta Cellulose Content [g]} \\ = 1.5 \text{ g} - \left( \frac{L}{0.5 \text{ g}} \times 1.5 \text{ g} \right) - \text{Alpha Cellulose [g]} \\ - \text{Gamma Cellulose [g]} \end{aligned} \quad (3.12)$$

The mass of total cellulose content,  $C$  is the summation of alpha- and beta-cellulose, as presented by Equation 3.13. The percentage for cellulose recovery rate and hemicellulose (gamma-cellulose) removal rate were calculated via Equation 3.14 and 3.15 respectively.

$$\begin{aligned} \text{Total Cellulose Content, } C \text{ [g]} \\ = \text{Alpha Cellulose [g]} + \text{Beta Cellulose [g]} \end{aligned} \quad (3.13)$$

$$\text{Cellulose Recovery Rate [\%]} = \frac{C_f - C_i}{C_i} \times 100\% \quad (3.14)$$

$$\text{Hemicellulose Removal Rate [\%]} = \frac{H_i - H_f}{H_i} \times 100\% \quad (3.15)$$

where

$C$  = Total cellulose content, g

$C_i$  = Total cellulose content before treatment, g

$C_f$  = Total cellulose content after treatment, g

$H_i$  = Total hemicellulose content before treatment, g

$H_f$  = Total hemicellulose content after treatment, g

### 3.6 Spectroscopic Analysis

#### 3.6.1 Structural Morphology Analysis

Scanning Electron Microscopy (SEM) equipped with an Energy Dispersive X-ray Spectroscopy (EDX) was used to analyse the raw and treated biomass

sample qualitatively and quantitatively. Morphological characterisation by SEM was done by two-dimensional scanning of the electron probe at 40 kV. It was used to observe the fundamental physical properties and microstructure of the biomass sample under magnification ranging from 400 to 2000. Besides, the biomass samples were coated in gold by using a vacuum sputter coating system to improve their electrical conductivity and the quality of the images before characterisation. EDX was used to determine the composition of topographic characteristics found on the surface of the samples (Esmeraldo et al., 2010).

### 3.6.2 X-ray Diffraction (XRD)

The X-ray diffraction (XRD) patterns were obtained at room temperature with diffraction angles ranging between  $5^\circ < 2\theta < 60^\circ$ , adjusted with a scanning speed of  $2^\circ$  per minute with copper radiation at 40 kV and 30 mA. The crystallinity index (CrI) was determined according to Segal method by using Equation 3.16.

$$\text{CrI (\%)} = \frac{I_{002} - I_A}{I_{002}} \times 100\% \quad (3.16)$$

where

CrI = Crystallinity index

$I_{002}$  = Maximum peak intensity of the 002 lattice reflection

$I_A$  = Valley intensity between the peak of the 002 and 001 plane

The angles of  $I_{002}$  and  $I_A$  depend on the type of lignocellulosic biomass on tested. The typical characteristic peak of  $I_{002}$  is  $22^\circ$ , while  $I_A$  is  $18^\circ$ .

### 3.6.3 Fourier Transformation-infrared (FTIR)

Fourier Transformation-infrared (FTIR) Spectroscopy was used to analyse the chemical structure and functional groups of the biomass samples. It was also aimed to observe the structural changes of cellulose, hemicellulose, and lignin components before and after the organosolv pretreatment. Test sample was placed onto the universal diamond Attenuated Total Reflectance (ATR) top-plate. Thereafter, spectra were obtained in the range of  $400 - 4000 \text{ cm}^{-1}$  with  $4 \text{ cm}^{-1}$  resolution (16 scan).

## CHAPTER 4

### RESULTS AND DISCUSSION

#### 4.1 Organosolv Pretreatment of Pure Biomass Samples

Chemical composition and spectroscopic analysis were carried out for pure biomass sample which included the raw and treated coconut husk (CH), sugarcane bagasse (SB) and spent coffee ground (SCG).

##### 4.1.1 Compositional Analysis

The compositions of raw and treated biomass samples were analysed to identify the ( $\alpha$ - and  $\beta$ -) cellulose, hemicellulose ( $\gamma$ -cellulose) and (Klason and acid soluble) lignin content according to TAPPI T203cm-99 and T222om-02 methods. The chemical compositional analysis results are tabulated in Table 4.1. Table 4.2 shows the recovery and removal rate of chemical components for treated biomass samples (Experiment No. 1 to 3). Figure 4.1 gives a better illustration for comparison of chemical components recovery and removal rates between each type of biomass samples.

CH is recognised for its high durability and strength due to its high lignin content. The lignin content ( $36.89 \pm 1.3$  %) of CH was observed to be the highest among the three biomass samples. Raw CH also presented a high content of  $\alpha$ -cellulose of  $30.73 \pm 1.7$  % and  $\beta$ -cellulose of  $20.60 \pm 4.1$  %, which is an essential criteria as biorefinery feedstock. SB was composed of the high amount of cellulose, in which the  $\alpha$ -cellulose contributed  $41.01 \pm 4.3$  % and the  $\beta$ -cellulose was found to be  $9.506 \pm 7.2$  %. The lignin content of SB was observed to be moderate with  $24.62 \pm 0.3$  %, which could ease the hydrolysis process. Hemicellulose is more abundant in SCG, which amounted up to  $35.28 \pm 7.5$  %. Cellulose is also presenting in a significant amount in SCG, consisting of  $22.68 \pm 1.0$  %  $\alpha$ -cellulose and  $19.56 \pm 6.2$  %  $\beta$ -cellulose. Since the variation of chemical components in LCB is depending on their species, locality, age, etc., the chemical composition obtained in this study can be seen differed from those reported in other research papers (Kérzia et al., 2017).

The solid recovery of biomass samples decreased after organosolv pretreatment was ascribed to the degradation of lignin content accompanied

with some dissolution of hemicellulose content ( $\gamma$ -cellulose). Based on the results from Table 4.2 and Figure 4.1, treated SCG gives the highest solid yield, followed with treated SB, and then treated CH. Removal of  $\gamma$ -cellulose takes up the major role in reducing the samples weight as the delignification yield is relatively lower than hemicellulose removal rate. Moreover, solid recovery could be affected by the density of the lignocellulose material. It was recorded that, the increasing order in term of density for these three biomass samples are: SB ( $0.1 \pm 0.02 \text{ g/cm}^3$ ), CH ( $0.3 \pm 0.05 \text{ g/cm}^3$ ) and SCG ( $1.5 \pm 0.03 \text{ g/cm}^3$ ). Thus, this has satisfied the result obtained from the experiment.

The decreased of lignin and  $\gamma$ -cellulose content of treated biomass samples would lead to an increase of cellulose contents. This is proved as the biomass samples show a positive value for  $\alpha$ - and  $\beta$ -cellulose recovery rate. Lignin represents nature's cement along with hemicellulose, that exploits the strength of cellulose while conferring its flexibility (Esmeraldo et al., 2010). The solubilised of lignin and hemicellulose content after treatment destroyed the tightly packed assembly and provided a larger active area for the accessibility of cellulose component to be tested during compositional analysis, thus resulting in a noticeable cellulose enrichment.

The  $\alpha$ - and  $\beta$ -cellulose recovery rate is mostly contributed by delignification yield and has an indirect relationship with  $\gamma$ -cellulose removal rate. When the elimination of lignin content increased, more hemicellulose content is diminished, and thus leading to higher cellulose content. This phenomenon could be observed from results obtained in Table 4.2 and Figure 4.1. However, the treated SB has higher cellulose recovery rate with lower lignin and hemicellulose removal rate when compared to treated CH. This is mostly attributed by the high cellulose content in native SB which allowed higher cellulose exposure after organosolv pretreatment.

In this research study, the delignification yield is mainly due to the lignin compositions of biomass samples and solid to liquid loading (S/L). It was observed that the higher the lignin content, the lower the delignification yield. The raw CH contains a relatively higher lignin composition than SB and SCG. Lignin acts as an important structural material in support tissues, tends to protect the cellulose and hemicellulose content within the cell wall from being attacked

during treatment. Therefore, the higher lignin content in CH further strengthen its matrix fibre and reducing the delignification yield.

Furthermore, biomass loading is critical in determining the efficiency of organosolv pretreatment. The biomass loading mention here is the solid concentration in term of volume to be treated by the volume of aqueous ethylene glycol. It was observed that the lower the density of biomass sample, the lower the delignification yield. The low density of SB increase the volume required to achieve 5 wt.% solid loading for organosolv pretreatment. The S/L loading for SB reduces the efficiency of solution mixing (Ebrahimi et al., 2017). In other words, high solid loading of SB pretreatment reaction may increase viscosity and result in poor mixing and agitation under constant rotation speed (250 rpm) (Niju and Swathika, 2019). In comparison, the highest cellulose recovery rate was found in treated SCG with the best delignification yield due to its high density property, which is advantageous in achieving good solution mixing.

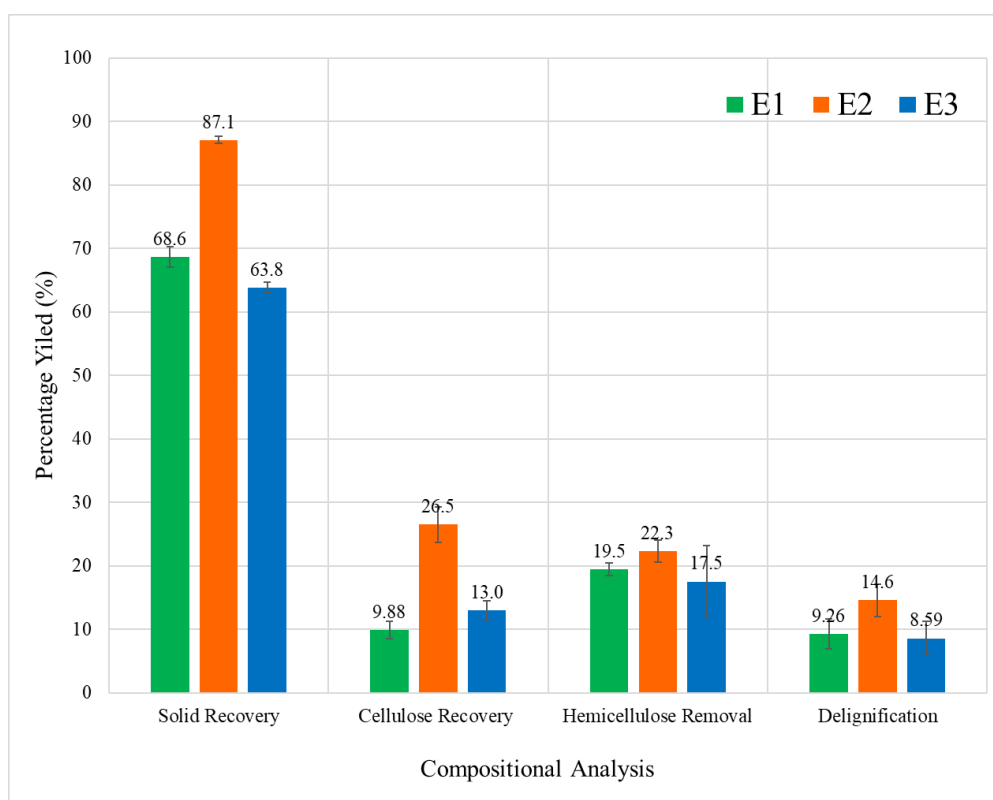


Figure 4.1: Chemical Components Recovery and Removal Rate for Various Types of Biomass Samples

Table 4.1: Chemical Composition of Raw and Treated Biomass Samples

| Experiment No.         | Chemical Component Percentage (wt.% dry basis) |                    |                     |                 |
|------------------------|--|--------------------|---------------------|-----------------|
|                        | $\alpha$ -Cellulose                            | $\beta$ -Cellulose | $\gamma$ -Cellulose | Lignin          |
| <b>Raw CH</b>          | 30.73 $\pm$ 1.7                                | 20.60 $\pm$ 4.1    | 12.62 $\pm$ 6.4     | 36.89 $\pm$ 1.3 |
| <b>E1, Treated CH</b>  | 35.05 $\pm$ 1.2                                | 21.74 $\pm$ 3.7    | 10.16 $\pm$ 1.4     | 33.48 $\pm$ 0.9 |
| <b>Raw SCG</b>         | 22.68 $\pm$ 1.0                                | 19.56 $\pm$ 6.2    | 35.28 $\pm$ 7.5     | 22.43 $\pm$ 0.2 |
| <b>E2, Treated SCG</b> | 28.02 $\pm$ 1.2                                | 21.31 $\pm$ 1.0    | 27.41 $\pm$ 0.6     | 19.16 $\pm$ 0.6 |
| <b>Raw SB</b>          | 41.01 $\pm$ 4.3                                | 9.506 $\pm$ 7.2    | 24.73 $\pm$ 2.7     | 24.62 $\pm$ 0.3 |
| <b>E3, Treated SB</b>  | 44.35 $\pm$ 2.8                                | 12.75 $\pm$ 2.2    | 20.40 $\pm$ 1.4     | 22.50 $\pm$ 0.7 |

Table 4.2: Chemical Components Recovery and Removal Rate for Various Types of Biomass Samples

| Experiment No.         | Percentage Yield (%) |  |                             |                 |
|------------------------|----------------------|--|-----------------------------|-----------------|
|                        | Solid Recovery       | $\alpha$ - and $\beta$ -Cellulose Recovery | $\gamma$ -Cellulose Removal | Delignification |
| <b>E1, Treated CH</b>  | 68.65 $\pm$ 1.6      | 9.879 $\pm$ 1.4                            | 19.46 $\pm$ 1.0             | 9.260 $\pm$ 2.4 |
| <b>E2, Treated SCG</b> | 87.07 $\pm$ 0.6      | 26.50 $\pm$ 2.8                            | 22.29 $\pm$ 1.7             | 14.60 $\pm$ 2.5 |
| <b>E3, Treated SB</b>  | 63.85 $\pm$ 0.8      | 13.04 $\pm$ 1.5                            | 17.54 $\pm$ 5.7             | 8.590 $\pm$ 2.7 |

## 4.1.2 Scanning Electron Microscopy (SEM) Analysis

The structural morphology of raw and treated biomass samples were determined by using SEM technique. The SEM images of biomass samples were observed at 500, 1000 and 2000 times magnification. Figure 4.2, 4.3 and 4.4 presents the surface morphology of CH, SB and SCG respectively. The SEM image for raw biomass samples were attached at the left side of the figure and right side for treated biomass samples.

### 4.1.2.1 Coconut Husk

Figure 4.2-A to D include the SEM images of CH in fibre and powder form. Figure 4.1 A1 and B1 clearly presence an intact surface of CH macrofiber. Macrofiber is formed by bundles of microfibers that aligned approximately parallel to each other. Numerous silica, SiO<sub>2</sub> phytoliths with a typical “rosette” shape (seen in red circles) could be observed at the lateral part of microfiber. The existence of Si and O elements had been verified by EDX analysis performed locally in these areas as shown in Table 4.3. The grinded CH surface is rather smooth and exhibiting some degrees of kinking and twisting as proved in Figure 4.2-C1 and D1.

There is a minor morphological change between the raw (left) and treated (right) SEM images. Owing to the elimination of hemicellulose and lignin, the treated CH fibre displayed a rougher and microporous surface as shown in Figure 4.2-A2 and B2. Besides, the lateral part of macrofibre exhibited lesser SiO<sub>2</sub> phytoliths, creating several groove-liked pore structure (Amaral et al., 2019). Grooves are expected to facilitate the accessibility of cellulose (Arsyad and Wardana, 2015) (Lomelí Ramírez et al., 2010).

Referring to Figure 4.2-C2 and D2, the pretreated fibres presence a distinct feature of cracking and splitting on the external surface, leading to terraces and steps on fibre surface. The loosely packed and separation of fibres indicated the removal of lignin which increased the amount of cellulose exposed in accordance to the result obtained in Table 4.1 (Bakri et al., 2018). Moreover, the physical appearance of the treated CH was found to be less yellowish after subjected to the attack of ethylene glycol.

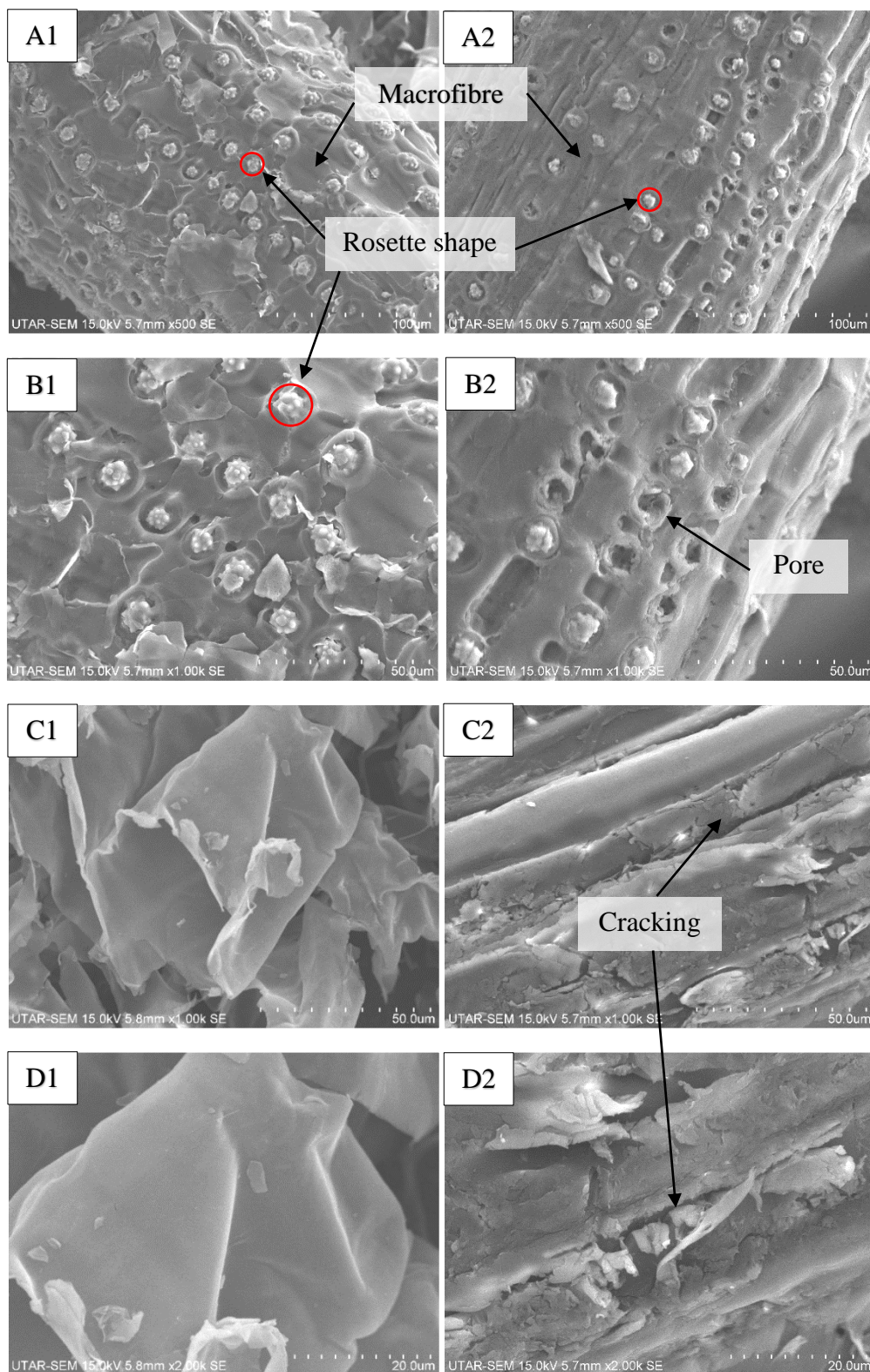
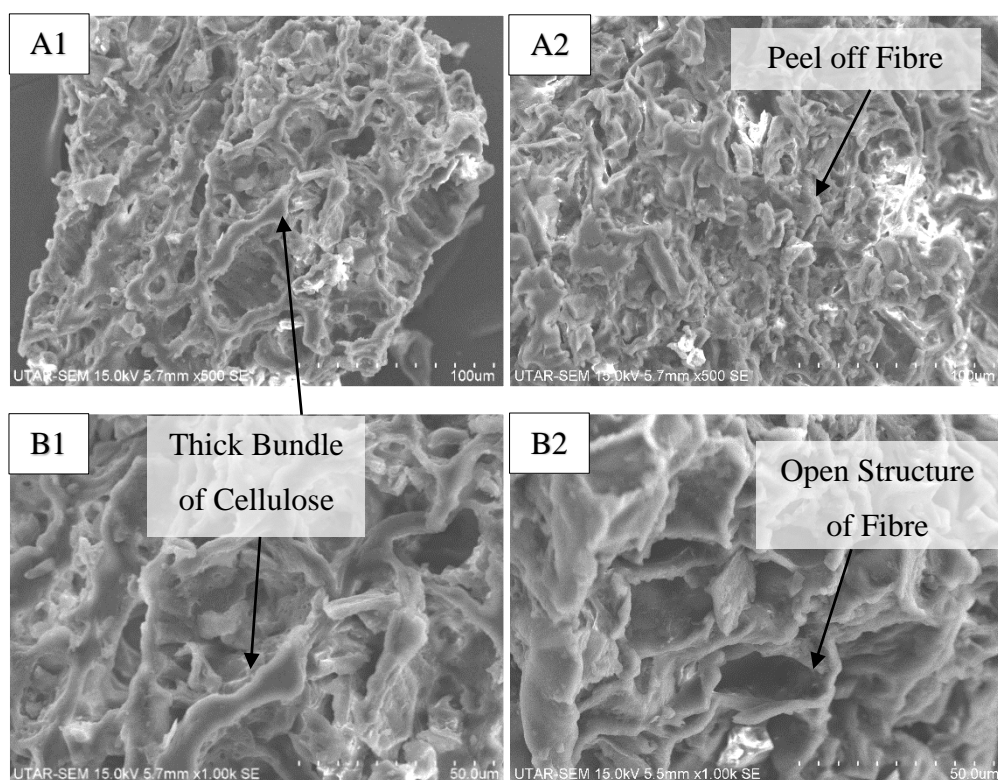


Figure 4.2: SEM images of CH (A1) Raw Fibre-500 $\times$  (B1) Raw Fibre-1000 $\times$  (C1) Raw Powder-1000 $\times$  (D1) Raw Powder-2000 $\times$  (A2) Treated Fibre-500 $\times$  (B2) Treated Fibre-1000 $\times$  (C2) Treated Fibre-1000 $\times$  (D2) Treated Fibre-2000 $\times$

#### 4.1.2.2 Spent Coffee Ground

The structural morphology of SCG is unlike other LCB. According to Figure 4.4-A1, the SEM images of SCG display a dense, non-fibrous, and porous honeycomb like surface texture. A dense and packed thick bundle of cellulose that attached with each other could be observed from Figure 4.3-A1 and B1. Majority of the surface of SCG are considered smooth even though there are tiny dents and pores that are more prominently observed in Figure 4.3-C1 which could be due to mechanical process of size reduction during brewing process.

Disintegration of honeycomb like structure of treated SCG could be observed in Figure 4.3-A2. Lignin fractions along with polyphenols contribute to structural integrity of SCG. Removal of these components may have resulted in structural disintegration. The treated SCG displayed a less regular and loosen honeycomb structure, brought by misalignment of peel off cellulose bundle. The disruption of component structures of SCG was attributed to the efficiency of the pretreatment in the removal of hemicellulose structures resulted in a substantial increase in external surface area. Thus resulting in higher cellulose recovery percentage as shown in Table 4.1.



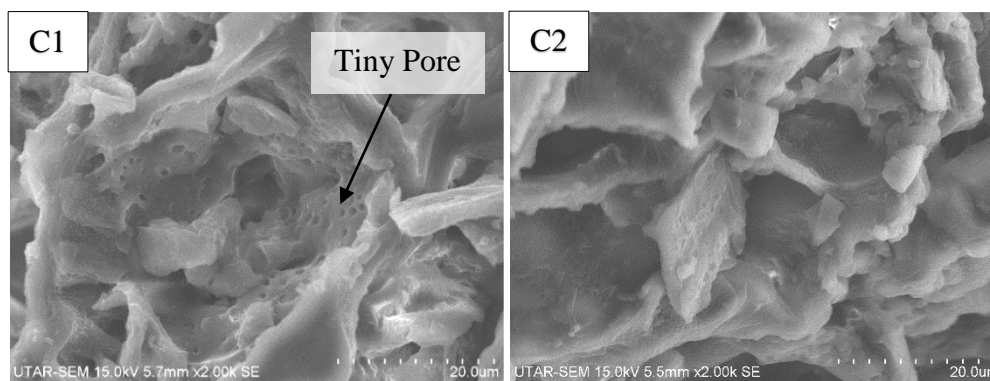


Figure 4.3: Surface Morphology of SCG (A1) Raw SCG-500 $\times$  (B1) Raw SCB-1000 $\times$  (C1) Raw SCG-2000 $\times$  (A2) Treated SCG-500 $\times$  (B2) Treated SCG-1000 $\times$  (C2) Treated SCG-2000 $\times$

#### 4.1.2.3 Sugarcane Bagasse

Figure 4.3-A1 to C1 show a smooth surface and compact structure of native sugarcane bagasse. The untreated bagasse also displayed a complete, rigid, and fibrous structure by parallel stripes, impeding the cellulose accessibility. Although exhibiting certain degree of rupture due to effective grinding, the untreated bagasse still presenting an enclosed and dense surface layer with almost no pore exists.

By contrast, a disordered morphology of treated SB could be observed from Figure 4.3-A2 to C2. The matrix structures of treated bagasse are destroyed and loosened due to the degradation of hemicellulose, lignin and some amorphous cellulose. Figure 4.3-C2 clearly presents the cracking structure on the fibre surface and tiny pores appeared after organosolv pretreatment. The effect of organosolv pretreatment on treated SB is corresponding to the result obtained in Table 4.1. The fragments surface of treated SB would expose more cellulose for enzyme attacking and beneficial for further enzymatic hydrolysis (Zhang et al., 2018b).

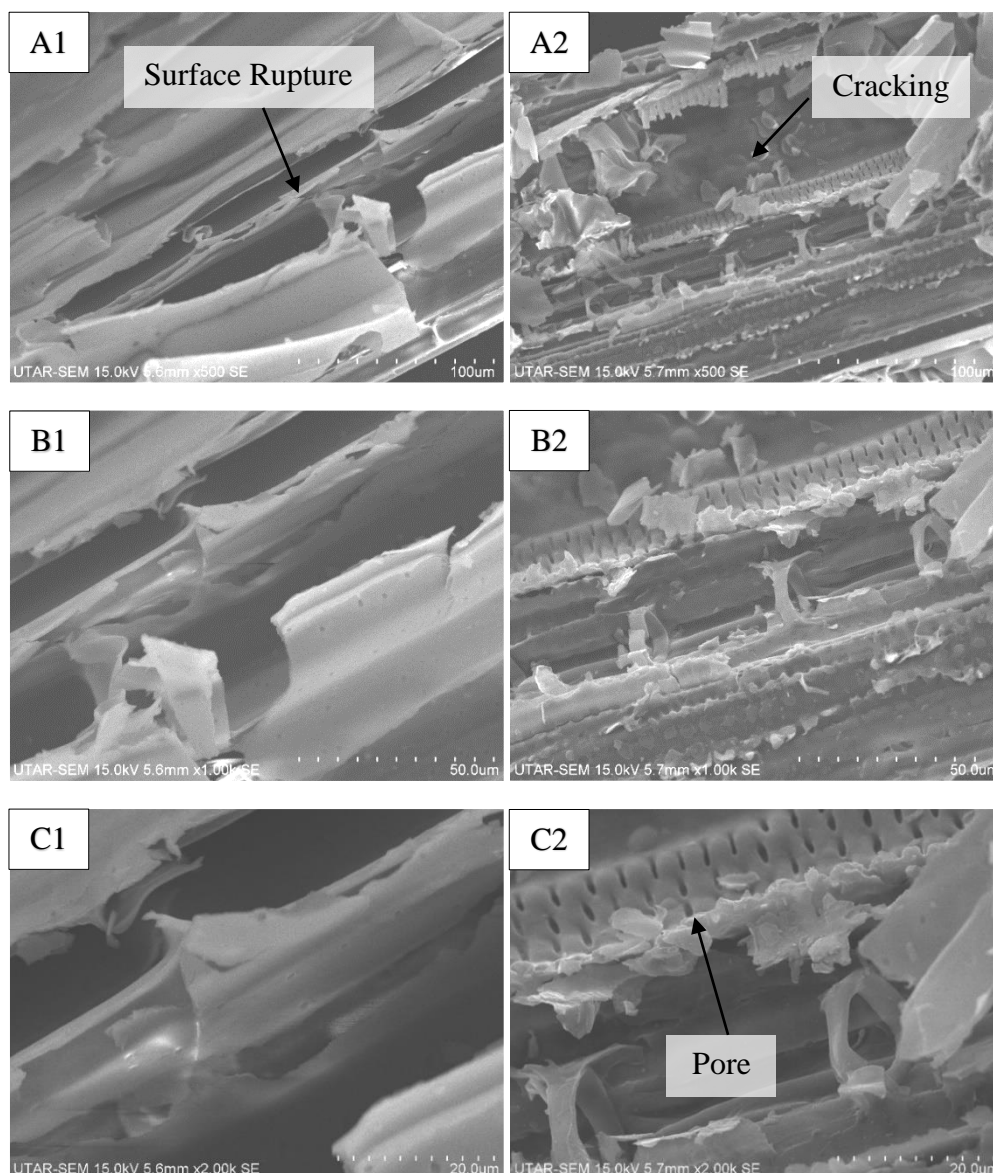


Figure 4.4: SEM images of SB (A1) Raw Fibre-500 $\times$  (B1) Raw Fibre-1000 $\times$  (C1) Raw Fibre-2000 $\times$  (A2) Treated Fibre-500 $\times$  (B2) Treated Fibre-1000 $\times$  (C2) Treated Fibre-2000 $\times$

#### 4.1.3 Energy Dispersive X-ray (EDX) Analysis

The elemental composition of three type biomass samples was determined by EDX technique. The amount of elements of raw and treated biomass samples are tabulated in Table 4.3.

LCB is generally organic structure which composed of mainly carbon (C) and oxygen (O) in its structure. Some other elements such as magnesium (Mg), sulphur (S) and chlorine (Cl) were found as well in the biomass samples. EDX chemical analysis showed that the bulk coconut husk contained silicon (Si)

component and this amount decreased after organosolv pretreatment, which satisfied the SEM images obtained from Figure 4.2-A and B. CHs are expected to be rich with carbon when compared with SB and SCG. Some amount of gold (Au) can be seen too as gold coating was applied to the sample before analysis due to non-conducting behaviour of LCB samples.

Moreover, EDX analysis revealed a change in elementary composition on the surface of biomass sample before and after pretreatment. The oxygen to carbon (O/C) ratio expresses the surface lignin content of the substrate. Research have showed that the theoretical O/C ratios of cellulose and lignin were 0.83 and 0.33, respectively. Therefore, lower lignin content has a higher O/C ratio (Yu et al., 2015).

Based on Table 4.3, raw CH presented the lowest O/C ratio denoted the highest amount of lignin content. Raw SB possessed relatively high O/C ratio which represented its high cellulose content. The pretreatment increased the O/C ratio, indicated that the surface lignin was removed. The O/C ratios observed for treated CH and SCG having a substantial improvement, indicating a higher delignification rate relative to treated SB. Indeed, treated SB showed a minor positive change of O/C ratio which is corresponding to the result obtained from Table 4.1.

Table 4.3: Element Quantification in Dried Weight Percent of Biomass Samples by EDX Analysis

| Element<br>(wt.%) | Biomass Sample |       |                                      |       |        |       |
|-------------------|----------------|-------|--------------------------------------|-------|--------|-------|
|                   | Raw CH         | E1    | Raw SCG                              | E2    | Raw SB | E3    |
| <b>C</b>          | 56.32          | 50.75 | 52.38                                | 53.89 | 52.16  | 45.27 |
| <b>O</b>          | 24.91          | 39.75 | 30.85                                | 40.50 | 39.12  | 40.61 |
| <b>Mg</b>         | 0.32           | 0.86  | 0.43                                 | 0.92  | 0.30   | 0.72  |
| <b>S</b>          | 0.29           | 0.61  | 0.37                                 | 0.61  | 0.76   | 0.23  |
| <b>Cl</b>         | 1.68           | 0.77  | 0.31                                 | 0.00  | 0.59   | 0.33  |
| <b>Au</b>         | 3.83           | 15.41 | 4.70                                 | 13.02 | 5.66   | 12.5  |
| <b>Si</b>         | 3.05           | 0.63  | Element Weight Percent is Not Tested |       |        |       |
| <b>O/C</b>        | 0.44           | 0.78  | 0.58                                 | 0.75  | 0.75   | 0.90  |

#### 4.1.4 Fourier Transform-Infrared (FTIR) Analysis

FTIR spectroscopy was used to characterise the functional groups of lignocellulosic materials. The function groups corresponding to their vibrational frequencies are tabulated in Table 4.4. Table 4.5 compares the peak intensities of various type of biomass samples. The vibrational frequencies lower than  $800\text{ cm}^{-1}$  are considered as out of the plane bending mode. Basically, the FTIR analysis revealed that all the biomass samples have a typical LCB's adsorption bands with the presence of peaks around  $3500\text{ to }3200\text{ cm}^{-1}$ ,  $2900\text{ to }2800\text{ cm}^{-1}$  and  $1700\text{ cm}^{-1}$ , as shown in Figure 4.5. The conspicuous peaks of adsorption for each of the biomass samples were discussed accordingly.

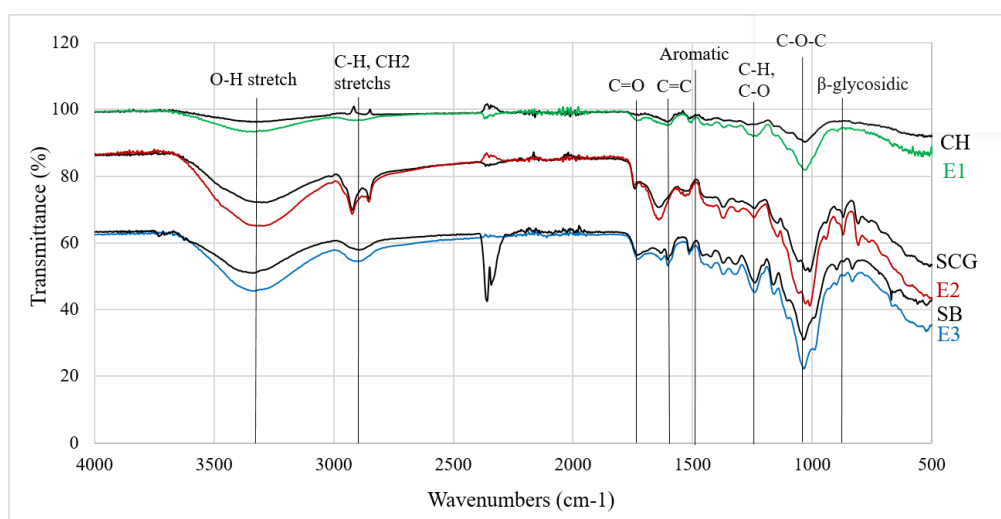


Figure 4.5: FTIR Spectrum of Raw and Treated Biomass Samples

##### 4.1.4.1 Coconut Husk

Cellulose associated peaks was found at wavenumber  $3337$ ,  $1372$  and  $1027\text{ cm}^{-1}$ , as shown in Figure 4.6. The increased band strength at  $3337\text{ cm}^{-1}$  could be assigned to the increased of cellulose recovery after removal of lignin. Besides, a marginally higher band intensity at  $2916\text{ cm}^{-1}$  and  $1372\text{ cm}^{-1}$  was observed as well, indicated strong H-bonds in the crystalline cellulose of CH were disrupted after pretreatment (Ebrahimi et al., 2017). Furthermore, treated CH samples clearly exhibited increased intensities at the peak  $1027\text{ cm}^{-1}$  may be correlated to the increase in porosity and exposure of the cellulose component in treated CH sample.

Hemicellulose and lignin related peaks could be distinguished at  $1733\text{ cm}^{-1}$  and  $1600$  to  $1400\text{ cm}^{-1}$ , respectively. Treated CH displayed a small peak at  $1733\text{ cm}^{-1}$ , implying that a proportion of hemicellulose underwent partial dissolution after elimination of lignin. Moreover, treated CH demonstrated a slight increase in intensity at the peak near  $1600$  to  $1400\text{ cm}^{-1}$ , which suggested the presence of remaining lignin content or other recalcitrance elements exist in the sample.

Additionally, the peak at  $2916\text{ cm}^{-1}$  which was assigned to lignin was present and revealed that the lignin was not completely eliminated from the treated CH. Guaiacyl-type lignin could be observed at the absorption peak near  $1247\text{ cm}^{-1}$  (Pacheco et al., 2018).

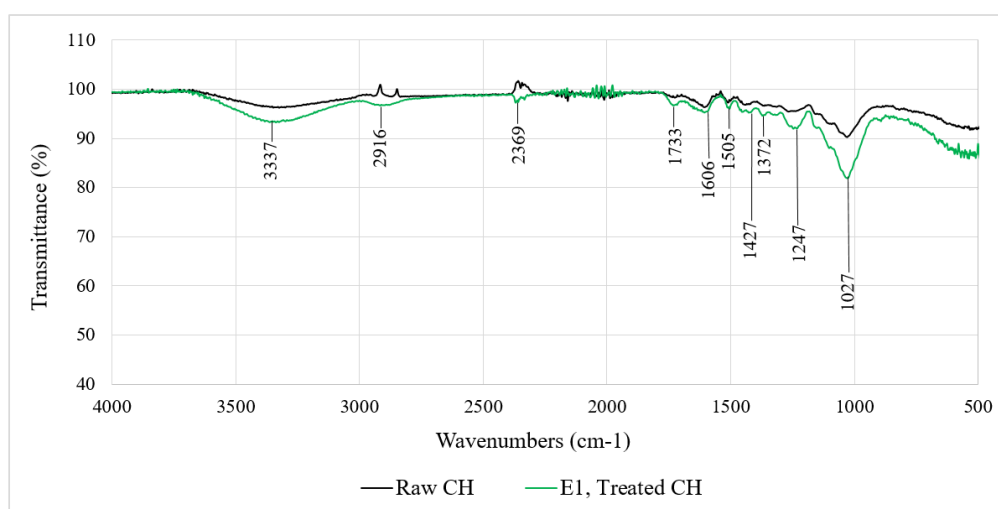


Figure 4.6: FTIR Spectrum of Raw and Treated Coconut Husk

#### 4.1.4.2 Spent Coffee Ground

Based on Figure 4.7, the broadening bands at  $3500$  to  $3000\text{ cm}^{-1}$  of treated SB could be translated into the  $\text{-OH}$  stretching or intermolecular disruption of this linkage of cellulose and lignin structure. The transmittance at  $1010\text{ cm}^{-1}$  represents  $\text{C-O}$  stretching of cellulose. The increase peak intensity at  $1010\text{ cm}^{-1}$  is an indicative of cellulose enrichment. The FTIR spectrum also shows an increase band strength from  $807$  to  $871\text{ cm}^{-1}$ , suggesting that the  $\beta$ -glycosidic linkages of cellulose is altered. This explains that the cellulose content in SCG has been transformed into a more porous and irregular structure after organosolv pretreatment. Besides, a weaker peak associated with hemicellulose ( $1745\text{ cm}^{-1}$

<sup>1</sup>) was observed indicated the removal of hemicellulose, as proven in the result of from Table 4.1.

Characteristic peak associated with lignin content fall in between 1600 to 1400  $\text{cm}^{-1}$  as indicated. The bands of treated SCG overlapped with the raw SCG at these wavenumber which denoted the insignificant lignin removal rate. The result was opposed to the pretreatment result obtained in Table 4.1 where the delignification effect was expected to be higher. This could be due to the higher composition of impurities in the solid. According to EDX analysis, treated SCG presented relatively higher concentration of Mg, S and Au elements.

Furthermore, according to the report of Ballesteros, Teixeira and Mussatto (2014), the bands at 1700 and 1600  $\text{cm}^{-1}$  is highly due to the existence of chlorogenic acids and caffeine in SCG. The peak at 1643  $\text{cm}^{-1}$  is being intense can be attributed to the absorption of these compounds when their concentration in the sample increases. Ballesteros, Teixeira and Mussatto (2014) also revealed that the transmittances at 2882 and 2829  $\text{cm}^{-1}$  are related to the asymmetric stretching of C–H bonds of methyl ( $-\text{CH}_3$ ) group in the caffeine molecule.

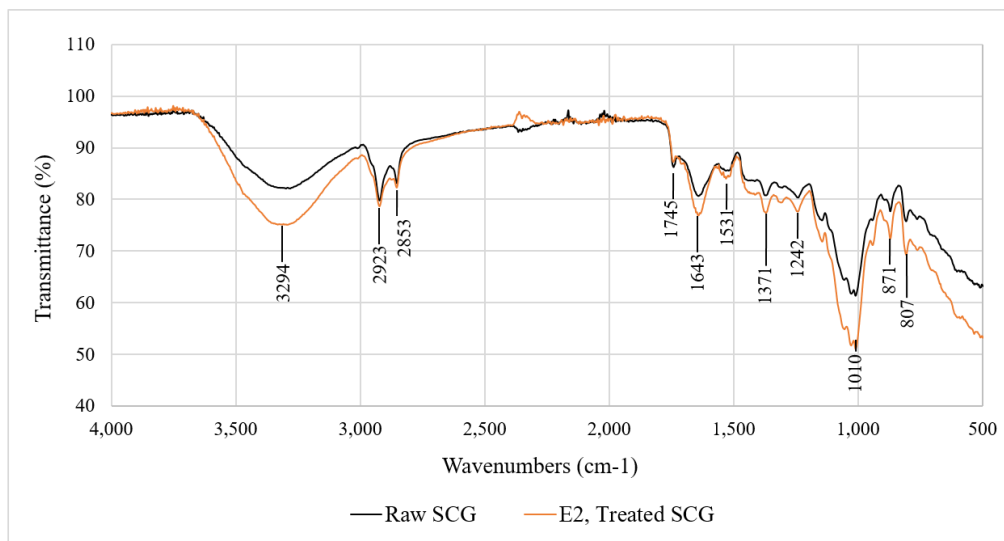


Figure 4.7: FTIR Spectrum of Raw and Treated Spent Coffee Ground

#### 4.1.4.3 Sugarcane Bagasse

Referring to Figure 4.8, absorption peaks associated with cellulose (3330, 1324 and 1034  $\text{cm}^{-1}$ ) were shown to be stronger for treated SB in comparison with the raw SB, suggesting the increase in cellulose content in the solid residue (Jin et

al., 2020). Treated SB displayed a higher band strength at  $832\text{ cm}^{-1}$  indicated that the glycosidic linkages in cellulose was disrupted and led to the enhancement in surface area and porosity of treated SB sample. Besides, the samples showed a weak peak at  $1727\text{ cm}^{-1}$  indicated the low concentration of hemicellulose in SB.

Lignin structure was characterised by the peaks at  $2896\text{ cm}^{-1}$  and  $1600$  to  $1400\text{ cm}^{-1}$ . Guaiacyl lignin unit could be observed at the absorption peak near  $1240\text{ cm}^{-1}$  (Pacheco et al., 2018). The peaks associated with lignin underwent little or no reduction in the intensity for treated bagasse, proved the inefficiency of delignification or might be resulted from the impurities exist in the sample during conducting FTIR analysis.

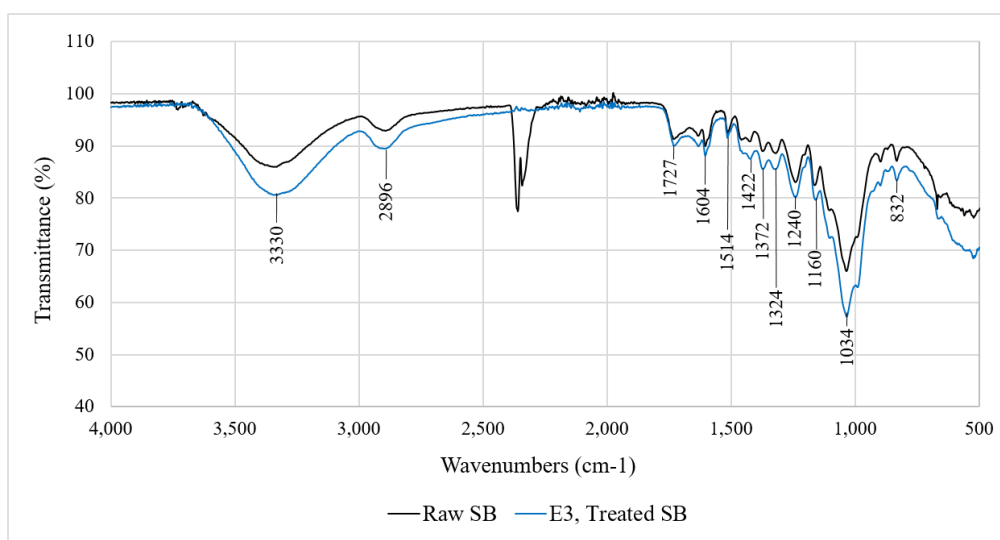


Figure 4.8: FTIR Spectrum of Raw and Treated Sugarcane Bagasse

Table 4.4: Polymers and Functional Groups of their respective Vibrational Frequencies

| Vibrational Frequencies<br>(cm <sup>-1</sup> ) | Peak Assignment   | Polymer                    | Reference   |
|--|---|----------------------------|---|
| <b>3,500 – 3,200</b>                           | O–H stretching vibrations for strong inter- and intra-molecular H-bonds     | Cellulose<br>Lignin        | (Ebrahimi et al., 2017)<br>(Jin et al., 2020)     |
| <b>2,900 – 2,800</b>                           | C–H stretching of alkyl structures and CH <sub>2</sub> stretching vibration | Lignin                     | (Pacheco et al., 2018)                            |
| <b>1,750 – 1,700</b>                           | C=O stretching vibration in acetyl groups and ester groups                  | Hemicellulose<br>Lignin    | (Ebrahimi et al., 2017)<br>(Pacheco et al., 2018) |
| <b>1,600</b>                                   | C=C stretching vibration  | Lignin                     | (Ebrahimi et al., 2017)                           |
| <b>1,500</b>                                   | Aromatic skeletal vibration   | Lignin                     | (Ebrahimi et al., 2017)                           |
| <b>1,460 – 1,400</b>                           | Asymmetric bending in CH <sub>3</sub>                                       | Lignin                     | (Ebrahimi et al., 2017)                           |
| <b>1,371 – 1,319</b>                           | C-H and C-O bending vibration in polysaccharides aromatic rings             | Cellulose<br>Hemicellulose | (Pacheco et al., 2018)                            |
| <b>1,270 – 1,230</b>                           | C–O vibration in the guaiacyl and syringyl ring                             | Lignin                     | (Pacheco et al., 2018)                            |
| <b>1,200 – 1000</b>                            | C–O stretch and deformation bands   | Cellulose<br>Lignin        | (Ebrahimi et al., 2017)                           |
| <b>1000</b>                                    | C-O-C vibrations of pyranose ring skeleton                                  | Cellulose                  | (Jin et al., 2020)                                |
| <b>800 – 900</b>                               | β-glycosidic bond between sugar units                                       | Cellulose                  | (Jin et al., 2020)                                |

Table 4.5: Functional Groups of their respective Vibrational Frequencies

| Vibrational<br>Frequencies<br>(cm <sup>-1</sup> ) | Polymer       | Biomass Sample |          |           |           |          |           |
|---|---------------|----------------|----------|-----------|-----------|----------|-----------|
|   |               | Raw CH         | E1       | Raw SCG   | E2        | Raw SB   | E3        |
| 3,500 – 3,200                                     | Cellulose     | Weakest        | Weaker   | Stronger  | Strongest | Weak     | Strong    |
|   | Lignin        |                |          |           |           |          |           |
| 2,900 – 2,800                                     | Lignin        | Weakest        | Weaker   | Stronger  | Strongest | Weak     | Strong    |
| 1,750 – 1,700                                     | Hemicellulose | Weakest        | Weaker   | Strongest | Stronger  | Weak     | Weak      |
|   | Lignin        |                |          |           |           |          |           |
| 1,600   | Lignin        | Weakest        | Weaker   | Stronger  | Strongest | Weak     | Weak      |
| 1,500   | Lignin        | Weakest        | Weaker   | Weak      | Weak      | Weak     | Weak      |
| 1,460 – 1,400                                     | Lignin        | Weak           | Moderate | Absent    | Absent    | Weak     | Moderate  |
| 1,371 – 1,319                                     | Cellulose     | Weakest        | Weaker   | Stronger  | Strongest | Weak     | Strong    |
|   | Hemicellulose |                |          |           |           |          |           |
| 1,270 – 1,230                                     | Lignin        | Weaker         | Weak     | Weak      | Strong    | Stronger | Strongest |
| 1,200 – 1000                                      | Cellulose     | Moderate       | Strong   | Stronger  | Strongest | Stronger | Strongest |
|   | Lignin        |                |          |           |           |          |           |
| 1000  | Cellulose     | Moderate       | Strong   | Stronger  | Strongest | Stronger | Strongest |
| 800 – 900   | Cellulose     | Absent         | Absent   | Stronger  | Strongest | Weak     | Moderate  |

#### 4.1.5 X-ray Diffraction (XRD) Analysis

XRD analysis was carried out to characterise the structural modifications of LCB after organosolv pretreatment. The CrI for raw and treated biomass samples are calculated by using Equation 3.16. The intense peak represented by crystallinity cellulose ( $I_{002}$ ), and the peak contributed by the amorphous region of biomass ( $I_A$ ) were tabulated in Table 4.6 accordingly. In general, the organosolv pretreatments of LCB will promote an increase in CrI because they preferentially remove the lignin and hemicellulose component, and to lesser extent some amorphous cellulose, which leading to the exposure of crystalline cellulose (Chandrasah, Rajamane and Jeyalakshmi, 2014).

Table 4.6: Crystallinity Index of Raw and Treated Biomass Samples

| Biomass Sample         | Intensity |       | Crystallinity Index,<br>CrI (%) |
|------------------------|-----------|-------|---------------------------------|
|                        | $I_{002}$ | $I_A$ |                                 |
| <b>Raw CH</b>          | 300       | 150   | 50.00                           |
| <b>E1, Treated CH</b>  | 378       | 106   | 71.96                           |
| <b>Raw SCG</b>         | 406       | 194   | 52.22                           |
| <b>E2, Treated SCG</b> | 382       | 168   | 56.02                           |
| <b>Raw SB</b>          | 368       | 142   | 61.41                           |
| <b>E3, Treated SB</b>  | 438       | 166   | 62.10                           |

After pretreatment of aqueous ethylene glycol, the increased of CrI for all the biomass samples is likely due to the partial dissolution of amorphous hemicellulose and lignin in accordance with the results obtained from Table 4.2. This revealed that the EG pretreatment was unable eliminate the lignin content completely, but it probably degraded the hemicellulose content in the samples (Kérzia et al., 2017).

Furthermore, the XRD analysis showed raw SG consists of the highest CrI as it possesses relatively higher amount of crystalline cellulose among the biomass samples. Meanwhile, a subtle change of CrI was found for raw and treated SB, implying that the pretreatment has low efficiency on changing the degree of cellulose crystallinity of sugarcane bagasse (Jin et al., 2020). SCG presented a mild increased of CrI after pretreatment which could be mainly

contributed by the elimination of disorder hemicellulose in accordance to its high hemicellulose removal rate as shown in Table 4.2. The highest increment in CrI was achieved by the treated CH, suggesting that organosolv pretreatment had effectively removed the hemicellulose, lignin, and amorphous cellulose content. This results the exposure of more crystalline cellulose and contribute to the increase of CrI.

The presence of crystalline cellulose in the LCB do not produce sharp diffraction peaks in XRD diffractogram but not amorphous materials. Based on Figure 4.9 to 4.11, the untreated biomass samples (seen in grey graphs), display a typical XRD pattern of amorphous structure in LCB, as not obvious sharp diffraction peak was observed. The amorphous nature is mostly attributed to the existence of large amounts of lignin, hemicellulose and amorphous cellulose content. Normally, hemicelluloses are more easily degraded under attack of organic solvent than amorphous cellulose due to their low degree of polymerisation and crystallinity (Santos et al., 2013).

The examination of crystallinity change in XRD profile by Segal approach through utilising the peak intensity is convenient for evaluating the relative difference between same types of LCBs. However, the quantity of crystalline and amorphous component in LCB could not be estimated accurately. Since, some samples will generate more than one crystalline peaks, but only the highest intensity of peak ( $I_{002}$ ) is taken into account for calculation. This ignores the contributions from other crystalline peaks and too much attentions are focused on single alignment of cellulose crystal lattice. Additionally, peaks in the cellulose diffratograms are very broad and greatly differ in their width. Thus, a simple intensity comparison cannot be expected to provide an accurate estimation of cellulose crystallinity (Schroeder, Gentile and Atalla, 1986).

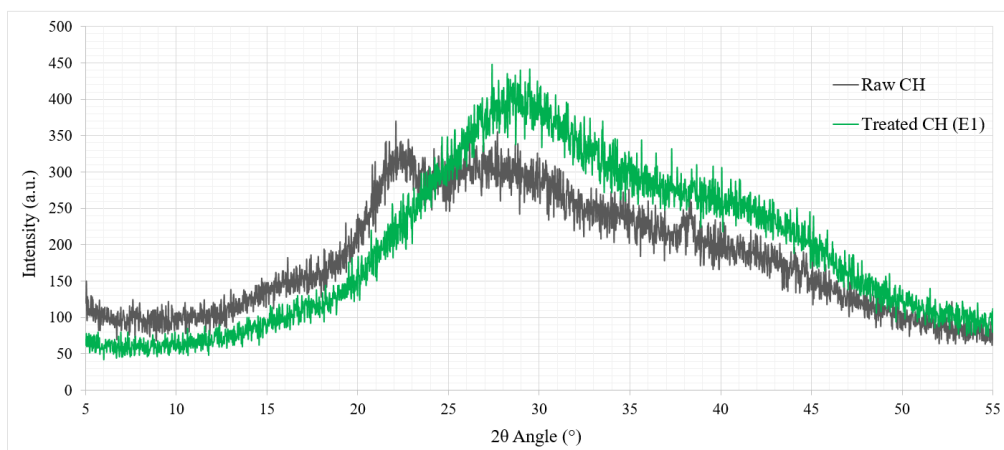


Figure 4.9: Diffractogram of Raw and Treated Coconut Husk

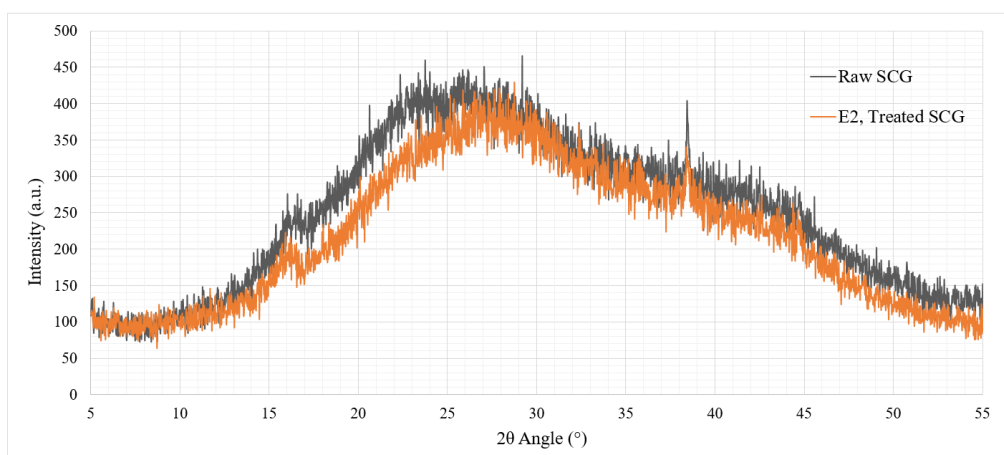


Figure 4.10: Diffractogram of Raw and Treated Spent Coffee Ground

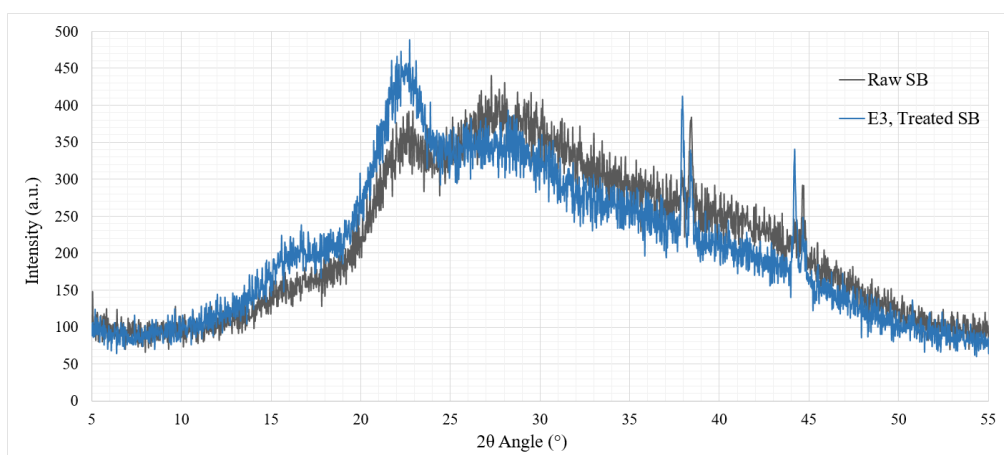


Figure 4.11: Diffractogram of Raw and Treated Sugarcane Bagasse

## 4.2 Organosolv Pretreatment of Biomass Mixture

A comprehensive study of organosolv pretreatment for various types of biomass mixture had been performed to investigate the interaction behaviours between CH, SCG and SB, and thus further verify the results obtained from pure biomass pretreatment. Different proportion of CH, SCG and SB were mixed well prior to pretreatment according to the fraction provided in Table 3.4. Similar procedures of TAPPI tests and spectroscopic analysis were carried out for treated biomass mixtures to examine their physiochemical properties.

### 4.2.1 Chemical Compositional Analysis

The outcomes of Experiment No. 4 to 9 are tabulated in Table 4.7 and Table 4.8, which included the chemical components recovery and removal rates, O/C ratios computed from EDX analysis and CrI obtained from XRD characterisation. Whereas, Table 4.9 lists the element presence in the samples in dried weight percent. Each of the data displayed are interrelated with each other, depending on the efficacy of organosolv pretreatment on the particular combination of biomass mixture.

Table 4.7: Chemical Composition of Treated Biomass Mixture

| Exp. No.  | Chemical Component Percentage (wt.% dry basis) |                     |                 |
|-----------|--|---------------------|-----------------|
|           | $\alpha$ - and $\beta$ -Cellulose              | $\gamma$ -Cellulose | Lignin          |
| <b>E4</b> | 53.68 $\pm$ 0.3                                | 19.83 $\pm$ 0.3     | 26.50 $\pm$ 0.6 |
| <b>E5</b> | 57.66 $\pm$ 1.2                                | 22.57 $\pm$ 1.2     | 19.77 $\pm$ 0.3 |
| <b>E6</b> | 54.94 $\pm$ 0.6                                | 16.68 $\pm$ 0.3     | 28.38 $\pm$ 0.9 |
| <b>E7</b> | 52.30 $\pm$ 0.7                                | 23.96 $\pm$ 0.8     | 23.73 $\pm$ 0.1 |
| <b>E8</b> | 54.51 $\pm$ 0.5                                | 23.05 $\pm$ 0.6     | 22.44 $\pm$ 0.3 |
| <b>E9</b> | 57.30 $\pm$ 0.2                                | 12.21 $\pm$ 0.2     | 30.49 $\pm$ 0.2 |

Based on Table 4.7, the overall result of total cellulose content has an average value of more than 50 %. The gamma-cellulose or hemicellulose concentration is mainly contributed by the SCG in the sample. Hence, the sample with high proportion of SCG showed an extensive percentage of hemicellulose content. For instance, E7 consists of 75 wt.% SCG possessed the

highest hemicellulose content, followed by E8 (25 wt.% SCG), E5 (50 wt.% SCG) and E4 (50 wt.% SCG). While, the increased of lignin composition is due to the increased quantity of CH in the sample, such as E9 (75 wt.% CH), E6 (50 wt.% CH) and E4 (50 wt.% CH)

According to Table 4.8, E5 (50 wt.% SCG + 50 wt.% SB) showed the highest delignification yield of  $15.98 \pm 1.4$  % and hemicellulose removal rate of  $24.77 \pm 1.4$  % among the biomass mixtures. This has resulted in a significant amount of cellulose enrichment in the sample with  $24.34 \pm 2.5$  % of recovery rate and a considerably low solid yield of  $66.21 \pm 1.0$  %. The efficacious of organosolv pretreatment on this combination of biomass mixture is mostly attributed to the high density of SCG that has gradually increased the solution mixing between solvent and solid, thus improved the hemicellulose degradation rate. Besides, the high cellulose concentration in native SB also contributed to its high cellulose recovery. The O/C ratio (0.7065) of E5 also reflected the existence of high cellulose content in the sample.

In contrast, E8 (25 wt.% SCG + 75 wt.% SB) represents a non-ideal biomass combination for organosolv pretreatment with the lowest delignification yield of  $6.762 \pm 1.4$  % and a moderate hemicellulose removal rate of  $15.79 \pm 2.3$  %. A poor solubilisation and dissolution of lignin and hemicellulose content leading to a low cellulose recovery in E8 ( $12.52 \pm 1.1$  %) with a relatively high solid yield ( $68.17 \pm 0.5$  %). The fairly low O/C ratio (0.4423) of E8 also indicated the deficient of lignin removal in the sample. This is most probably caused by the agitation issues as per mentioned, which is raised by SB that existed in a large proportion in the mixture.

Furthermore, a conspicuous small range of cellulose increment of  $7.928 \pm 1.2$  % was observed for E6 (50 wt.% CH + 50 wt.% SB) with a low O/C ratio of 0.4611. E6 also displayed a relatively low percentage yield for both lignin and hemicellulose removal rates. One of the reason is ascribed to the high biomass loading, leading to high viscosity of the suspension, in which the solvent could not wet the solid completely during organosolv pretreatment. Hence, resulted in an undesired elimination of lignin and hemicellulose component in E6.

Table 4.8: Chemical Components Recovery and Removal Rate of Treated Biomass Mixtures

| Exp. No. | Solid Recovery (%) | $\alpha$ - and $\beta$ -Cellulose Recovery (%) | $\gamma$ -Cellulose Removal (%) | Delignification Yield (%) |
|----------|--------------------|--|---------------------------------|---------------------------|
| E4       | 72.95 $\pm$ 1.4    | 14.77 $\pm$ 0.7                                | 17.20 $\pm$ 1.3                 | 10.68 $\pm$ 1.9           |
| E5       | 66.21 $\pm$ 1.0    | 24.34 $\pm$ 2.5                                | 24.77 $\pm$ 3.9                 | 15.98 $\pm$ 1.4           |
| E6       | 64.59 $\pm$ 1.3    | 7.928 $\pm$ 1.2                                | 10.68 $\pm$ 1.8                 | 7.726 $\pm$ 2.9           |
| E7       | 66.74 $\pm$ 0.7    | 17.53 $\pm$ 1.7                                | 19.08 $\pm$ 2.5                 | 8.883 $\pm$ 0.4           |
| E8       | 68.17 $\pm$ 0.5    | 12.52 $\pm$ 1.1                                | 15.79 $\pm$ 2.3                 | 6.762 $\pm$ 1.4           |
| E9       | 71.31 $\pm$ 2.5    | 12.14 $\pm$ 0.5                                | 21.96 $\pm$ 1.2                 | 9.861 $\pm$ 0.7           |

Table 4.9: Element Quantification of Treated Biomass Mixtures from EDX Analysis

| Exp. No. | Element (wt.%) |        |           |            |          |            |            | O/C Ratio |
|----------|----------------|--------|-----------|------------|----------|------------|------------|-----------|
|          | Carbon         | Oxygen | Magnesium | Sulphur    | Chlorine | Sodium     | Silicon    |           |
| E4       | 58.69          | 39.73  | 1.08      | Not Tested | 0.77     | Not Tested | 2.67       | 0.6769    |
| E5       | 58.37          | 41.24  | 0.00      | Not Tested | 0.38     | Not Tested | Not Tested | 0.7065    |
| E6       | 34.18          | 15.76  | 0.80      | 0.62       | 0.51     | Not Tested | 1.76       | 0.4611    |
| E7       | 66.92          | 31.55  | 0.46      | 0.28       | 0.44     | 0.35       | Not Tested | 0.4715    |
| E8       | 56.32          | 24.91  | 0.86      | 0.61       | 0.77     | 0.48       | 0.63       | 0.4423    |
| E9       | 59.00          | 30.47  | 0.37      | 0.65       | 0.69     | 0.45       | 1.60       | 0.5164    |

Additionally, a pretty good hemicellulose removal rate was achieved with the presence of SCG in the sample, such as E4, E5, E7 and E8. As indicated, SCG consists of major quantity of hemicellulose, thus an obvious disparity of hemicellulose concentration could be observed after effective organosolv pretreatment. When there is CH exists in the sample, the lignin removal rate was observed to be low, especially E9 (75 wt.% CH + 25 wt.% SB). This is because lignin is the major hindrance for breaking the intermolecular bonds of plant cell wall that block the accessibility of cellulose content.

The homogeneity of biomass mixture is difficult to achieve by simple mixing due to the density and particle size are varied among CH, SCG and SB. Although the blending and shaking of two lignocellulosic materials in an enclosed container was carried out, certain extent of uneven mixing is still exist. Thus, the ratio of biomass mixture is altered during the TAPPI tests for a small portion of treated samples. For this reason, the results obtained from Table 4.7 and Table 4.8 are lacking accuracy and cannot fully represent the chemical compositional of each samples.

#### **4.2.2 Structural and Morphology Analysis**

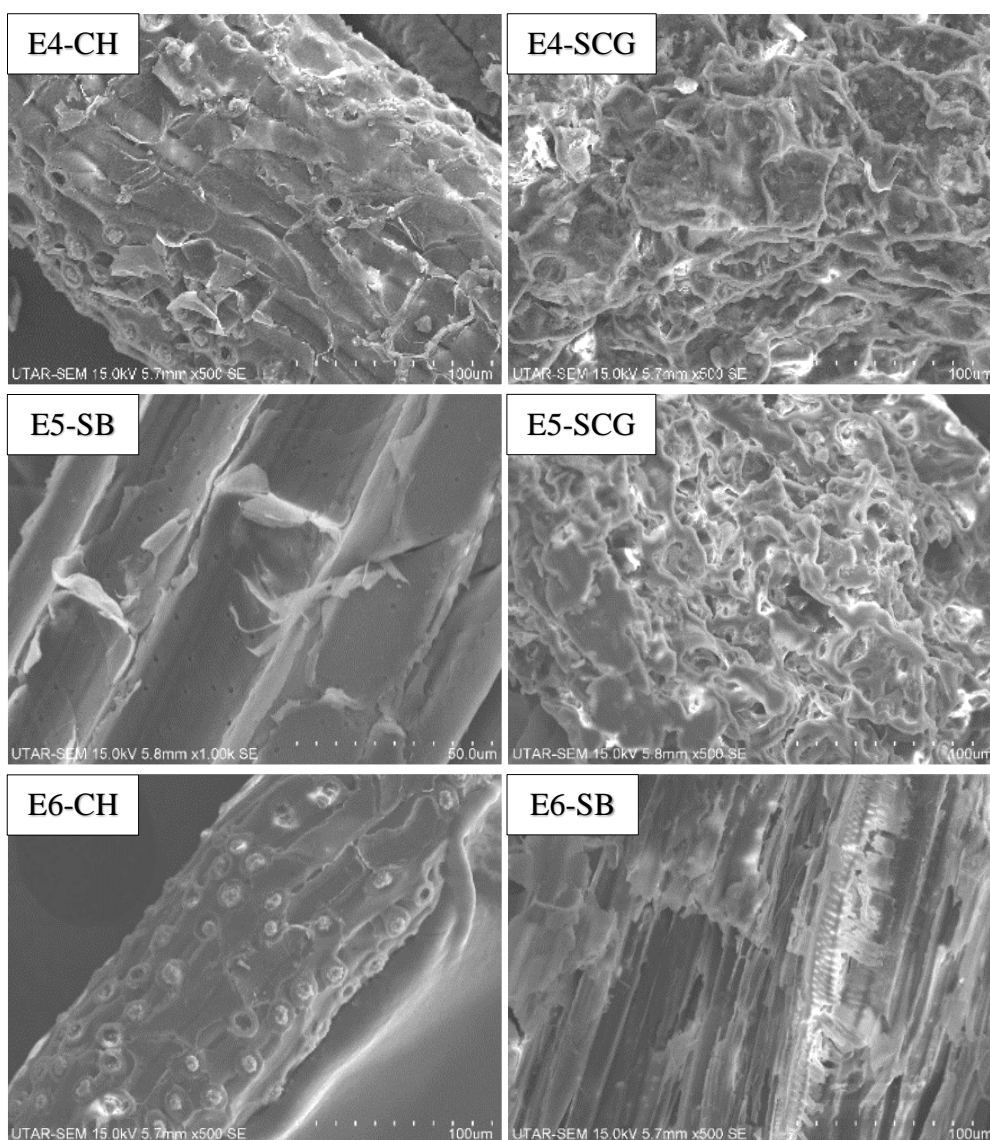
Figure 4.12 depicts the SEM images of treated biomass mixtures with their respective combination of biomass labelled at the top left corner of each picture.

The SEM images of CH macrofibres exhibit a rod-like structure with different surface characteristics. E4 and E9-CH display a porous and rough surface texture on the lateral part of fibres due to the detaching of SiO<sub>2</sub> phytoliths and unstructured of lignin fragment, in accordance to their delignification yield attained. E7-CH shows the parallel strip alignment structure, suggested that it is the microfiber of CH. A rift like cracking on the microfiber was observed, indicated the solvation of lignin and hemicellulose content. However, E6-CH displays a relatively intact microfiber surface with less pores and little detach of SiO<sub>2</sub> phytoliths due to the inefficient of organosolv pretreatment, which is corresponding to the result obtained from Table 4.8.

The SEM images for SCG in E4, E5 E7 and E8 show a typical porous structure of coffee ground. It was observed that their structures become disorder and irregular after pretreatment when compared with untreated SCG. An

obvious contrast is showed in E8-SCG, the splitting of fibre from SCG matrix was captured. However, it is difficult to distinguish the differences between untreated and treated SCG after mild conditions of pretreatment owing to its highly complex honeycomb like structure.

The surface layer of treated SB were removed after organosolv pretreatment, creating an opening structure of SB fibres. Tiny pores were observed in the pit of E5-SB, indicated higher chance of cellulose accessibility and cellulose recovery rate. E6 and E8-SB present a rougher and porous surface due to the splitting of fibre bundle. The cracking of fibre can be seen in E9-SB owing to the removal of lignin and hemicellulose content and physical reduction of bagasse.



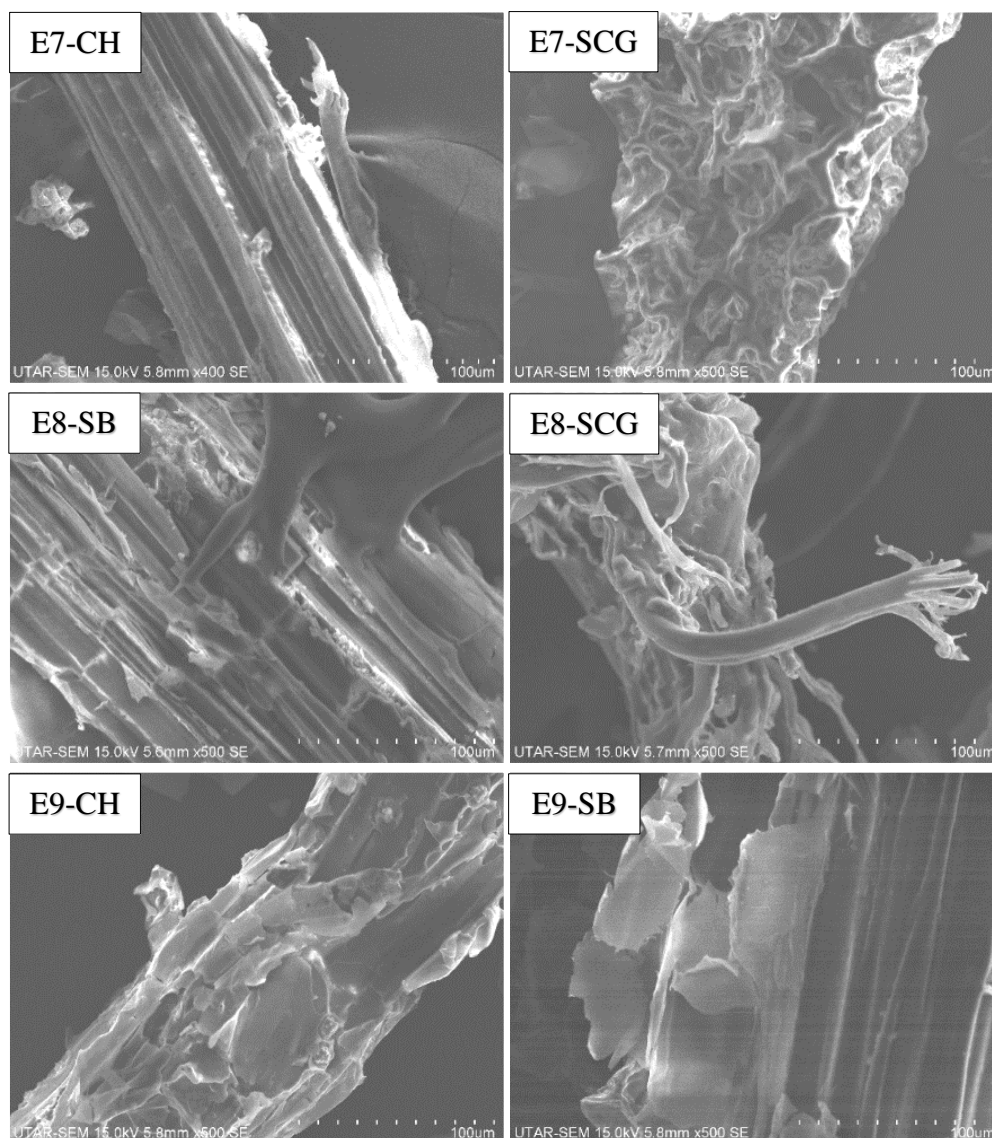


Figure 4.12: SEM images of Treated Biomass Mixtures under Magnification ranging from 400× to 1000×

### 4.2.3 FTIR Analysis

FTIR analysis was applied to examine the difference in chemical structure and functional groups for various types of biomass mixture. Figure 4.13 arranges the FTIR spectra of each biomass mixture according to their band strength. The prominent peaks of adsorption were discussed region by region with the aid of Table 4.4.

The overall FTIR analysis shows the characteristic band strength at the regions around  $3500 - 3200 \text{ cm}^{-1}$ ,  $2900 - 2800 \text{ cm}^{-1}$  and  $1750 - 1700 \text{ cm}^{-1}$ ,

revealed the existence of cellulose, hemicellulose and lignin content in a typical lignocellulosic material.

E6 shows the most intense peaks at  $3330\text{ cm}^{-1}$ ,  $2900\text{ cm}^{-1}$  and  $1730\text{ cm}^{-1}$ , which are associated with cellulose, lignin and hemicellulose biopolymers, respectively. E6 also exhibits the strongest band strength from  $1400 - 1600\text{ cm}^{-1}$ , denoted it consists of large amount of lignin. Besides, high intensity of peaks were observed at  $1030\text{ cm}^{-1}$  and  $896\text{ cm}^{-1}$ , indicated  $\beta$ -glycosidic bond between sugar units is altered and resulted in a high cellulose content. This is further supported by the result obtained in Table 4.7, where E6 contained a considerably quantity of three major biopolymer.

Higher band intensities were found at the region  $1000 - 1230\text{ cm}^{-1}$  for E5, indicated it possesses higher cellulose content than E6, in accordance to the chemical composition analysis. The FTIR spectra of E9 also displays a comparatively strong band strength at all the mentioned regions, especially the characteristic peak associated with cellulose at  $1024\text{ cm}^{-1}$ , as it contains a significant amount of cellulose in the sample.

The weakest adsorption of spectra was observed for E8, followed by E7 and E4, even though they have a considerably large quantity of biopolymer in the samples. This could be attributed to the inhomogeneous behaviour of the biomass mixture during undergoing the FTIR analysis and leading to an unfairly test. Besides, the presence of impurities in the samples such as Mg, S, Cl, Na, etc. content will tend to affect the analysis result as well.

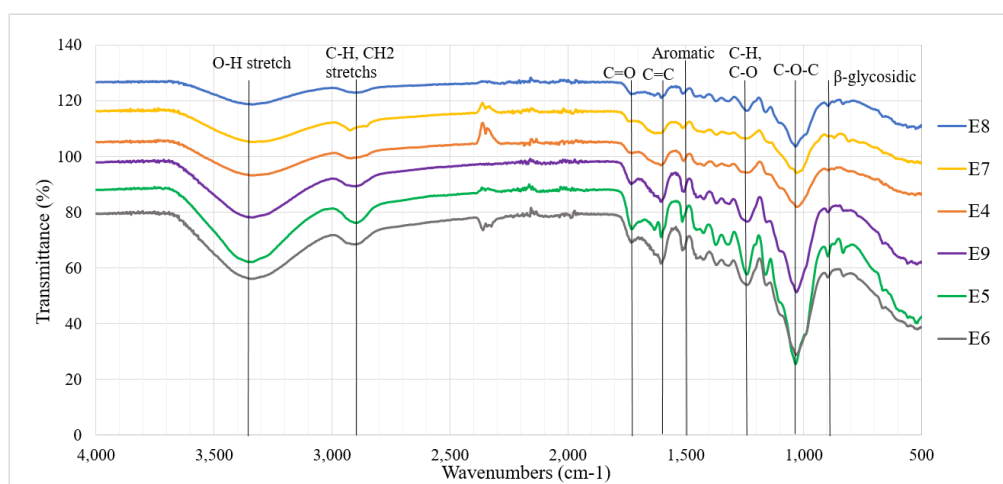


Figure 4.13: FTIR Spectrum of Treated Biomass Mixtures

#### 4.2.4 XRD Analysis

XRD analysis was used to determine the amount of crystalline cellulose in the biomass mixture by computation of CrI, as shown in Table 4.10. Figure 4.14 depicts the XRD spectrum for E4 to E9.

E4 possesses the highest CrI of 62.76 %, indicated that most of the amorphous regions are removed after organosolv pretreatment, as it has relatively high delignification yield and hemicellulose removal rate. However, an unexpectedly low CrI (52.57 %) was obtained for E5, even though it has the best lignin and hemicellulose removal rates. This is likely due to the incomplete removal of amorphous cellulose in the sample.

Additionally, the CrI of E6 and E7 are opposed to the chemical compositional analysis as tabulated in Table 4.7 and 4.8. This is mostly attributed to the homogeneity issue of biomass mixture as mentioned before. The proportion used for TAPPI tests is different from the one used for XRD analysis, hence leading to variation of result.

E8 has no outstanding performance in the elimination of lignin and hemicellulose content but it shows a high CrI of 56.21 %, implying that the sample might consists of mainly crystalline cellulose, especially in treated SB fraction. E9 gives a medium CrI of 47.98 % due its moderate performance in both hemicellulose and lignin removal rates, which is corresponding to its chemical composition result and further supported by its FTIR spectra.

Table 4.10: Crystallinity Index of Raw and Treated Biomass Mixtures

| Biomass Sample | Intensity |       | Crystallinity Index,<br>CrI (%) |
|----------------|-----------|-------|---------------------------------|
|                | $I_{002}$ | $I_A$ |                                 |
| <b>E4</b>      | 580       | 216   | 62.76                           |
| <b>E5</b>      | 506       | 240   | 52.57                           |
| <b>E6</b>      | 318       | 138   | 56.60                           |
| <b>E7</b>      | 222       | 142   | 36.04                           |
| <b>E8</b>      | 338       | 148   | 56.21                           |
| <b>E9</b>      | 346       | 180   | 47.98                           |

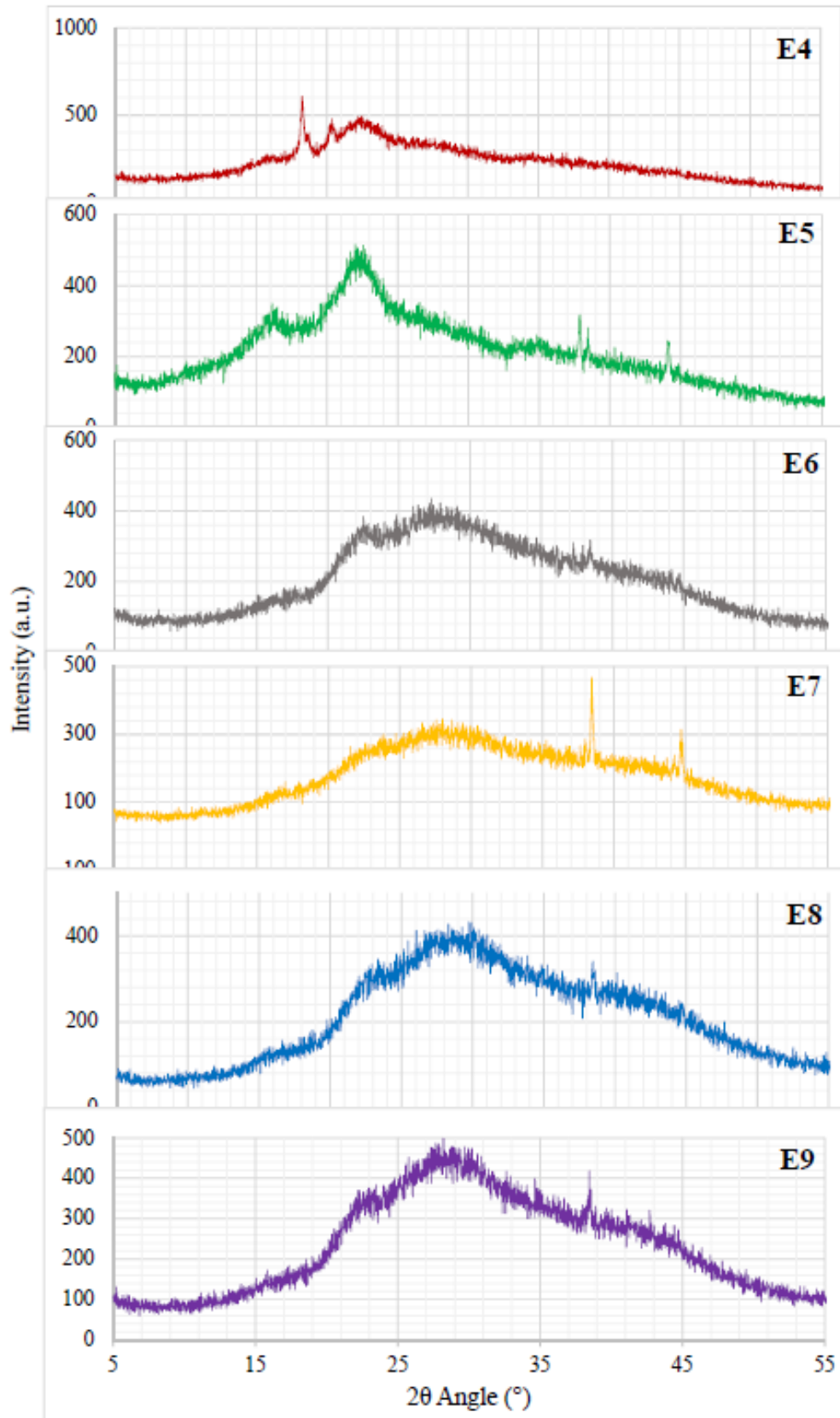


Figure 4.14: Diffractograms of Treated Biomass Mixtures

### 4.3 Model Development of Organosolv Pretreatment

A systematic investigation of the effect of lignin and hemicellulose composition on delignification, hemicellulose degradation and cellulose recovery rates after organosolv pretreatment has been performed through computing the mathematical models. Firstly, the model (M1) is built for pure biomass samples (E1, E2 and E3) based on the results obtained in Table 4.1 and Table 4.2. Secondly, a model (M2) which included the pure biomass samples and biomass mixtures (E1 to E9) were developed based on the results obtained in Table 4.7 and Table 4.8, to further verify the correlation acquired from the first model.

#### 4.3.1 Lignin Composition and Delignification Yield

The relationship between lignin composition and delignification yield was plotted in Figure 4.15. A trend line of  $R^2 = 0.2854$  was found for M1, showing a low influence of lignin concentration on organosolv delignification. Lignin confers mechanical strength to the plant cell wall which act as ‘adhesives’ and ‘fillers’ in between holocellulose components (Ding et al., 2018). It also acts like natural barrier that protect the plant cell wall from the exposure of carbohydrates. The high lignin content would make it possible for the fibre to resist the attack of organic solvent (EG) due to its stable coexistence structure. The increase of lignin composition would tend to rise the difficulty level in delignification but in less significant way, in accordance to the correlation obtained.

Additionally, the  $R^2 = 0.0907$  of M2 further proves that the relationship between two variables is weak. As discussed in Chapter 4.1.1, solid to liquid ratio had proven will affect the lignin removal rate of organosolv pretreatment. The biomass loading is depending on the density of LCB. When the weight of sample is set as controlled variable, the lower the density of sample, the greater the amount of sample subjected to organosolv pretreatment. This would result in low efficiency of mixing and delignification. Therefore, the statement of delignification yield is highly dependent on lignin composition is invalid.

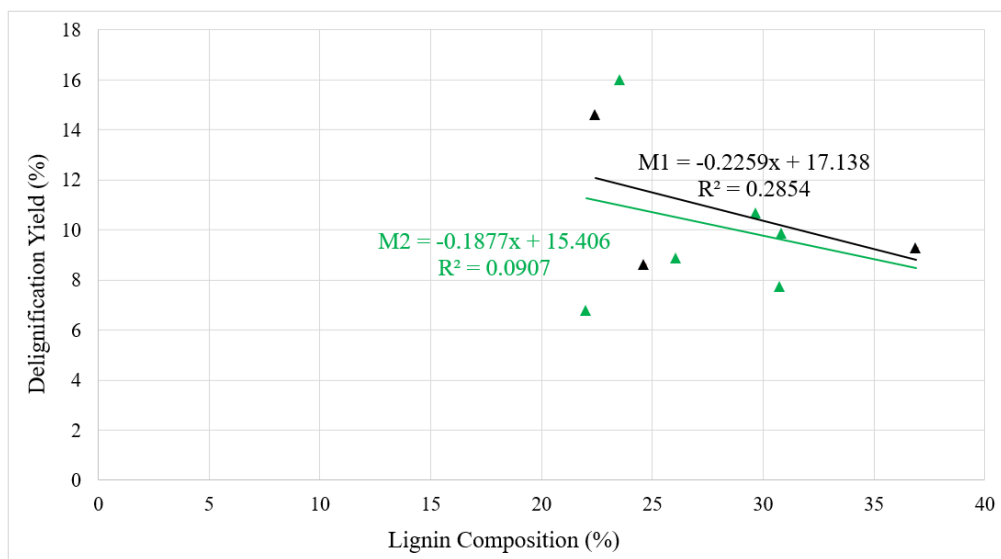


Figure 4.15: Relationship between Lignin Composition (%) and Delignification Yield (%)

#### 4.3.2 Hemicellulose Composition and Hemicellulose Removal Rate

The relationship between hemicellulose composition and hemicellulose removal rate was plotted in Figure 4.16. It was determined that the rate of hemicellulose degradation is related to the hemicellulose composition with a strong correlation of  $R^2 = 0.7140$  for M1. This is mostly contributed by the remarkable organosolv pretreatment on SCG. The pretreatment of SCG provides the best solution of mixing due its low biomass loading and thus promote the dissolution of hemicellulose.

However, a weak correlation of  $R^2 = 0.5363$  was determined for M2, reflected that the mixing of biomass will tend to affect the hemicellulose removal rate. With the presence of other high lignin compound biomass, the hindrance that lower down the hemicellulose degradation rate increases. Though, it still shows a relationship between them. Since higher hemicellulose content provides greater removal, it is reasonable to assume that high hemicellulose samples become solvated by EG during organosolv pretreatment.

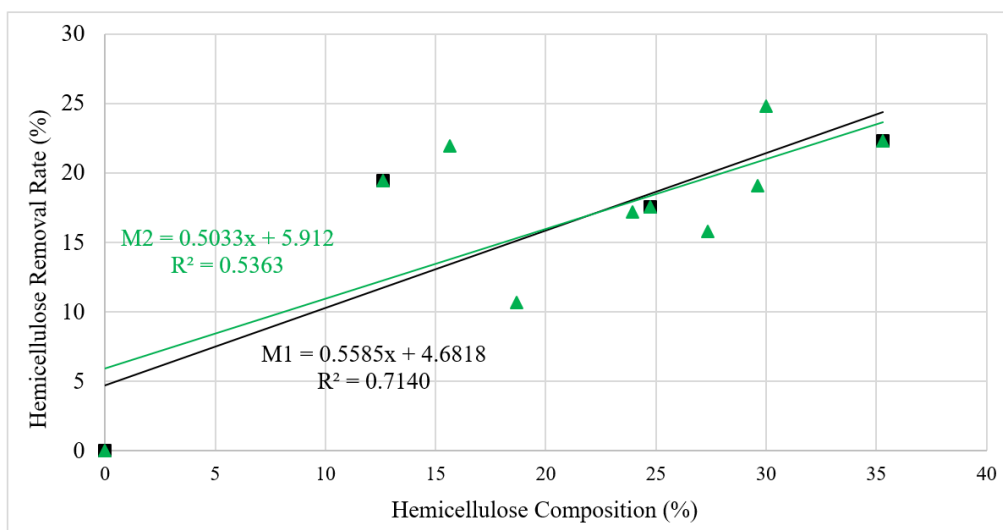


Figure 4.16: Relationship between Hemicellulose Composition (%) and Hemicellulose Removal Rate (%)

### 4.3.3 Delignification Yield and Hemicellulose Removal Rate

The relationship between delignification yield and hemicellulose removal rate was plotted, as shown in Figure 4.17. A superior correlation of hemicellulose composition and hemicellulose removal rate was found for M1 with  $R^2 = 0.9224$ . The correlation of this two variables appears to be an indirect relationship. Hemicelluloses are intermediates that connect cellulose and lignin through intermolecular bonds to form secondary cell wall. The increased of lignin elimination would improve the exposure of holocellulose components, allowing better accessibility of the solvent to break the lignin-hemicellulose bonds. Hence, more hemicellulose will be readily for dissolution and results in faster reactions of hemicellulose degradation (Santos et al., 2013).

Furthermore, a trend line of  $R^2 = 0.8226$  was determined for M2, which further confirmed the strong correlation between each variable. Delignification yield and hemicellulose removal rate seem to be closely associated, and this mathematical model appears to be more responsible to apply for other LCBs.

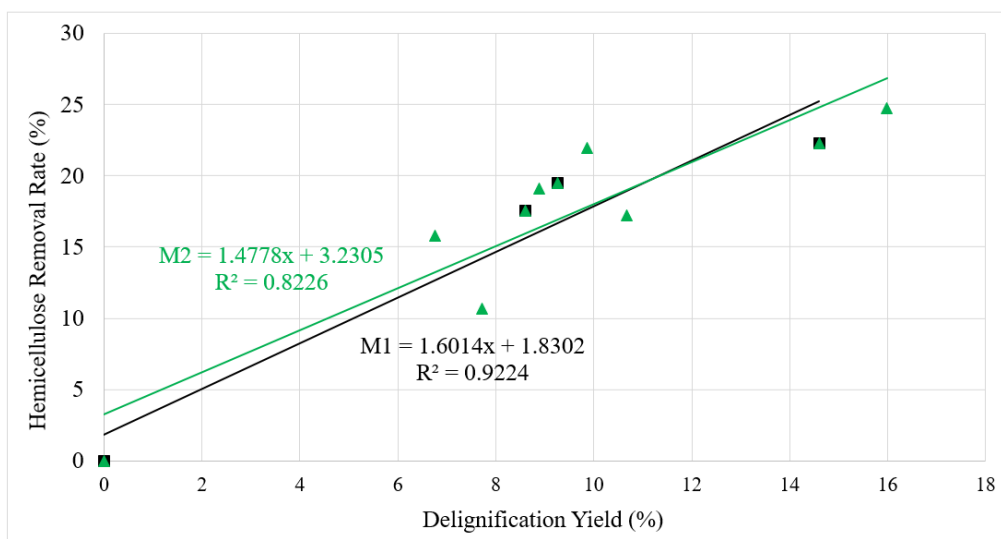


Figure 4.17: Relationship between Delignification Yield (%) and Hemicellulose Removal Rate (%)

#### 4.3.4 Delignification Yield, Hemicellulose Removal Rate and Cellulose Recovery

The relationship between delignification yield and cellulose recovery was plotted in Figure 4.18. The  $R^2$ -values for M1 and M2 are 0.9132 and 0.8500 respectively, indicating a high influence of organosolv delignification on cellulose recovery. Whereas, Figure 4.19 shows the relationship between hemicellulose removal rate and cellulose recovery. It was noticed that hemicellulose removal rate is correlated with cellulose recovery with  $R^2 = 0.7124$  for M1 and  $R^2 = 0.7026$  for M2.

Lignin represents the major recalcitrant in plant cell wall which is covalently bonded with hemicellulose, while hemicellulose is linked with cellulose by hydrogen bonds. When the matrix structure of fibre was interrupted after subjected to organic solvent (EG), the holocellulose components are released due to the cleavage of these linkages (Santos et al., 2013). Thus, higher amount of hemicellulose are readily for degradation and retained the cellulose content in the cell wall. It can be concluded that, the higher the delignification yield, the faster the hemicellulose degradation rate, the more the cellulose being recovered.

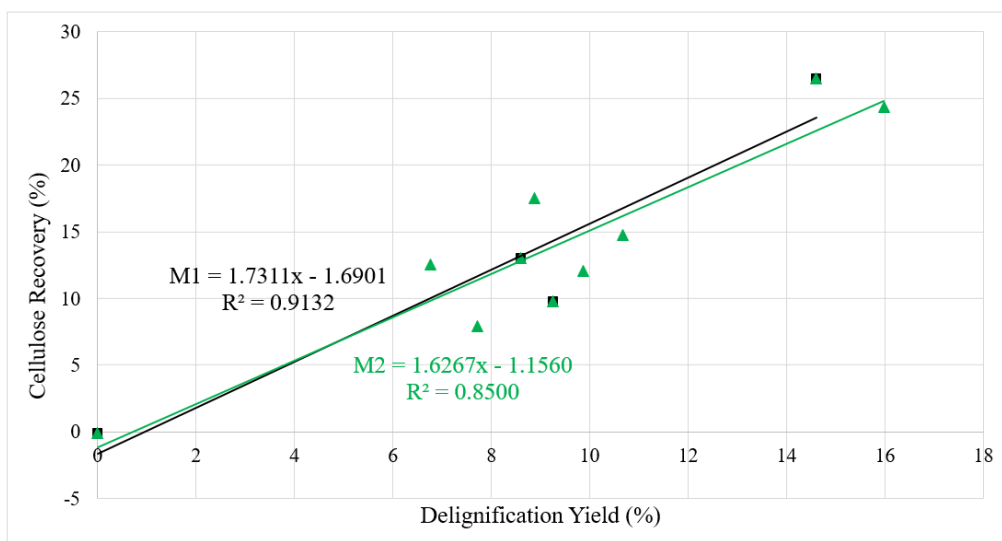


Figure 4.18: Relationship between Delignification Yield (%) and Cellulose Recovery (%)

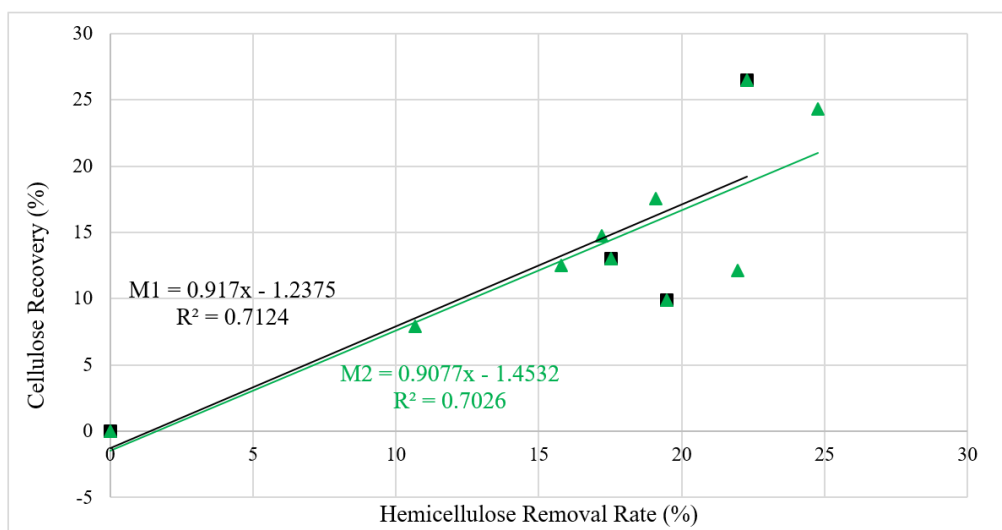


Figure 4.19: Relationship between Hemicellulose Removal Rate (%) and Cellulose Recovery (%)

## CHAPTER 5

### CONCLUSIONS AND RECOMMENDATIONS

#### 5.1 Conclusions

In this research study, the chemical compositional analysis was carried for CH, SCG and SB according to the TAPPI method. The raw CH consists of the highest lignin content of  $36.89 \pm 1.3$  %, followed by SB of  $24.62 \pm 0.3$  %, and SCG of  $22.43 \pm 0.2$  %. Raw SB yields the greatest amount of alpha-cellulose with  $41.01 \pm 4.3$  %, followed by CH with  $30.73 \pm 1.7$  %, and SCG with  $22.68 \pm 1.0$  %. The beta-cellulose composition of CH, SCG and SB are  $20.60 \pm 4.1$  %,  $19.56 \pm 6.2$  % and  $9.506 \pm 7.2$  %, respectively. SCG is rich with gamma-cellulose with  $35.28 \pm 7.5$  %, while CH and SB consist of  $12.62 \pm 6.4$  % and  $24.73 \pm 2.7$  % gamma-cellulose respectively. Aqueous ethylene glycol (30 v/v%) pretreatment of pure biomass samples and biomass mixtures were performed at 80 °C for 40 minutes with solid to liquid loading of 1:20.

The potential factors that tend to affect the efficacy of organosolv pretreatment had been discovered. Firstly, the higher the lignin content, the lower the delignification yield. Treated SCG with the lowest lignin content showed the best delignification yield of  $14.60 \pm 2.5$  %. Secondly, the lower the density of the biomass sample, the higher the biomass loading required to fulfil the S/L ratio. Then, the more viscous the pretreatment solution, the lower the delignification yield. The lightest SB sample showed the lowest delignification yield of  $8.590 \pm 2.7$  %.

Several characterisation techniques had been underwent to investigate the physical and chemical changes of biomass before and after the pretreatment process. SEM analysis of CH showed that the treated coconut macrofibre exhibited a rougher and porous surface texture accompanied with the detaching of SiO<sub>2</sub> phytoliths. Whereas, treated SCG displayed a less order and loosening honeycomb like structure. While, an opening structure with several tiny holes could be observed from treated SB due to the cracking of fibre after organosolv pretreatment. FTIR analysis showed that the spectrum generated by treated biomass samples exhibit a broader and higher intensity of band strength. The

biomass samples also displayed a typical FTIR spectra of LCB with the presence of cellulose, hemicellulose and lignin content. The crystallinity of cellulose can be improved through modification of cellulose structure and removal of amorphous regions in the plant cell wall by organosolv pretreatment. CH showed the greatest enhancement of CrI from 50.00 % to 71.96 %. The CrI of treated SCG and SB are 56.02 % and 62.10 % respectively.

For organosolv pretreatment of various combinations of biomass mixture, E5 showed the best performance of organosolv pretreatment with the highest delignification yield of  $15.98 \pm 1.4$  %, highest hemicellulose removal rate of  $24.77 \pm 3.9$  % and highest total cellulose recovery of  $24.34 \pm 2.5$  %. In contrast, E6 showed the most undesired result of organosolv pretreatment, with the second lowest delignification yield of  $7.726 \pm 2.9$  %, lowest hemicellulose removal rate of  $10.68 \pm 1.8$  % and lowest total cellulose recovery of  $7.928 \pm 1.2$  %.

Several models of organosolv pretreatment was developed. Firstly, the delignification yield possessed a weak relationship with lignin composition, with  $0.2854 \leq R^2 \leq 0.0907$ . Secondly, the hemicellulose removal rate is correlated with hemicellulose composition with  $0.5363 \leq R^2 \leq 0.7140$ . Thirdly, hemicellulose removal rate is highly correlated with delignification yield with  $0.8226 \leq R^2 \leq 0.9224$ . It can be concluded that the higher the delignification yield and hemicellulose removal rate, the higher the cellulose recovery.

In a nutshell, all the objectives were achieved in the end of this study. The chemical composition of each biomass sample were determined. Characterisation of the biomass samples were carried out. The mathematical models for organosolv pretreatment were established. Lastly, possible factors of organosolv pretreatment were discovered and discussed as well.

## **5.2 Recommendations for Future Work**

The research methodology was conducted accordingly based on the scope of study. However, some deviations of result caused by materials, human errors equipment and analytical instruments limitations are inevitable. Therefore, it is significant to propose any useful recommendations to enhance the accuracy and

reliability of the experiments results for future work. The suggested recommendations are listed as below.

- (i) The composition of other minor components such as ash, protein and lipid content that presence in the CH, SCG and SB should be determined accordingly.
- (ii) The fractions of hemicellulose such as arabinose, mannose, galactose and xylose should be determined as well.
- (iii) The inter-unit linkages *p*-hydroxyphenyl, guaiacyl and syringyl lignin units present in the CH, SCG and SB should be investigated to examine the major recalcitrant within lignin content.
- (iv) Perform additional parameter study for ethylene glycol-based organosolv pretreatment, such as concentration of solvent used, temperature, contact time and solid to liquid loading to investigate the optimal pretreatment conditions for CH, SCG and SB, thus broader the range of input value for the model developed.
- (v) A wider range of samples from different types of lignocellulosic biomass should be included, such as hardwood, softwood and grass.
- (vi) Chemical composition and spectroscopic analyses should be conducted as soon as the samples were generated to reduce and prevent the contamination of samples.
- (vii) Any equipment used such as weighing machine, heating mantle, hot plate, etc. should be consistent throughout the research study to minimise discrepancies.
- (viii) An advanced mixer should be applied to promote perfect mixing of biomass mixture before pretreatment process and any analysis procedures.

## REFERENCES

- Abbott, D., 2015. *Defining Measures of Success for Predictive Models*. [online] Available at: <<https://www.predictiveanalyticsworld.com/machinelearningtimes/defining-measures-of-success-for-predictive-models-0608152/5519/>> [Accessed 20 July 2019].
- Ahorsu, R., Medina, F. and Constantí, M., 2018. Significance and challenges of biomass as a suitable feedstock for bioenergy and biochemical production: A review. *Energies*, 11(3366), pp. 1–19.
- Alghooneh, A., Mohammad Amini, A., Behrouzian, F. and Razavi, S.M.A., 2017. Characterisation of cellulose from coffee silverskin. *International Journal of Food Properties*, 20(11), pp. 2830–2843.
- Amaral, H.R., Cipriano, D.F., Santos, M.S., Schettino, M.A., Ferreti, J.V.T., Meirelles, C.S., Pereira, V.S., Cunha, A.G., Emmerich, F.G. and Freitas, J.C.C., 2019. Production of high-purity cellulose, cellulose acetate and cellulose-silica composite from babassu coconut shells. *Carbohydrate Polymers*, 210(2018), pp. 127–134.
- Amore, A., Ciesielski, P. and Lin, C., 2016. Development of Lignocellulosic Biorefinery Technologies: Recent Advances and Current Challenges. *Australian Journal of Chemistry*, 1(1), pp. 1–42.
- Anwar, Z., Gulfraz, M. and Irshad, M., 2014. Agro-industrial lignocellulosic biomass a key to unlock the future bio-energy: A brief review. *Journal of Radiation Research and Applied Sciences*, 7(2), pp. 163–173.
- Arsyad, M. and Wardana, I.N.G., 2015. The morphology of coconut fiber surface under chemical treatment. *Revista Materia*, 20(1), pp. 169–177.
- Bakri, B., Naharuddin, Putra, A.E.E., Renreng, I. and Arsyad, H., 2018. Characterization of coir fibers after alkali and microwave treatments. *ARPN Journal of Engineering and Applied Sciences*, 13(4), pp. 1335–1339.
- Ballesteros, L.F., Teixeira, J.A. and Mussatto, S.I., 2014. Chemical, Functional, and Structural Properties of Spent Coffee Grounds and Coffee Silverskin. *Food and Bioprocess Technology*, 7(12), pp. 3493–3503.
- Baruah, J., Nath, B.K., Sharma, R. and Kumar, S., 2018. Recent Trends in the Pretreatment of Lignocellulosic Biomass for Value-Added Products. *Front. Energy Res.*, 6(141), pp. 1–19.
- Bernama, 2019. *Lack of local company participation in renewable energy: Jomo*. [online] Available at: <<https://www.nst.com.my/news/nation/2019/03/466141/lack-local-company-participation-renewable-energy-jomo>> [Accessed 18 April 2020].

De Bhowmick, G., Sarmah, A.K. and Sen, R., 2018. Lignocellulosic biorefinery as a model for sustainable development of biofuels and value added products. *Bioresource Technology*, 247(9), pp. 1144–1154.

Bildirici, M. and Özaksoy, F., 2018. An analysis of biomass consumption and economic growth in transition countries. *Economic Research-Ekonomska Istrazivanja*, 31(1), pp. 386–405.

Burton, J., 2018. *The World Leaders In Coconut Production - WorldAtlas*. [online] Available at: <<https://www.worldatlas.com/articles/the-world-leaders-in-coconut-production.html>> [Accessed 15 April 2020].

Cequier-Sánchez, E., Rodríguez, C., Ravelo, Á.G. and Zárate, R., 2008. Dichloromethane as a solvent for lipid extraction and assessment of lipid classes and fatty acids from samples of different natures. *Journal of Agricultural and Food Chemistry*, 56(12), pp. 4297–4303.

Chan, Y.H., Cheah, K.W., How, B.S., Loy, A.C.M., Shahbaz, M., Singh, H.K.G., Yusuf, N.R., Shuhaili, A.F.A., Yusup, S., Ghani, W.A.W.A.K., Rambli, J., Kansha, Y., Lam, H.L., Hong, B.H. and Ngan, S.L., 2019. An overview of biomass thermochemical conversion technologies in Malaysia. *Science of the Total Environment*, 680(1), pp. 105–123.

Chandrasasa, R., Rajamane, N. and Jeyalakshmi, 2014. Development of Cellulose Nanofibres from Coconut Husk. *International Journal of Emerging Technology and Advanced Engineering Website: www.ijetae.com ISO Certified Journal*, 9001(4), pp. 88–93.

Chin, D.W.K., Lim, S., Pang, Y.L., Leong, L.K. and Lim, C.H., 2019. Investigation of Organosolv Pretreatment to Natural Microbial-Degraded Empty Fruit Bunch for Sugar based Substrate Recovery. *Energy Procedia*, 158(1), pp. 1065–1071.

Council, N.R., 2007. *Models in Environmental Regulatory Decision Making*. Washington, DC: The National Academies Press. pp. 83–84.

Ding, K., Le, Y., Yao, G., Ma, Z., Jin, B., Wang, J. and Jin, F., 2018. A rapid and efficient hydrothermal conversion of coconut husk into formic acid and acetic acid. *Process Biochemistry*, 68(3), pp. 131–135.

Duzevik, D., 2017. *Advantages and Disadvantages of Simulation*. Hoboken, New Jersey: Blackwell Publishing Ltd.

Ebrahimi, M., Caparanga, A.R., Ordone, E.E. and Villa, O.B., 2017. Evaluation of organosolv pretreatment on the enzymatic digestibility of coconut coir fibers and bioethanol production via simultaneous saccharification and fermentation. *Renewable Energy An International Journal*, 109(1), pp. 41–48.

Eduardo, C., Silva, D.F., Maria, I.R. and Garcia, R., 2016. Bioethanol production from coconut husk fiber. *Food Technology*, 46(10), pp. 1872–1877.

Efthymiopoulos, I., Hellier, P., Ladommatos, N., Kay, A. and Mills-Lampsey, B., 2018. Integrated strategies for water removal and lipid extraction from coffee industry residues. *Sustainable Energy Technologies and Assessments*, 29(4), pp. 26–35.

Enerdata, 2019. *Global Energy Statistical Yearbook 2019 | World Energy Consumption Statistics*. [online] Available at: <<https://yearbook.enerdata.net/total-energy/world-consumption-statistics.html>> [Accessed 18 April 2020].

Esmeraldo, M.A., Barreto, A.C.H., Freitas, J.E.B., Fechine, P.B.A., Sombra, A.S.B., Corradini, E., Mele, G., Maffezzoli, A. and Mazzetto, S.E., 2010. Dwarf-green coconut fibers: A versatile natural renewable raw bioresource. Treatment, morphology, and physicochemical properties. *BioResources*, 5(4), pp. 2478–2501.

Espirito Santo, M., Rezende, C.A., Bernardinelli, O.D., Pereira, N., Curvelo, A.A.S., deAzevedo, E.R., Guimarães, F.E.G. and Polikarpov, I., 2018. Structural and compositional changes in sugarcane bagasse subjected to hydrothermal and organosolv pretreatments and their impacts on enzymatic hydrolysis. *Industrial Crops and Products*, 113(1), pp. 64–74.

Fatmawati, A., Agustriyanto, R. and Liasari, Y., 2013. Enzymatic hydrolysis of alkaline pretreated coconut coir. *Bulletin of Chemical Reaction Engineering and Catalysis*, 8(1), pp. 34–39.

Huzir, N.M., Aziz, M.M.A., Ismail, S.B., Abdullah, B., Mahmood, N.A.N., Umor, N.A. and Syed Muhammad, S.A.F. ad, 2018. Agro-industrial waste to biobutanol production: Eco-friendly biofuels for next generation. *Renewable and Sustainable Energy Reviews*, 94(11), pp. 476–485.

Jin, Y., Shi, Z., Xu, G., Yang, H. and Yang, J., 2020. A stepwise pretreatment of sugarcane bagasse by alkaline and hydroxymethyl reagent for bioethanol production. *Industrial Crops and Products*, 145(1), pp. 1–8.

Kérzia, C., Araújo, C. De, Campos, A.D.O., Eduardo, C., Padilha, D.A., Canindé, F., Júnior, D.S., Jéssica, R. and Macedo, G.R. De, 2017. Bioresource Technology Enhancing enzymatic hydrolysis of coconut husk through *Pseudomonas aeruginosa* AP 029 / GLVIIA rhamnolipid preparation. *Bioresource Technology*, 237(1), pp. 20–26.

Kim, S. and Dale, B.E., 2004. Global potential bioethanol production from wasted crops and crop residues. *Biomass and Bioenergy*, 26(4), pp. 361–375.

Lalman, J.A., Shewa, W.A. and Gallagher, J., 2016. Biofuels Production from Renewable Feedstocks. In: Peter C.K. Lau, eds. *Quality Living Through Chemurgy and Green Chemistry*. Berlin: Springer. pp. 193–214

Lee, M., Yang, M., Choi, S., Shin, J., Park, C., Cho, S.K. and Kim, Y.M., 2019. Sequential production of lignin, fatty acid methyl esters and biogas from spent coffee grounds via an integrated physicochemical and biological process. *Energies*, 12(12), pp.1–13.

Lindsey, R., 2020. *Climate Change: Atmospheric Carbon Dioxide* / NOAA *Climate.gov*. [online] Available at: <<https://www.climate.gov/news-features/understanding-climate/climate-change-atmospheric-carbon-dioxide>> [Accessed 18 April 2020].

Mahmood, K. and Shafique, F., 2010. Model development as a research tool: an example of PAK-NISEA. *Library Philosophy and Practice*, 1522(0222), pp. 1–13.

Mesa, L., López, N., Cara, C., Castro, E., González, E. and Mussatto, S.I., 2016. Techno-economic evaluation of strategies based on two steps organosolv pretreatment and enzymatic hydrolysis of sugarcane bagasse for ethanol production. *Renewable Energy*, 86(1), pp. 270–279.

Moreira-Vilar, F.C., Siqueira-Soares, R.D.C., Finger-Teixeira, A., De Oliveira, D.M., Ferro, A.P., Da Rocha, G.J., Ferrarese, M.D.L.L., Dos Santos, W.D. and Ferrarese-Filho, O., 2014. The acetyl bromide method is faster, simpler and presents best recovery of lignin in different herbaceous tissues than klason and thioglycolic acid methods. *PLoS ONE*, 9(10), pp. 1–7.

Nantnarphirom, P., Kraithong, W., Viriya-Empikul, N. and Eiad-Ua, A., 2017. Organosolv pretreatment transformation process of bagasse to porous carbon material. *Materials Today: Proceedings*, 4(5), pp. 6261–6266.

Nguyen, Q.A., Cho, E., Trinh, L.T.P., Jeong, J. su and Bae, H.J., 2017. Development of an integrated process to produce D-mannose and bioethanol from coffee residue waste. *Bioresource Technology*, 244(1), pp. 1039–1048.

Niju, S. and Swathika, M., 2019. Delignification of sugarcane bagasse using pretreatment strategies for bioethanol production. *Biocatalysis and Agricultural Biotechnology*, 20(1), pp. 1–7.

Nitsos, C. and Rova, U., 2018. Organosolv Fractionation of Softwood Biomass for Biofuel and Biorefinery Applications. *Energies*, 11(5), pp. 193–220.

Ozturk, M., Saba, N., Altay, V., Iqbal, R., Hakeem, K.R., Jawaid, M. and Ibrahim, F.H., 2017. Biomass and bioenergy: An overview of the development potential in Turkey and Malaysia. *Renewable and Sustainable Energy Reviews*, 79(1), pp. 1285–1302.

Pacheco, C.M., Bustos, C., Reyes, G., Aguayo, M.G. and Rojas, O.J., 2018. Characterization of Residues from Chilean Blueberry Bushes: A Potential Source of Cellulose. *BioResources*, 13(4), pp. 7345–7359.

Park, Y.C., Kim, J.S. and Kim, T., 2018. Pretreatment of Corn Stover Using Organosolv with Enzymatic Saccharification. *Energies*, 11(5) pp. 1–9.

Pereira, A.P., Woodman, T.J., Brahmabhatt, P. and Chuck, C.J., 2019. The optimized production of 5-(hydroxymethyl)furfural and related products from spent coffee grounds. *Applied Sciences*, 9(3390), pp. 1–21.

Rajah, F.T., 2018. *Coconut-cross-section - Coconut-Shell Carbon Water Filters - Rajah Filter Technics*. [online] Available at: <<https://rajahfiltertechnics.com/water-filtration/the-advantages-of-using-indian-coconuts-for-activated-carbon/attachment/coconut-cross-section/>> [Accessed 15 April 2020].

Ravindran, R., Desmond, C., Jaiswal, S. and Jaiswal, A.K., 2018. Optimisation of organosolv pretreatment for the extraction of polyphenols from spent coffee waste and subsequent recovery of fermentable sugars. *Bioresource Technology Reports*, 3(1), pp. 7–14.

Ravindran, R., Jaiswal, S., Abu-Ghannam, N. and Jaiswal, A.K., 2017. Two-step sequential pretreatment for the enhanced enzymatic hydrolysis of coffee spent waste. *Bioresource Technology*, 239(1), pp. 276–284.

Rawangkul, R., Khedari, J., Hirunlabh, J. and Zeghmati, B., 2010. Characteristics and performance analysis of a natural desiccant prepared from coconut coir. *ScienceAsia*, 36(3), pp. 216–222.

Ritchie, H. and Roser, M., 2018. *Energy - Our World in Data*. [online] Available at: <<https://ourworldindata.org/energy>> [Accessed 18 April. 2020].

Rodríguez, A., Espinosa, E., Domínguez-Robles, J., Sánchez, R., Bascón, I. and Rosal, A., 2018. Different Solvents for Organosolv Pulping. In: S.N. Kazi, eds. *Pulp and Paper Processing*. Malaysia: IntechOpen. pp. 33–54.

Rogers, K., 2012. *Scientific modeling | science |*. [online] Available at: <<https://www.britannica.com/science/scientific-modeling>> [Accessed 18 June. 2019].

Romanov, A., 2020. *Sugarcane bagasse - the waste of sugar manufacture | Mostphotos*. [online] Available at: <<https://www.mostphotos.com/en-us/3577291/sugarcane-bagasse>> [Accessed 19 April 2020].

Salapa, I., Katsimpouras, C., Topakas, E. and Sidiras, D., 2017. Organosolv pretreatment of wheat straw for efficient ethanol production using various solvents. *Biomass and Bioenergy*, 100(1), pp. 10–16.

Santos, R.B., Jameel, H., Chang, H.M. and Hart, P.W., 2013. Impact of lignin and carbohydrate chemical structures on degradation reactions during hardwood kraft pulping processes. *BioResources*, 8(1), pp. 158–171.

Schroeder, L.R., Gentile, V.M. and Atalla, R.H., 1986. Nondegradative preparation of amorphous cellulose. *Journal of Wood Chemistry and Technology*, 6(1), pp. 1–14.

Shahbandeh, M., 2020. *Global coconut production 2000-2017*. [online] Available at: <<https://www.statista.com/statistics/577497/world-coconut-production/>> [Accessed 15 April 2020].

Sidiras, D.K., 2015. Organosolv Pretreatment as a major step of Lignocellulosic Biomass Refining. *Engineering Conferences International ECI Digital Archives*, 1(1), pp. 1–9.

Sudhakar, K., Mamat, R., Samykano, M., Azmi, W.H., Ishak, W.F.W. and Yusaf, T., 2018. An overview of marine macroalgae as bioresource. *Renewable and Sustainable Energy Reviews*, 91(1), pp. 165–179.

Tan, Z.Y., 2019. *Agriculture: A coconut revival | The Edge Markets*. [online] Available at: <<https://www.theedgemarkets.com/article/agriculture-coconut-revival>> [Accessed 15 April 2020].

Tappi, 2011. Lignin in Wood and Pulp. *T222 Om-02*, pp.1–7.

TAPPI, 1999. Alpha-, beta- and gamma-cellulose in pulp. *Test Methods T 203 cm-99*. Atlanta: Technical Association of the Pulp and Paper Industry, pp.5–9.

Vallejos, M.E., Zambon, M.D., Area, M.C. and Curvelo, A.A. da S., 2015. Low liquid-solid ratio fractionation of sugarcane bagasse by hot water autohydrolysis and organosolv delignification. *Industrial Crops and Products*, 65(1), pp. 349–353.

Walton, J., 2020. *The 5 Countries That Produce the Most Sugar*. [online] Available at: <<https://www.investopedia.com/articles/investing/101615/5-countries-produce-most-sugar.asp>> [Accessed 19 Apr. 2020].

Welker, C.M., Balasubramanian, V.K., Petti, C., Rai, K.M., Debolt, S. and Mendu, V., 2015. Engineering Plant Biomass Lignin Content and Composition for Biofuels and Bioproducts. pp. 7654–7676.

Wongsiridetchai, C., Chiangkham, W., Khlaihiran, N., Sawangwan, T., Wongwathanarat, P., Charoenrat, T. and Chantorn, S., 2018. Alkaline pretreatment of spent coffee grounds for oligosaccharides production by mannanase from *Bacillus* sp. GA2(1). *Agriculture and Natural Resources*, 52(3), pp. 222–227.

Worldometer, 2017. *China Coal Reserves and Consumption Statistics*. [online] Available at: <<https://www.worldometers.info/coal/china-coal/>> [Accessed 18 April 2020].

Yu, H., You, Y., Lei, F., Liu, Z., Zhang, W. and Jiang, J., 2015. Comparative study of alkaline hydrogen peroxide and organosolv pretreatments of sugarcane bagasse to improve the overall sugar yield. *Bioresource Technology*, 187(1), pp. 161–166.

Zabed, H., Sahu, J.N., Boyce, A.N. and Faruq, G., 2016. Fuel ethanol production from lignocellulosic biomass: An overview on feedstocks and technological approaches. *Renewable and Sustainable Energy Reviews*, 66(1), pp. 751–774.

Zafar, S., 2019. *Uses of Coconut Wastes | BioEnergy Consult. Bioenergy Consult*. [online] Available at: <<https://www.bioenergyconsult.com/coconut-biomass/>> [Accessed 19 April 2020].

Zarrinbakhsh, N., Wang, T., Rodriguez-Uribe, A., Misra, M. and Mohanty, A.K., 2016. Characterization of wastes and coproducts from the coffee industry for composite material production. *BioResources*, 11(3), pp. 7637–7653.

Zhang, H., Fan, M., Li, X., Zhang, A. and Xie, J., 2018a. Enhancing enzymatic hydrolysis of sugarcane bagasse by ferric chloride catalyzed organosolv pretreatment and Tween 80. *Bioresource Technology*, 258(1), pp. 295–301.

Zhang, H., Fan, M., Li, X., Zhang, A. and Xie, J., 2018b. Enhancing enzymatic hydrolysis of sugarcane bagasse by ferric chloride catalyzed organosolv pretreatment and Tween 80. *Bioresource Technology*, 258(2), pp. 295–301.

Zhang, H., Zhang, S., Yuan, H., Lyu, G. and Xie, J., 2018c. FeCl<sub>3</sub>-catalyzed ethanol pretreatment of sugarcane bagasse boosts sugar yields with low enzyme loadings and short hydrolysis time. *Bioresource Technology*, 249(9), pp. 395–401.

Zhang, K., Pei, Z. and Wang, D., 2016. Organic solvent pretreatment of lignocellulosic biomass for biofuels and biochemicals: A review. *Bioresource Technology*, 199(1), pp. 21–33.

Zhang, Z., Harrison, M.D., Rackemann, D. and Doherty, W., 2016. Organosolv Pretreatment of Plant Biomass for Enhanced Enzymatic Saccharification. *Green Chemistry*, 1(1-3), pp. 1–33.

Zhao, X., Cheng, K. and Liu, D., 2009. Organosolv pretreatment of lignocellulosic biomass for enzymatic hydrolysis. *Applied Microbiology and Biotechnology*, 82(5), pp. 815–827.